THE JOURNAL
OF
CHEMICAL PHYSICS

VOLUME 10 JULY, 1942 NUMBER 7

Valence and Central Forces in Bent Symmetrical XY_2 Molecules

W. H. SHAFFER AND R. R. NEWTON
Mendenhall Laboratory of Physics, Ohio State University, Columbus, Ohio

(Received April 1, 1942)

Appropriate generalized coordinates and potential functions are set up for studying the zero- and first-order vibration problem of the best symmetrical XY_2 molecular model under the assumption of valence and central forces. The force constants in the quadratic and cubic parts of the potential function of the water vapor molecule are evaluated for these two types of forces by using the data of Darling and Dennison.

I. INTRODUCTION

THE data obtained from experiment on the normal frequencies of vibration of polyatomic molecules are usually insufficient to allow evaluation of all the force constants in the most general form of the harmonic potential function consistent with the symmetry of a molecule. Consequently it is necessary to adopt simplified potential functions, such as those based on valence- or central-forces, involving a number of force constants not greater than the number of independent data available. These approximations often lead to consistent results and appear to give fairly good interpretation of experimental data. However, their validity should be tested in cases where it is possible to evaluate all the constants in the most general form of the harmonic potential function and it would be desirable to investigate the possibility of extending the same types of approximations to higher order parts of the potential function.

In this paper the vibrations of the bent symmetrical XY_2 molecular model are discussed for valence- and central-forces. Appropriate generalized coordinates are selected for describing these two types of forces and the most general zero- (harmonic) and first-order (cubic) parts of the potential function are set up in terms of these coordinates. Relations are derived giving the force constants in the valence- and central-force expressions in terms of those occurring in the normal coordinate form of potential function. The results are applied to the interpretation of the data on the vibrations of the water vapor molecule which Darling and Dennison[1] obtained from a study of the vibration-rotation spectra of H_2O and D_2O. This is the first case in which sufficient data have been available on the vibrations of a polyatomic molecule to make it feasible to extend the valence- and central-force types of potential function to include the cubic terms.

II. NORMAL MODES OF OSCILLATION

Several writers[1–5] have discussed the normal modes and frequencies of vibration of the bent symmetrical XY_2 molecular model. A brief sum-

[1] B. T. Darling and D. M. Dennison, Phys. Rev. **57**, 128 (1940).
[2] N. Bjerrum, Verh. d. D. Phys. Ges. **16**, 737 (1914).
[3] D. M. Dennison, Phil. Mag. **1**, 195 (1926).
[4] E. O. Salant and J. E. Rosenthal, Phys. Rev. **42**, 812 (1932).
[5] W. H. Shaffer and H. H. Nielsen, Phys. Rev. **56**, 188 (1939).

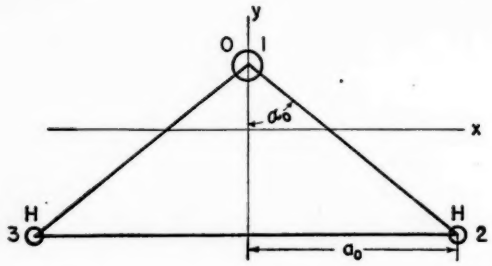

FIG. 1a.

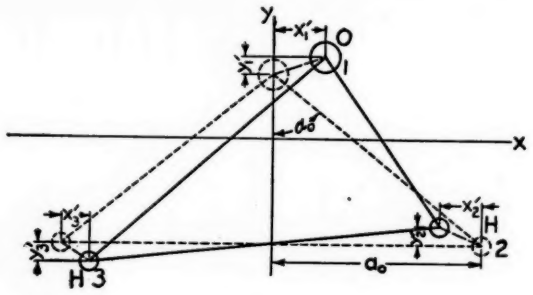

FIG. 1b.

mary of the problem is given here in order to clarify the notation used in this paper.

The equilibrium configuration of the model is shown in Fig. 1a. The positions of the particles are referred to a right-handed coordinate system, xyz, so oriented that its origin lies at the center of gravity, its xy plane coincides with the plane of the molecule, and its z axis points upward from the xy plane. In the equilibrium configuration the coordinate axes coincide with the principal axes of inertia as shown in Fig. 1a and the equilibrium coordinates are $x^0_1=0$, $x^0_2=-x^0_3=a_0$, $y^0_1=(\mu/M)a_0\cot\alpha_0$, $y^0_2=y^0_3=-(\mu/2m)a_0\cot\alpha_0$, $z^0_1=z^0_2=z^0_3=0$, where m is the mass of a Y-particle, M the mass of the X-particle and $\mu=2mM/(2m+M)$.

When the system is oscillating, the components of displacement of the ith particle ($i=1,2,3$) from equilibrium are denoted by x'_i, y'_i, z'_i as illustrated in Fig. 1b, where the z'_i vanish because the molecule lies in the xy plane. It has been shown[4,5] that appropriate symmetry coordinates for studying the small oscillations of the XY_2 model are

$$\begin{aligned} u&=x'_1-(1/2)(x'_2+x'_3),\\ v&=y'_1-(1/2)(y'_2+y'_3),\\ w&=x'_2-x'_3. \end{aligned} \tag{1a}$$

These coordinates are also suitable for studying the interactions between rotation and vibration since they are consistent with the Eckart[6,7] conditions:

$$\begin{aligned} Mx'_1+m(x'_2+x'_3)&=0,\\ My'_1+m(y'_2+y'_3)&=0, \end{aligned}$$

and

$$M(x^0_1y'_1-y^0_1x'_1)+m(x^0_2y'_2-y^0_2x'_2+x^0_3y'_3-y^0_3x'_3)=0. \tag{1b}$$

It can readily be shown from Eqs. (1a) and (1b) that

$$\begin{aligned} x'_1&=(\mu/M)u, \quad x'_2=-(\mu/2m)u+(w/2), \quad x'_3=-(\mu/2m)u-(w/2),\\ y'_1&=(\mu/M)v, \quad y'_2=(\mu/2m)(-v+u\cot\alpha_0), \quad y'_3=(\mu/2m)(-v-u\cot\alpha_0). \end{aligned} \tag{2}$$

The kinetic energy of oscillation (see reference 5) is

$$T_v=(1/2)\{\mu_1\dot{u}^2+\mu\dot{v}^2+(m/2)\dot{w}^2\},$$

where $\mu_1=\mu[1+(\mu/2m)\cot^2\alpha_0]$, and the most general quadratic potential energy function* consistent with the symmetry of the molecule is

$$U_0=(1/2)\{Aw^2+Bu^2+Cv^2+2Dvw\}.$$

The normal frequencies of oscillation ω_j (in cm^{-1}) are given by the relations $\omega_j=(2\pi c)^{-1}\lambda_j^{\frac{1}{2}}$, ($j=1,2,3$), where c is the velocity of light in cm/sec. and the λ_j are roots of Lagrange's secular determinant, $|\lambda T_v-U_0|=0$. The λ_i satisfy the following relations:

$$\begin{aligned} (\lambda_1+\lambda_2)&=[(2A/m)+(C/\mu)],\\ (\lambda_1-\lambda_2)^2&=[(2A/m)-(C/\mu)]^2+(8D^2/\mu m),\\ \lambda_1\lambda_2&=(2/\mu m)(AC-D^2), \quad \lambda_3=(B/\mu_1). \end{aligned}$$

The three constants A, C, and D which are related to the two roots λ_1 and λ_2 can be determined if the roots, λ'_1 and λ'_2, of the isotopic molecule $X'Y'_2$ are known. If m' denotes the mass of Y', M' the mass of X', and $\mu'=2m'M'/(2m'+M')$,

[6] C. Eckart, Phys. Rev. **47**, 552 (1932).

[7] E. B. Wilson and J. B. Howard, J. Chem. Phys. **4**, 260 (1936).

* For comparison with reference 5 where the generalized force constants are $k'_1\cdots k'_4$, note that $A=k'_1$, $B=k'_3$, $C=k'_2$, $2D=k'_4$.

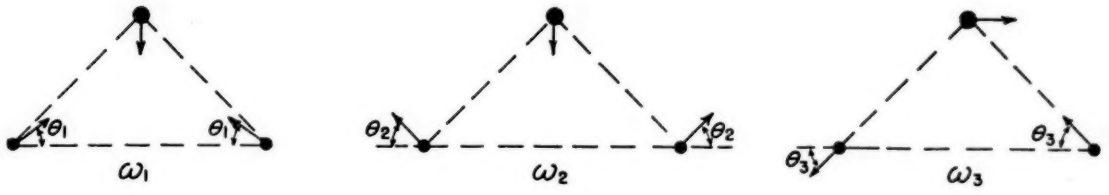

FIG. 2.

the following relations hold:

$$A=[\mu(\lambda_1+\lambda_2)-\mu'(\lambda'_1+\lambda'_2)]/[(2\mu/m)-(2\mu'/m')];$$
$$C=[m(\lambda_1+\lambda_2)-m'(\lambda'_1+\lambda'_2)]/[(m/\mu)-(m'/\mu')];$$
$$D^2=AC-(\mu m/2)\lambda_1\lambda_2; \quad (3)$$
$$(\mu^2/\mu_1)\lambda_3=(\mu'^2/\mu'_1)\lambda'_3, \quad (\lambda_1\lambda_2/\lambda'_1\lambda'_2)=(\mu'm'/\mu m).$$

The following relations give the symmetry coordinates u, v, and w, in terms of the normal coordinates $q_j=A_j\cos(\lambda_j^{\frac{1}{2}}t-\epsilon_j)$ associated with the normal frequencies, ω_j:

$$w=(m/2)^{-\frac{1}{2}}(\sigma_1q_1-\sigma_2q_2), \quad (4)$$
$$v=\mu^{-\frac{1}{2}}(\sigma_2q_1+\sigma_1q_2), \quad u=\mu_1^{-\frac{1}{2}}q_3,$$

where

$$\sigma_1=2^{-\frac{1}{2}}(1+K)^{\frac{1}{2}}, \quad \sigma_2=2^{-\frac{1}{2}}(1-K)^{\frac{1}{2}}$$

and

$$K=+\{1-8(\mu m)^{-1}(\lambda_1-\lambda_2)^{-2}D^2\}^{\frac{1}{2}}.$$

It follows from Eqs. (3) and (4) that the displacement coordinates x'_i and y'_i are related to the normal coordinates q_j in the following manner:

$$x'_i=\sum_j l_{ij}q_j, \quad y'_i=\sum_j m_{ij}q_j, \quad (5)$$

where

$$l_{11}=l_{12}=m_{13}=0, \quad l_{13}=(\mu/M)\mu_1^{-\frac{1}{2}},$$
$$l_{21}=-l_{31}=(2m)^{-\frac{1}{2}}\sigma_1, \quad -l_{22}=l_{32}=(2m)^{-\frac{1}{2}}\sigma_2,$$
$$l_{23}=-l_{33}=-(\mu/2m)\mu_1^{-\frac{1}{2}}, \quad m_{11}=(\mu/M)\mu^{-\frac{1}{2}}\sigma_2,$$
$$m_{12}=(\mu/M)\mu^{-\frac{1}{2}}\sigma_1, \quad m_{21}=m_{31}=-(\mu/2m)\mu^{-\frac{1}{2}}\sigma_2,$$
$$m_{22}=m_{32}=-(\mu/2m)\mu^{-\frac{1}{2}}\sigma_1,$$
$$m_{23}=-m_{33}=(\mu/2m)\mu_1^{-\frac{1}{2}}\cot\alpha_0.$$

The normal modes of oscillation are illustrated in Fig. 2 where $\tan\theta_1=(\sigma_2/\sigma_1)(\mu/2m)^{\frac{1}{2}}$ and $\tan\theta_2=(\sigma_1/\sigma_2)(\mu/2m)^{\frac{1}{2}}$.

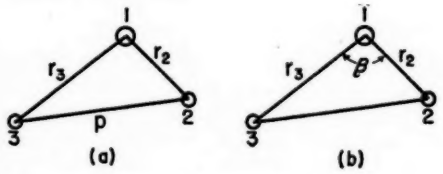

FIG. 3.

III. VALENCE- AND CENTRAL-FORCE COORDINATES

Two common types of force fields which are used in discussions of molecular vibrations are (a) the central-force field in which it is assumed that there are restoring forces acting essentially along the lines connecting the atomic nuclei and (b) the valence-force field in which it is assumed that there are restoring forces acting along the valence bonds and restoring torques tending to maintain the angles between valence bonds. Suitable coordinates for describing the central- and valence-force fields are illustrated in Figs. 3a and 3b, respectively, where $r_2=r_0+\delta r_2$, $r_3=r_0+\delta r_3$, $p=p_0+\delta p$, and $\beta=\beta_0+\delta\beta$, if r_0, p_0, and β_0 denote equilibrium values of the respective coordinates and δr_2, δr_3, δp, and $\delta\beta$ denote changes in the coordinates occurring during oscillation. Assuming small oscillations and using Eqs. (1) and (3), one can show that

$$\delta p=w, \quad \delta r_2+\delta r_3=w\sin\alpha_0+2v\cos\alpha_0,$$
$$\delta r_3-\delta r_2=2u(\mu_1/\mu)\sin\alpha_0, \quad (6)$$
$$\delta\beta=(1/r_0)(w\cos\alpha_0-2v\sin\alpha_0).$$

It follows from Eqs. (4) and (6) that the normal coordinates are related to the central- and valence-force coordinates in the following manner:

$$q_1=\beta_1(\delta r_2+\delta r_3)+\beta_2\delta p,$$
$$q_2=\beta_3(\delta r_2+\delta r_3)+\beta_4\delta p, \quad (7)$$
$$q_3=\beta_5(\delta r_3-\delta r_2),$$

and

$$q_1=\gamma_1(\delta r_2+\delta r_3)+\gamma_2 r_0\cos\alpha_0\delta\beta,$$
$$q_2=\gamma_3(\delta r_2+\delta r_3)+\gamma_4 r_0\cos\alpha_0\delta\beta, \quad (8)$$
$$q_3=\gamma_5(\delta r_3-\delta r_2),$$

where

$$\beta_1=[\mu^{\frac{1}{2}}\sigma_2/2\cos\alpha_0], \quad \beta_3=[\mu^{\frac{1}{2}}\sigma_1/2\cos\alpha_0],$$
$$\gamma_2=\beta_2=(1/2)[(2m)^{\frac{1}{2}}\sigma_1-\mu^{\frac{1}{2}}\sigma_2\tan\alpha_0],$$
$$\gamma_4=\beta_4=(1/2)[-(2m)^{\frac{1}{2}}\sigma_2-\mu^{\frac{1}{2}}\sigma_1\tan\alpha_0],$$
$$\gamma_5=\beta_5=[\mu\mu_1^{-\frac{1}{2}}/2\sin\alpha_0],$$
$$\gamma_1=\beta_1+\beta_2\sin\alpha_0, \quad \gamma_3=\beta_3+\beta_4\sin\alpha_0.$$

It follows from (7) and (8) that the zero-order or harmonic potential function U_0 can be expressed in terms of the central-force coordinates as

$$U_0=(1/2)\{K_1(\delta r_2^2+\delta r_3^2)+K_2\delta p^2 +2K_3\delta p(\delta r_2+\delta r_3)+2K_4\delta r_2\delta r_3\} \quad (9)$$

and in terms of the valence-force coordinates as

$$U_0=(1/2)\{c_1(\delta r_2^2+\delta r_3^2)+c_2r_0^2\cos^2\alpha_0\delta\beta^2 +2c_3r_0\cos\alpha_0\delta\beta(\delta r_2+\delta r_3)+2c_4\delta r_2\delta r_3\} \quad (10)$$

where

$$K_1=[(C/4\cos^2\alpha_0)+(\mu/\mu_1)^2(B/4\sin^2\alpha_0)],$$
$$K_2=[A+(C/4)\tan^2\alpha_0-D\tan\alpha_0],$$
$$2K_3=[-(C/2)\tan\alpha_0+D]/\cos\alpha_0,$$
$$2K_4=[(C/2\cos^2\alpha_0)-(\mu^2/\mu_1)(B/2\sin^2\alpha_0)];$$

and

$$\begin{aligned}c_1&=A\sin^2\alpha_0+(C/4)\cos^2\alpha_0\\&\quad+(\mu/\mu_1)^2(B/4\sin^2\alpha_0)+D\sin\alpha_0\cos\alpha_0,\\c_2&=K_2,\\c_3&=A\sin\alpha_0-(C/4)\sin\alpha_0\\&\quad+(D/2\cos\alpha_0)\cos 2\alpha_0,\\c_4&=A\sin^2\alpha_0+(C/4)\cos^2\alpha_0\\&\quad-(\mu/\mu_1)^2(B/4\sin^2\alpha_0)+D\sin\alpha_0\cos\alpha_0.\end{aligned} \quad (11)$$

IV. CUBIC POTENTIAL FUNCTION

It can be shown[1,5,8] from consideration of the symmetry properties of the normal modes that the first-order part of the anharmonic potential energy function contains the following terms cubic in the normal coordinates q_1, q_2, and q_3:

$$U_1=a_1q_1^3+a_2q_2^3+a_3q_1^2q_2+a_4q_1q_2^2 +a_5q_1q_3^2+a_6q_2q_3^2. \quad (12)$$

It follows from Eqs. (7), (8), and (12) that U_1 can be expressed in terms of the central-force coordinates as

$$U_1=L_1(\delta r_2^3+\delta r_3^3)+L_2\delta p^3 +3L_3(\delta r_2^2\delta r_3+\delta r_2\delta r_3^2)+6L_4\delta r_2\delta r_3\delta p +3L_5(\delta r_2+\delta r_3)\delta p^2 +3L_6(\delta r_2^2+\delta r_3^2)\delta p, \quad (13)$$

and in terms of the valence-force coordinates as

$$U_1=l_1(\delta r_2^3+\delta r_3^3)+l_2r_0^3\cos^3\alpha_0\delta\beta^3 +3l_3(\delta r_2^2\delta r_3+\delta r_2\delta r_3^2) +6l_4r_0\cos\alpha_0\delta r_2\delta r_3\delta\beta +3l_5r_0^2\cos^2\alpha_0(\delta r_2+\delta r_3)\delta\beta^2 +3l_6r_0\cos\alpha_0(\delta r_2^2+\delta r_3^2)\delta\beta, \quad (14)$$

where the L's are defined as

$$\begin{aligned}L_1&=(a_1\beta_1+a_3\beta_3)\beta_1^2+(a_2\beta_3+a_4\beta_1)\beta_3^2\\&\quad+(a_5\beta_1+a_6\beta_3)\beta_5^2,\\L_2&=(a_1\beta_2+a_3\beta_4)\beta_2^2+(a_2\beta_4+a_4\beta_2)\beta_4^2,\\L_3&=L_1-(4/3)(a_5\beta_1+a_6\beta_3)\beta_5^2,\\L_4&=(a_1\beta_1+a_3\beta_3)\beta_1\beta_2+(a_2\beta_3+a_4\beta_1)\beta_3\beta_4\\&\quad+(1/3)[(\beta_1\beta_4-\beta_2\beta_3)(a_3\beta_1-a_4\beta_3)\\&\quad-(a_5\beta_2+a_6\beta_4)\beta_5^2],\\L_5&=(a_1\beta_1+a_3\beta_3)\beta_2^2+(a_2\beta_3+a_4\beta_1)\beta_4^2\\&\quad+(2/3)(a_3\beta_2-a_4\beta_4)(\beta_1\beta_4-\beta_2\beta_3),\\L_6&=L_4+(2/3)(a_5\beta_2+a_6\beta_4)\beta_5^2,\end{aligned}$$

and the definitions of the l's can be obtained from those of the corresponding L's simply by replacing the β's by γ's.

V. APPLICATION TO WATER VAPOR MOLECULE

The expressions developed in the preceding sections for the valence- and central-force coordinates are now applied to the case of the water vapor molecule. For this purpose we use the following data obtained by Darling and Dennison:[1]

(a) Normal frequencies of H_2O:
$\omega_1=3825.32\ \text{cm}^{-1}$, $\omega_2=1653.91\ \text{cm}^{-1}$,
$\omega_3=3935.59\ \text{cm}^{-1}$.

(b) Normal frequencies of D_2O:
$\omega'_1=2758.06\ \text{cm}^{-1}$, $\omega'_2=1210.25\ \text{cm}^{-1}$,
$\omega'_3=2883.79\ \text{cm}^{-1}$.

(c) Equilibrium coordinates:
$\beta_0=2\alpha_0=104°31'$, $r_0=0.9508\text{A}$.

(d) Cubic constants† in the potential energy:
$a_1=-3.615\times10^{49}$, $a_2=1.500\times10^{48}$,
$a_3=-7.391\times10^{46}$, $a_4=1.049\times10^{49}$,
$a_5=-1.050\times10^{50}$,
$a_6=-1.217\times10^{49}$ dynes per cm² per g$^{\frac{1}{2}}$.

[8] L. G. Bonner, Phys. Rev. **46**, 458 (1934).

† The constants a_1, a_2, etc., of Eq. (12) can readily be obtained from the α_1, α_2, etc., of Darling and Dennison by means of the relations $a_1=C\omega_1^{\frac{1}{2}}\alpha_1$, $a_2=-C\omega_2^{\frac{1}{2}}\alpha_2$, $a_3=-C\omega_1\omega_2^{\frac{1}{2}}\alpha_3$, $a_4=C\omega_1^{\frac{1}{2}}\omega_2\alpha_4$, $a_5=C\omega_1^{\frac{1}{2}}\omega_3\alpha_5$, $a_6=-C\omega_2^{\frac{1}{2}}\omega_3\alpha_6$,

The above values for the normal frequencies of H_2O and D_2O lead to the following values of the generalized force constants defined in (3): $A=3.129\times10^5$, $C=7.197\times10^5$, and $D=3.161\times10^5$ dynes per cm. The coefficients σ_1 and σ_2 of (4) have for H_2O the values $\sigma_1=0.8101$, $\sigma_2=0.5863$, and for D_2O the values $\sigma_1'=0.7876$, $\sigma_2'=0.6161$. The angles describing the normal modes in Fig. 2 are for H_2O, $\theta_1=34°17'30''$, $\theta_2=46°2'$ and for D_2O, $\theta_1'=34°57'30''$, $\theta_2'=48°48'30''$; if the vibrations of the hydrogen atoms were exactly parallel and perpendicular to the OH bonds in modes ω_1 and ω_2, respectively, it would be true that $\theta_1=\theta_1'=37°44'30''$ and $\theta_2=\theta_2'=52°15'30''$.

The constants defined in (11) for the valence- and central-force forms of the zero-order potential function have the following values in units of 10^5 dynes per cm:

Central, $K_1=9.064$, $K_2=2.049$, $K_3=-1.215$, $K_4=0.5398$;
Valence, $c_1=8.423$, $c_2=2.049$, $c_3=0.4047$, $c_4=-0.1015$.

It is interesting to compare the above values of the valence-force constants with the corresponding ones obtained by Ta-You Wu[9] from earlier values of the normal frequencies: $c_1=8.23$, $c_2=2.00$, $c_3=0$, $c_4=-0.076$.

The constants occurring in the valence- and central-force forms of the first-order potential function given in (13) and (14) have the following values in units of 10^{13} dynes per cm per cm:

Central, $L_1=-8.48$, $L_2=-0.258$, $L_3=1.91$, $L_4=-1.61$, $L_5=0.825$, $L_6=-1.19$;
Valence, $l_1=-9.89$, $l_2=-0.258$, $l_3=-0.163$, $l_4=-0.510$, $l_5=0.624$, $l_6=-0.084$.

The constants in the valence- or central-force forms of the second-order or quartic part of the anharmonic potential function cannot be computed from the data available. It can easily be shown that such a calculation would require knowledge of all the constants in the normal-coordinate form of the second-order potential function. The study of Darling and Dennison, which was based on a second-order calculation of the vibration-rotation energies of the bent XY_2 molecule, yielded the values of only six of the nine constants in the second-order function.

VI. CONCLUSIONS

These results show that the cross-product terms in the generalized valence-force form of both the zero-order and the first-order potential function are smaller than in the generalized central-force form, and hence the usual simplified valence-force potential function should give a better approximation to the true potential of the water vapor molecule than would the simplified central-force form. A very good three-term approximation to the zero-order potential can be obtained by neglecting the constant c_4 in the valence-force form.

A possible type of approximation to the first-order potential function for water vapor is suggested by the values of the constants in the valence-force form. This approximation would be

$$U_1=l_1(\delta r_2^3+\delta r_3^3)+6l_4r_0\cos\alpha_0\delta r_2\delta r_3\delta\beta+3l_5r_0^2\cos^2\alpha_0(\delta r_2+\delta r_3)\delta\beta^2.$$

---

where $C=8\pi^3c^{6/2}\hbar^{-4}$ if $c=2.9986\times10^{10}$ cm/sec. and $\hbar=(6.624\times10^{-27}/2\pi)$ erg-sec. The minus signs in a_2, a_3, and a_6 occur because q_2 of Eq. (5) is the negative of the corresponding quantity in the paper of Darling and Dennison. In the calculations in this paper the following constants are used: $m_H=1.6734\times10^{-24}$ g, H=1.00813, D=2.01473, O=16.000.

[9] Ta-You Wu, *Vibrational Spectra and Structure of Polyatomic Molecules* (Prentice-Hall, New York, 1940).

Electronic Structure and Stability of Hydrogen Halides and of Complex Ions XO_4

KASIMIR FAJANS AND NORMAN BAUER
Department of Chemistry, University of Michigan, Ann Arbor, Michigan

(Received April 9, 1942)

(1) It is shown that in the hydrogen halide molecules (internuclear distance r_0) the proton penetrates the electronic shell of the anion to a depth which for the simplified case of spherical symmetry can be characterized by the condition: The amount of negative charge beyond the sphere of radius r_0 equals $-1e$. (2) From the dipole moments $\mu = xer_0$ of the hydrogen halide molecules it can be concluded: The wave mechanical distribution of the negative charge of the free halide ions is changed by the introduction of the proton in such a way that the center of gravity of an amount of charge equal to $-(1-x)e$ is shifted from the halogen nucleus to the proton. The fraction $(1-x)$ increases with the electronic polarizability of the anion, and would be equal to 1 for an ion of infinitely large polarizability, leading to a completely unpolar type of binding in this case. (3) It is shown that for the complex ions SiO_4^{4-}, PO_4^{3-}, $SO_4^{=}$, and ClO_4^{-}, the gradation of the X–O distances and of the molar dispersion can be easily understood from the point of view used in 1924 for the case of the molar refraction: These ions represent the result of the polarization of $O^{=}$ by Si^{4+}, P^{5+}, S^{6+}, and Cl^{7+}, and the X–O binding in them shows gradual changes toward the unpolar type. (4) It is pointed out that the relatively unstable HI and ClO_4^{-} approach the unpolar type of binding more closely than any other of the compounds considered here. The generalization of this connection between instability and the degree of deformation of electronic shells explains why compounds like FO_4^{-} and BrO_4^{-} are unknown.

INTRODUCTION

THE problem of the electronic structure of chemical compounds has been approached in many more or less different ways. Limiting ourselves here to simple inorganic substances we shall characterize four points of view by mentioning how they describe the structure of the hydrogen halide molecules (HX) and of the sulphate ion.

(a) According to the extreme ionic point of view used by W. Kossel (1916), in HX the proton is attached to the spherical halide ion of definite size; in $SO_4^{=}$ four $O^{=}$ are attached to the S^{6+} ion.

(b) In the well-known theory of the covalent bond of G. N. Lewis (1916) one has the formulae

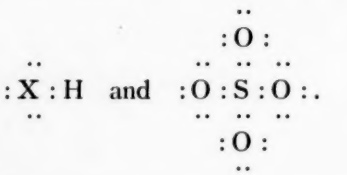

(c) According to the polarization or deformation point of view (especially since 1923[1]), the hydrogen halides or $SO_4^{=}$ can be thought of as the result of interaction between the anion X^{-} or $O^{=}$ with the proton or S^{6+}, respectively, and represent examples of a type of binding intermediate between (a) and (b).

(d) From the resonance point of view (especially L. Pauling[2] since 1931), the real HX molecule is considered to be the result of the resonance between two hypothetical extreme forms of HX, one ionic, the other covalent.[3] The Lewis formula for $SO_4^{=}$ is concluded to be unsatisfactory on the basis of the interatomic S–O distance. It is suggested that one should use the old structural valence line formula with two double and two single bonds and for a more precise electronic description to add several (seven are mentioned specifically) of the possible resonating structures (see reference 2, pp. 239–243).

Here we shall extend the former descriptions[4] based on the polarization theory making use of some newer theoretical and experimental results with special emphasis on such points as

[1] See the presentation in K. Fajans, *Chemical Forces and Optical Properties of Substances* (Cornell Lectures), (McGraw-Hill Book Company, New York, 1931).

[2] See the presentation in L. Pauling, *Nature of the Chemical Bond*, second edition (Cornell University Press, Ithaca, New York, 1940).

[3] In respect to HF, its ionic character is estimated in reference 2, p. 49 to be 60 percent. On p. 297, however, the extreme ionic concept of the H–F bond is supported by the statement that calculations on this basis lead to an excellent agreement with the observed value for the internuclear distance in HF and to a close agreement for the F–F distance in HF_2^{-}. See also Fig. 38–1.

[4] K. Fajans and G. Joos, Zeits. f. Physik **23**, 1, 1924. See also reference 1, pp. 21 and 86, and reference 6b.

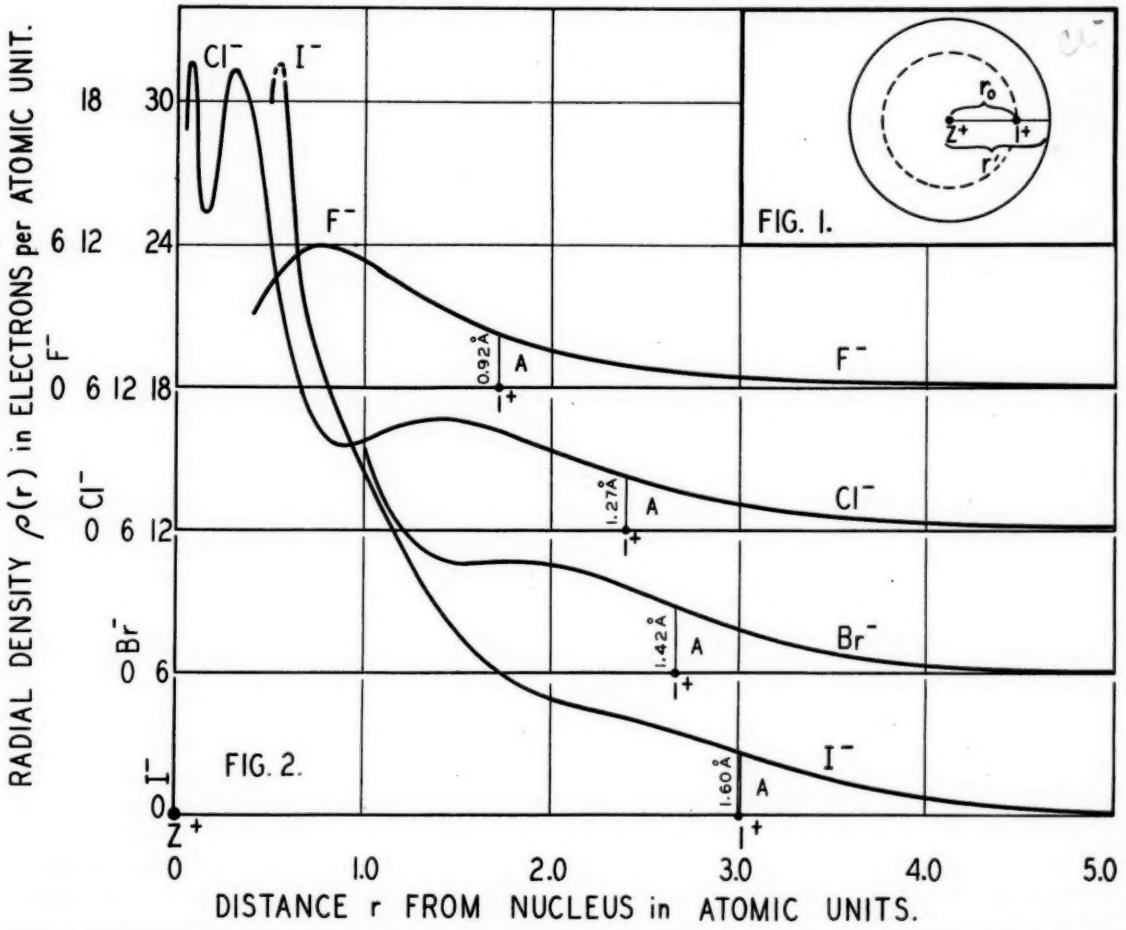

FIGS. 1 and 2 show the position of the proton within the electronic shells of halide ions. Figure 1 is for the simplified case of a spherically symmetrical anion of definite radius r'. Figure 2 gives the wave mechanical electron distribution in the free halide ions, with the proton at the actual internuclear distance r_0 it has in the hydrogen halide molecule.

will be necessary for the discussion of certain open questions in the valence theory, such as the hydrogen bond, boron hydrides, etc.[5]

1. HALIDE IONS OF DEFINITE RADIUS

Considering the process $X^- + H^+ = HX$, it will be helpful first to use the following simplified models (a) and (b):

(a) The electronic system of the free halide ion (nuclear charge $+Ze$) represents a penetrable sphere of definite radius r' (see Fig. 1). The spherically symmetrical distribution of the negative charge remains unaltered when the distance r between proton and nucleus changes from very large values to the equilibrium distance r_0 in the HX molecule.

(b) The proton changes the charge distribution of the electronic system; i.e., it polarizes and deforms the anion.

re (a): For the free ion the center of gravity of the $-(Z+1)e$ charge of the electronic system coincides with that of the $+Ze$ charge of the nucleus. For values $r \gtrsim r'$, the full attractive force of the excess charge $-1e$ is the only force acting on the proton. Thus the latter must penetrate the electronic system. With $r < r'$ the force becomes smaller because, according to the well-known result of the potential theory, one is led to the conclusion that that part of the negative charge outside the sphere of radius r does not act on the proton. Therefore, the latter

[5] See K. Fajans and W. M. Spurgeon, 103rd meeting of the Am. Chem. Soc., April 1942, Symposium on the Hydrogen Bond, and papers to follow.

will come to the equilibrium distance r_0 when the charge within the shell between r_0 and r' is equal to $-1e$.

re (b): We start with the rigid model (a), fix the position of the proton, and allow the charges of the anion to move. Since by the introduction of the proton into the ion an additional attractive force acts on the electronic system, its volume will diminish. The distance r_0 will also be somewhat different from the case (a) but this question does not need to be considered here. The actual loss of spherical symmetry makes quantitative predictions[6] about the details of the electronic distribution extremely difficult.

2. HALIDE IONS WITH WAVE MECHANICAL ELECTRON DISTRIBUTION

Figure 2 brings us somewhat nearer to reality. The curves correspond to the radial electron distribution in the free halide ion;[7] the proton (1+) is placed at a distance from the nucleus ($+Ze$) which it actually has in the hydrogen halide molecules. Thus if the halide ion were not polarized by the introduction of the proton, in applying appropriately the result obtained under 1(a) we would have to expect that the charge corresponding to the area A under the curves for r values between r_0 and ∞ is $-1e$. Instead, one finds that these areas correspond very nearly to $-2e$ for all four hydrogen halide molecules. Assuming these theoretical distribution curves for the free ions to be exact enough, this result means that the charge distribution in all four hydrogen halide molecules is different from that in the free ions. If the spherical symmetry of the electronic system were retained in the halide molecules we could draw the additional conclusion that a charge of approximately $-1e$ has been shifted from the space beyond r_0 into the region between the two nuclei. For the real (non-spherically symmetrical) case such a quantitative theoretical statement does not seem to be possible at present,[6] and one has to consult the experimental facts concerning the dipole moments and molar refraction in order to obtain more information about the change in the electron distribution due to the proton.

3. CHANGE OF ELECTRON DISTRIBUTION BY THE PROTON

With the undisturbed electronic cloud of Fig. 2 the dipole moment of the molecule would be $\mu=er_0$; in reality for HCl, HBr, and HI it is $\mu=xer_0$, where x has the values 0.17, 0.11, 0.05 (see references 6b and 2, p. 46), respectively. One can express this fact by saying either that the dipole length is $l=xr_0$ or that the positions of the halogen nucleus and the proton, separated by the distance r_0, represent the center of gravity of the charges $-xe$ and $+xe$. This means, when starting with the picture in Fig. 2, that the center of gravity of the charge $-(1-x)e$ has been drawn over from the halogen nucleus to the proton.

It can be expected that $(1-x)$ is closely connected with the polarizability of the halide ion. In Fig. 3, curve A, the values of $(1-x)$ are plotted against the molar refraction R[8] of Cl^-, Br^-, I^-. In addition it is obvious that for a rigid ion ($R=0$) one would have $(1-x)=0$, and that within an extremely easily polarizable electronic shell ($R=\infty$) the proton would be completely neutralized; i.e., here $(1-x)=1$. The curve allows one to interpolate, giving the value $(1-x)=0.5\pm0.1$ for HF, not known experi-

[6] a. F. Haber, Verh. d. D. Phys. Ges. **21**, 750 (1919); b. K. Fajans, Zeits. f. Elektrochemie **34**, 502 (1928); c. P. Debye, *Polar Molecules* (The Chemical Catalog Company, 1929), p. 59; d. J. G. Kirkwood, Physik. Zeits. **33**, 259 (1932); e. L. Pauling, J. Am. Chem. Soc. **54**, 988 (1932); f. Th. Neugebauer, Zeits. f. Physik **102**, 305 (1936); g. H. Hellmann and S. J. Pshejetzkij, Acta Physicochemica **7**, 621 (1937).

[7] The values of $\rho(r)$ in the curve for Cl^- are taken from D. R. Hartree and W. R. Hartree, Proc. Roy. Soc. **156**, 59 (1936) who used the well-known method of the self-consistent field; those for F^- are based on values of the wave functions which were calculated by D. R. Hartree, Proc. Roy. Soc. **151**, 96 (1935) by a similar method. The curve for Cl^- is the more reliable, exchange terms having been included.

The values of $\rho(r)$ for Br^- and I^- were calculated on the basis of empirical rules given by J. C. Slater, Phys. Rev. **36** (2), 57 (1930) for the screening constants and effective quantum numbers in his analytical expression for the wave functions. This empirical method is likely to give too small values of $\rho(r)$ at low electron densities, when compared with the Hartree curves. This is the case for Cl^-.

[8] The R values for the D line of the aqueous ions (see K. Fajans and R. Lühdemann, Zeits. f. physik. Chemie **B29**, 150 (1935)) were used in the figure because they are better known than the theoretically more significant R values for $\lambda=\infty$ of the gaseous ions.

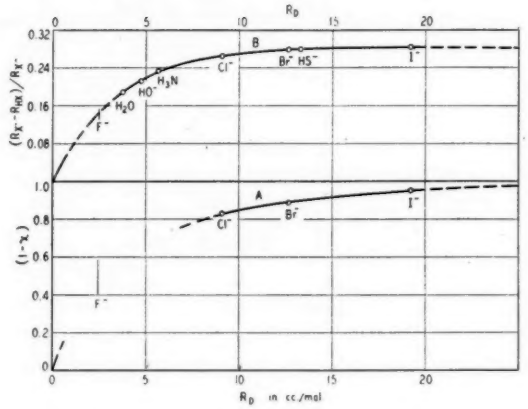

FIG. 3. Curve A: the ordinate gives the amount of charge $-(1-x)e$, the center of gravity of which is shifted by the introduction of the proton from the nucleus of the free halide ion to the position of the proton in the hydrogen halide molecule. Curve B: the ordinate gives the relative change of refraction of F^-, H_2O, $\cdots I^-$ caused by the introduction of a proton. For both curves, the abscissa is a measure of the polarizability of the initial particle.

mentally. With $r_0=0.92$A, $\mu=xer_0=2.4\pm0.5$ debyes.[8a]

From this result it follows that the type of binding in HF is far from that in the extreme case of rigid ions.[3]

4. TIGHTENING OF THE HALIDE IONS BY THE PROTON

It is of interest to note that curve A has a form similar to that of curve B in Fig. 3, which shows the relative diminution $-\Delta R/R$ of the molar refraction resulting from the introduction of a proton into anions and neutral molecules (their symbols are given near the points on the curve) as a function of the electronic polarizability (R) of the initial particle. This decrease of polarizability, i.e., tightening of the electronic system of anions or neutral molecules, is always found when they combine with an additional positive charge of a cation.[9] Curve B, showing this influence in the special case of protons, can be represented[10] by the exponential relation:

$$Q=-\Delta R/R=0.2859(1-e^{-0.2848R}). \quad (1)$$

The meaning of relation (1) is that $-\Delta R/R$, which can be considered as a measure of the tightening effect, tends towards the limiting value 0.2859 for $R=\infty$, which, as the curve indicates, is already closely approached by the easily polarizable iodide ion. The comparison with curve A shows that this limiting value of Q is reached when the field of the proton becomes completely neutralized by the charge drawn from the polarized electronic shell and that hydrogen iodide is close ($1-x=0.95$) to this state of unpolarity of the molecule.[11]

We shall show in Section 6 that this type of unpolarity of binding has some connection with the instability of the corresponding compounds (as shown by HI) but let us first discuss the structure of XO_4 ions.

5. DEFORMATION OF THE OXYGEN OCTET IN IONS XO_4

Here, instead of considering the polarizing action of a given particle (proton) on different electronic systems, we can compare the effect which different particles exert on the same electronic system, that of oxygen. The electron affinity of the oxygen atom, i.e., its tendency to complete an octet, is not large enough to make a free gaseous $O^=$ stable. The process $O+e^-=O^-$ is exothermic;[12] the second step however is endothermic[13] because of the repulsion between the excess charges of $O^=$. However, by combination with positively charged particles like the proton or other cations the electronic shell of $O^=$ can be stabilized and it is quite appropriate to treat many oxygen compounds as derivatives

[8a] *Note added in proof:* This agrees as closely as can be expected with the experimental value (between 2.47 and 2.71 debyes) of the dipole moment of HF in dioxane, communicated by M. E. Hobbs, A. J. Weith, and P. M. Gross at the 103rd meeting of the American Chemical Society, April 22, 1942.

[9] As molar refraction generally goes parallel to size and is sometimes considered as a measure of the "true" volume of a particle, the negative value of ΔR is in full agreement with the conclusion reached under 1 and 2 that the extension of halide ions is diminished by the combination with a proton.

[10] K. Fajans, Zeits. f. physik. Chemie **B24**, 133 (1934).

[11] It appears surprising that in spite of the great differences in the values $(1-x)$, the areas between r_0 and ∞ under the four curves in Fig. 2 are approximately equal, i.e., exceed the charge $-1e$ by about the same amount for all hydrogen halides. It is difficult to decide how much this is due to the lack of spherical symmetry and how much to uncertainties in the curves in the region of small electron density. (See footnote 7.)

[12] See, e.g., E. E. Hanson, Phys. Rev. **48**, 476 (1935); D. R. Hartree, Trans. Roy. Soc. **A238**, 229 (1939).

[13] See J. E. Mayer and M. M. Maltbie, Zeits. f. Physik **75**, 748 (1932); H. Hellmann and M. Mamotenko, Acta Physicochimica **7**, 127 (1937); O. K. Rice, *Electronic Structure and Chemical Binding* (McGraw-Hill Book Company, 1940), p. 101.

of $O^=$ and the corresponding cations, even in such cases as CO_2 and ClO_4^- which are usually considered as covalent. But in every case one must consider the changes of the state of the oxygen octet. The molar refraction has proven to be a very sensitive property for such purposes and is only exceeded in this respect by the molar dispersion of light.[14]

The apparent refraction R_D per single oxygen octet has the values 7.91, 6.81, 6.03, 4.27[15] for the oxides BaO, SrO, CaO, MgO, respectively. This shows that the stronger the electrostatic field of the cation, i.e., the larger its polarizing power, the greater the tightening of the oxygen octet. Therefore, if we consider the complex ions SiO_4^{4-}, PO_4^{3-}, $SO_4^=$, ClO_4^- to be formed from $O^=$ and the corresponding cations Si^{4+}, P^{5+}, S^{6+}, Cl^{7+} we must expect that refraction, dispersion, and size of the oxygen octet in the complex ions will diminish in the given order, which is that of increasing charge and slightly decreasing size of the small central ion of neon structure. Table I confirms this expectation.[16a] The decrease of refraction between SiO_4^{4-} and ClO_4^- per octet is 1.11 cc ~28 percent; the corresponding relative change of the linear dimension X−O (0.12~8 percent) is, as one would expect, about 3 times smaller. On the other hand, the decrease in molar dispersion between $SO_4^=$ and ClO_4^- is 0.014~22 percent, i.e., relatively about twice as large as the corresponding change in refraction of 0.37 cc ~11 percent.

TABLE I. Interatomic distance, refraction, and dispersion of the oxygen octet in the complex ions XO_4.

Central cation	Si^{4+}	P^{5+}	S^{6+}	Cl^{7+}
X−O in A*	1.60	1.55	1.51	(1.48)
$R_{O^=}$ in cc/mole**	4.42	4.05	3.68	3.31
$R_D - R_\infty$ in cc/mole***			0.071	0.057

* From Pauling (reference 2, p. 240). The selection of these distances from crystal structure data is not easy to make in view of the uncertainty of the parameter determination in many cases, and because of the influence of the surroundings on these values. The parallelism with the refractometric data indicates, however, that the selection made by Pauling is as satisfactory as possible.

** From K. Fajans and G. Joos, reference 4, p. 38. The value for the silicate ion is based on measurements of A. Heydweiller on $SiO_3^=$ in which the bonding cannot differ appreciably from that in SiO_4^{4-}. The values for $SO_4^=$ and ClO_4^- differ slightly from those in reference 4 according to newer measurements (see reference 8).

*** See reference 14.

This tightening effect, as in the case of the hydrogen halides, is the result of the drawing over of the electronic shell of the anion toward the positive charge of the cation and must, therefore, be accompanied by a diminution of the polarity of the X−O binding. Thus these complex ions represent, as do the hydrogen and silver halides, typical transition cases between the extremes of ideal ionic binding and completely unpolar binding (e.g., in H_2). In the case of ClO_4^-, in which the deformation of $O^=$ is strongest, the binding character is certainly very much nearer to the non-polar type. If one wishes to formulate these ions as covalent structures with both atoms having their octets completed, there is no objection to the Lewis formula,[16] which represents in the correct way the tetrahedral symmetry of these ions (see Introduction).

6. INSTABILITY OF ELECTRONIC SYSTEMS

It is noteworthy that the smallest polarity in the series of proton compounds as well as in the series of complex ions is found in HI and ClO_4^-, which are relatively unstable substances. Attachment of a proton or cations of heavy metals, which disturb the symmetry of ClO_4^-, leads to explosive properties. This recalls the case of cupric halides in which the deformation of the halide ions by the Cu^{++} and consequent decrease in polarity increases from the fluoride to the bromide, and leads ultimately to the instability of CuI_2.[17]

The generalization of this relation furnishes an understanding of the instability or non-

[14] N. Bauer, Dissertation, University of Michigan, 1941. The results will be published soon; they show that the relative change of dispersion (defined by $R_D - R_\infty$) caused by a given influence on the electronic system is about twice that for the refraction R_D.

[15] Obtained by subtraction of the values for the gaseous cations (see reference 10, p. 118) from those for the crystals (see reference 6b, p. 511).

[16a] The values of refraction and dispersion are based on measurements of dilute solutions, whereas strictly one should compare gaseous ions. However, a comparison of crystallized salts, e.g., of potassium sulfate and perchlorate (see P. Wulff and D. Schaller, Zeits. f. Krist. **A87**, 64 (1934)) shows the same gradation. This is understandable because in the case of such large anions with small polarizability, one would not expect strong hydration or lattice effects.

[16] The contrary conclusion was reached by Pauling (see Introduction) because the S−O distance in $SO_4^=$ is not the sum of his single bond radii for S and O. As will be explained in a future paper this deviation from additivity is to be expected from the point of view of the polarization theory without the assumption of double bonds.

[17] K. Fajans, Naturwiss. **11**, 165 (1923).

existence of certain other compounds. Thus one would expect that the polarizability of the anion of the element 85 would be considerably higher than that of I^-. The discoverers[18] of the radioactive species of this element report that it does not co-precipitate with AgI and behaves like a metallic element rather than as a halogen. One can express this fact from the above point of view by saying that the large deformability expected for the anion of ekaiodine leads to the instability of its salts.

In $CO_3^=$ the refraction per oxygen octet (4.08) is smaller than in the analogous $SiO_3^=$ (4.42) because the field of the small C^{4+} (helium type) is stronger than that of Si^{4+} (neon type). Thus by analogy one would expect $O^=$ in FO_4^-, FO_3^+, or FO_2^{3+} to be deformed by the very small F^{7+} still more strongly than by Cl^{7+} in ClO_4^-. None of these complex ions of fluorine exists; however, F_2O is a stable compound, which can be considered as formed by interaction within the grouping $F^-O^{2+}F^-$. One can interpret the imaginary reaction $2KFO_4 \rightarrow F_2O + K_2O + 3O_2$ as the result of the strong deformation of the oxygen ions by F^{7+}. Obviously this is only a way of formulating the fact that the electron affinity of fluorine is larger than that of oxygen. However, the advantage of the above point of view becomes evident when one tries to explain why ClO_4^- exists but BrO_4^- is unknown. The probable reason is that Br^{7+} has a non-rare gas structure and must have a much larger deforming power[19] than Cl^{7+}, as does Cu^+ compared with Na^+. The ion I^{7+}, which also is of the non-rare gas type but which must be considerably larger than Br^{7+}, combines with $O^=$ to form relatively stable periodates. From our point of view, this would mean that I^{7+} exerts a smaller influence on the oxygen octet than does Br^{7+}, for the same reason the Cl^{7+} has a smaller influence than has F^{7+}.

[18] D. R. Corson, K. R. MacKenzie, and E. Segrè, Phys. Rev. **58**, 672 (1940).

[19] K. Fajans, J. Chem. Phys. **9**, 281, 378 (1941).

JULY, 1942 JOURNAL OF CHEMICAL PHYSICS VOLUME 10

Polarization of Light Scattered by Isotropic Opalescent Media*

FRANCIS PERRIN
University of Paris, Paris, France, and Department of Chemistry, Columbia University, New York, New York

(Received March 23, 1942)

A general study is given of the polarization of light scattered by isotropic media whose elements of heterogeneity are not very small in comparison with the wave-length, (suspensions, colloidal solutions, solutions of large molecules, . . .). This includes an extension of a theory by R. S. Krishnan, who, considering certain particular states of polarization of the incident light and applying the law of reciprocity, had proved the equality of two of the four coefficients which are to be considered in these cases. Using Stokes' linear representation of the polarization of light beams, it is shown that the scattering through a given angle and for a given wave-length is characterized by the 16 coefficients of the linear forms which express the four polarization parameters of the scattered beam in terms of the four corresponding parameters of the incident beam and that the law of reciprocity leads to six relations between these sixteen coefficients. For an isotropic asymmetrical medium (having rotatory power), the scattering is thus characterized by *ten* independent coefficients. In the case of a symmetrical medium, four of these coefficients must be zero, leaving only *six* scattering coefficients, and if the scattering particles are spherical, there are two additional relations between these coefficients. The comparison with dipolar scattering by very small elements shows that the best test to prove multipolar scattering is the existence of some ellipticity in the scattered light when the incident beam is linearly polarized in a direction oblique to the scattering plane.

I

THE scattering of light by a macroscopically homogeneous medium is caused by some microscopical structure. If the dimensions of the elements of this structure are very small in comparison with the wave-length of the light, the scattering has the well-known simple characteristics of secondary dipolar emission.[17-20] But if

* Publication assisted by the Ernest Kempton Adams Fund for Physical Research of Columbia University.

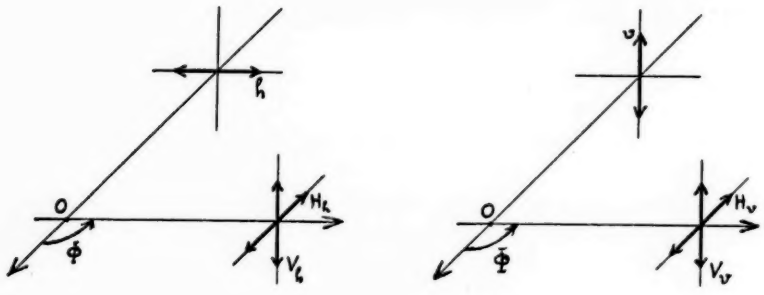

FIG. 1.

these elements have dimensions comparable to the wave-length, the phenomenon is more complicated, and has been experimentally studied only in particular conditions of excitation or observation, and theoretically only for spherical scattering particles.[7,21]

Our purpose is to extend a method used by R. S. Krishnan, and to point out the independent parameters which are necessary for specifying, in general, the intensity and polarization of the light scattered by any isotropic medium for given scattering angle and wave-length. A summary of this research has been read before the French Society of Physical Chemistry in May, 1939.[22]

We shall have to distinguish between *symmetrical* media, for which the center of any large spherical volume is a center of symmetry and any plane through this center a plane of symmetry, and the asymmetrical media, which usually have some optical rotatory power. The isotropy may be only statistical, as the result of an isotropic distribution of small anisotropic elements.

We shall see that for isotropic media, whose scattering elements are not very small compared with the wave-length, media which are more or or less turbid or opalescent, it is necessary to introduce several new parameters, whose values will contribute to the determination of the magnitude, shape, and optical properties of these elements. This method will be applicable in the study of smokes, fogs, suspensions, emulsions, colloidal solutions, solutions of large molecules, and also of media with widely extended fluctuations such as pure fluids, or liquid mixtures, near their critical state, glasses, etc.

My thanks are due to Dr. R. Wurmser with whom I had several discussions on these questions of scattering, which were the origin of this research.

II. THE RELATION OF R. S. KRISHNAN

In several papers published in 1938, R. S. Krishnan[1–5] has established theoretically, and has given the experimental verification of, a relation between the intensities of certain components of the light scattered by an isotropic symmetrical medium for some particular conditions of polarization of the incident light.

At a point of a horizontal light beam linearly polarized and of given intensity, he considered the scattering in a horizontal direction making an angle ϕ with the incident beam. He denoted by H_h and V_h the intensities of the horizontal and vertical vibrations of the scattered beam when the direction of vibration of the incident beam is horizontal, and by H_v and V_v these intensities when this direction is vertical (Fig. 1). He defined the corresponding depolarization factors of the scattered light by the ratios (generally smaller than 1)

$$\rho_h = V_h/H_h, \quad \rho_v = H_v/V_v. \tag{1}$$

The superposition without any phase relation, of the two considered incident beams, polarized at right angles and of the same intensity, gives an unpolarized incident beam to which corresponds a scattered beam whose horizontal and vertical intensities of vibration are $H_u = H_h + H_v$ and $V_u = V_h + V_v$. The depolarization factor of this scattered beam is defined by the ratio

$$\rho_u = H_u/V_u$$

and has thence the value

$$\rho_u = (H_h + H_v)/(V_h + V_v). \tag{2}$$

The measurements of the three depolarization

factors ρ_v, ρ_h, and ρ_u thus give the ratios of the four quantities H_h, V_h, H_v, V_v.

Using a general law of reciprocity due to Lord Rayleigh, R. S. Krishnan obtained the relation

$$H_v = V_h \tag{3}$$

for any symmetrical isotropic medium, and proved that this relation must be true also for a medium with only axial symmetry around the vertical direction perpendicular to the plane of scattering.[2]

This relation is verified in two particular cases already known: (1) For very small scattering particles (dipolar scattering) V_v, H_v, V_h are independent of ϕ, and (Lord Rayleigh)[6]

$$H_v = V_h,$$
$$H_h = V_v \cos^2\phi + H_v \sin^2\phi,$$

which gives for transverse scattering

$$H_v = V_h = H_h \quad \text{(dipoles, } \phi = \pi/2\text{)}. \tag{4}$$

(2) For spherical scattering particles of any dimension, and for all values of ϕ (G. Mie)[7]

$$H_v = V_h = 0 \quad \text{(spheres)}. \tag{5}$$

R. S. Krishnan gave, moreover, the experimental proof of Eq. (3) for various non-spherical large particles, for which the observed intensities H_v and V_h are always equal, but generally different from 0 and from H_h.

From the Eqs. (1), (2), and (3), the relation (6) results:

$$\rho_u = (1+1/\rho_h)/(1+1/\rho_v). \tag{6}$$

As a consequence of reciprocity it is thus unnecessary to measure the depolarization factor ρ_u for unpolarized excitation, if the depolarization factors ρ_h and ρ_v for horizontally and vertically polarized excitation have been measured.

Finally, in a paper published in November 1939, R. S. Krishnan[8] considered the case in which the direction of vibration of the linearly polarized incident beam makes an angle θ with the normal to the plane of scattering. Neglecting the correlation of phase which then exists between the horizontal and vertical components of vibration of the incident beam, he obtained for the ratio of the intensities of the horizontal and vertical components of vibration of the scattered light the equation,

$$\rho_\theta = H_\theta/V_\theta = (1+\mathrm{tg}^2\,\theta/\rho_h)/(\mathrm{tg}^2\,\theta+1/\rho_v). \tag{7}$$

This equation, though in agreement with the particular theoretical results of Lord Rayleigh (any small particles) and of G. Mie (large spheres) did not seem to him to be generally true, because of the arbitrariness of the hypothesis he had made to obtain it. He reported even a few measurements he had made of the scattering by large non-spherical particles showing some disagreement with it. However, we shall show that this equation must be valid for any symmetrical medium.

III. THE LAW OF RECIPROCITY IN OPTICS

In his book on the *Theory of Sound*, Lord Rayleigh established a theorem of reciprocity for the forces and displacements in the neighborhood of an equilibrium state of a mechanical system governed by linear equations.[9] Later on he extended to optics, without a new demonstration, the law of reciprocity; he merely indicated in a footnote the necessity of specifying the states of polarization.[10] R. S. Krishnan referred to this statement by Lord Rayleigh of the theorem of reciprocity to establish, in the case of light scattering, the relation we have given above. But the conditions he considered are particular, because he did not take into account the possible correlation of phases between the two components of vibration of each beam of light.

To apply the law of reciprocity to the most general phenomenon of scattering by an isotropic medium, it is necessary to start from a precise statement of this law.

Any monochromatic beam of light may be considered, in an infinite number of ways, as the superposition, with more or less phase correlation, of two completely polarized beams of complementary characters, for instance rectangular linear polarizations, or inverse circular polarizations. We shall choose as reference polarization states, for each direction of propagation, the states of linear polarization along two fixed rectangular axes.

Let us consider, given any system in which light can be scattered and absorbed, for an incident linearly polarized beam F_1 having an intensity I_1, coming from a linear polarizer N, a

particular emerging beam from which we may separate a linearly polarized component F'_1, having an intensity I'_1, by means of a linear polarizer N'. Let us associate with these beams the inverse beams, that is to say, an incident polarized beam F_2 coming from the polarizer N', with an intensity equal to I_1, in the direction opposite to that of the emerging beam F'_1, and the corresponding emerging beam F'_2 coming out of the polarizer N in the direction opposite to that of the incident beam F_1. The law of reciprocity states that the intensity I'_2 of this last beam F'_2 is equal to the intensity I'_1 of the beam F'_1: *If two incident polarized beams have equal intensities, the inverse emerging beams of the same polarization, which are associated with them, also have equal intensities.*

This law is true only if the considered optical system is not affected by a reversal of time, so that the sense of propagation of light be immaterial. There must be no movements, no electrical currents, no magnetic fields. To extend it to more general cases it is necessary to reverse, together with the direction of light propagation, all movements, electrical currents, and magnetic fields. For instance, it is well known that the law of reciprocity, as stated above, is not true for a system in which magnetic rotatory power comes into account, if the magnetic fields are not reversed with the sense of propagation of light.

Moreover, only monochromatic beams of the same frequency must be considered. At least it is necessary that the mechanisms which modify the frequency can be reversed with the propagation of light, as for instance a change of frequency caused by scattering by a moving body. The law of reciprocity is not valid for fluorescence or for Raman effect, in which the change of frequency is irreversible. In scattering phenomenon it is only relevant for Rayleigh scattering, with no or small symmetrical frequency changes.

It is also interesting to give the corpuscular statement of the law of reciprocity: If a photon associated with the incident polarized beam F_1 has a probability p to come out of the optical system associated with the polarized beam F'_1, then inversely, a photon associated with the beam F_2, reverse, to F'_1, has the same probability p to come out associated with the beam F'_2 reverse to F_1.

The law of reciprocity is thus seen to be connected with the general principle of quantum mechanics asserting the equal probability of inverse transitions between two states of the same energy.

IV. STOKES' LINEAR REPRESENTATION OF STATES OF POLARIZATION

Let us first consider a completely polarized monochromatic beam of light, whose electrical vibration may be represented by its components along two rectangular axes

$$\begin{aligned} E_x &= p_1 \cos(\omega t + \varphi_1), \\ E_y &= p_2 \cos(\omega t + \varphi_2), \end{aligned} \tag{8}$$

the amplitudes p_1, p_2, and the frequency $\omega/2\pi$ being positive. Let δ be the phase difference of these components

$$\delta = \varphi_1 - \varphi_2 \tag{9}$$

and I_e the total intensity of vibration

$$I_e = p_1^2 + p_2^2. \tag{10}$$

The terminal point of the oscillating vector **E** thus specified, describes, in the direct or reverse sense according to the positive or negative sign of $\sin\delta$, an ellipse with semi-axes a and b ($b \leqslant a$), whose major axis makes an angle α with the x axis. Let us set

$$\operatorname{tg}\beta = \pm b/a, \quad -\pi/4 \leqslant \beta \leqslant \pi/4, \tag{11}$$

taking the sign $+$ or $-$ according to the sense of rotation, i.e., so that always

$$\operatorname{tg}\beta \sin\delta > 0.$$

With such definitions, it is known that

$$\begin{aligned} p_1^2 - p_2^2 &= I_e \cos 2\beta \cos 2\alpha, \\ 2p_1p_2 \cos\delta &= I_e \cos 2\beta \sin 2\alpha, \\ 2p_1p_2 \sin\delta &= I_e \sin 2\beta. \end{aligned} \tag{12}$$

These three quantities, which we shall name M_e, C_e, S_e, determine the elliptic vibration (except its phase). In Poincaré's representation they are considered as the rectangular components of a vector in space, whose length is I_e, longitude 2α, and latitude 2β.

No actual light is strictly monochromatic. The amplitudes and phases of the components of any light vibration undergo slow variations without strict correlation. The ellipse of vibration, which

is still determined at each moment, changes its shape and magnitude, slowly in comparison with the period of vibration but extremely swiftly in comparison with the duration of any measurement. It is thus possible to measure only mean values.

The study of the polarization of a light beam requires the use of analyzers, each giving the mean intensity of a vibration E_a obtained as a linear combination, with given changes in phase, of the two components E_x and E_y of the initial vibration

$$E_a = c_1 p_1 \cos(\omega t + \varphi_1 + \eta_1) + c_2 p_2 \cos(\omega t + \varphi_2 + \eta_2). \quad (13)$$

This mean intensity has the value

$$\begin{aligned} I_a = {} & \tfrac{1}{2}(c_1^2 + c_2^2)(\langle p_1^2\rangle_{Av} + \langle p_2^2\rangle_{Av}) \\ & + \tfrac{1}{2}(c_1^2 - c_2^2)(\langle p_1^2\rangle_{Av} - \langle p_2^2\rangle_{Av}) \\ & + c_1 c_2 \cos(\eta_1 - \eta_2)\langle 2p_1 p_2 \cos\delta\rangle_{Av} \\ & - c_1 c_2 \sin(\eta_1 - \eta_2)\langle 2p_1 p_2 \sin\delta\rangle_{Av}, \end{aligned}$$

the notation $\langle\ \rangle_{Av}$ denoting the mean value with respect to time. By the use of four different (linearly independent) analyzers it is thus possible to calculate the quantities

$$\begin{aligned} I &= \langle p_1^2\rangle_{Av} + \langle p_2^2\rangle_{Av} = \langle I_e\rangle_{Av}, \\ M &= \langle p_1^2\rangle_{Av} - \langle p_2\rangle_{Av} = \langle M_e\rangle_{Av}, \\ C &= 2\langle p_1 p_2 \cos\delta\rangle_{Av} = \langle C_e\rangle_{Av}, \\ S &= 2\langle p_1 p_2 \sin\delta\rangle_{Av} = \langle S_e\rangle_{Av}, \end{aligned} \quad (14)$$

and if these four quantities are known, it is possible to calculate the intensity that will be measured with any analyzer corresponding to certain values of the coefficients c_1 and c_2 and of the phase shift $(\eta_1 - \eta_2)$. That is to say, the four quantities I, M, C, S give a complete description of the polarization properties of the light beam (Stokes).[11]

It is easy to prove that for any beam of light the parameters I, M, C, S, verify the inequality

$$I \geqslant (M^2 + C^2 + S^2)^{\frac{1}{2}}, \quad (15)$$

since the equality is true only for completely polarized light; and if four quantities satisfy this condition they may be considered the polarization parameters of a light beam.

Any light beam, having a partial polarization specified by the values I, M, C, S of the Stokes' parameters, may be considered as the superposition, without any phase correlation, of a beam of natural light having an intensity

$$I_N = I - (M^2 + C^2 + S^2)^{\frac{1}{2}} \quad (16)$$

and of a beam of completely polarized elliptic light having an intensity

$$I_E = (M^2 + C^2 + S^2)^{\frac{1}{2}} \quad (17)$$

and whose ellipse of vibration is defined by the angles α and β given by the relations

$$\begin{aligned} I_E \cos 2\beta \cos 2\alpha &= M, \\ I_E \cos 2\beta \sin 2\alpha &= C, \\ I_E \sin 2\beta &= S. \end{aligned} \quad (18)$$

The ratio

$$p = I_E / I = (M^2 + C^2 + S^2)^{\frac{1}{2}} / I, \quad (0 \leqslant p \leqslant 1) \quad (19)$$

is called the degree of polarization.

The essential property of the Stokes' parameters is their additivity in the superposition of two independent beams of light, i.e., without any correlation between the perturbations of their phases or amplitudes. This additivity corresponds to the absence of any interference.

When a beam of light passes through some optical arrangement, or more generally, produces a secondary beam of light, the intensity and the state of polarization of the emergent beam are functions of those of the incident beam. If two independent incident beams are superposed the new emergent beam will be, if the process is linear, the superposition without interference of the two emergent beams corresponding to the separate incident beams. Consequently, in such a linear process, from the additivity properties of the Stokes' parameters, the parameters I', M', C', S' which define the polarization of the emergent beam must be homogeneous linear functions of the parameters I, M, C, S corresponding to the incident beam; the sixteen coefficients of these linear functions will completely characterize the corresponding optical phenomenon. This fundamental remark is due in its general formulation to P. Soleillet.[12] We shall use it in the next section in the study of scattering. Let us give here only the linear transformation formulas of the Stokes' parameters in two simple cases which we shall have to consider:

When the light beam is rotated through an angle ψ around its direction of propagation, for instance by passing through a crystal plate with

simple rotatory power, we have

$$\begin{aligned} I' &= I, \\ M' &= M\cos 2\psi - C\sin 2\psi, \\ C' &= M\sin 2\psi + C\cos 2\psi, \\ S' &= S, \end{aligned} \tag{20}$$

and these equations also give the transformation of the Stokes' parameters when the reference axes are rotated through an angle $-\psi$.

When a difference in phase φ is introduced between the components of the vibration along the axes, for instance by a birefringent crystal plate with axes parallel to the reference axes (axes of maximum speed along Ox for $\varphi>0$), we have

$$\begin{aligned} I' &= I, \\ M' &= M, \\ C' &= C\cos\varphi - S\sin\varphi, \\ S' &= C\sin\varphi + S\cos\varphi. \end{aligned} \tag{21}$$

It is interesting to note how the method used by Stokes' to characterize a state of polarization may be generalized and connected with the wave statistics of J. von Neumann:[13] Let us consider a system of n harmonic oscillations of the same frequency subjected to small random perturbations; we may represent them by complex expressions

$$E_k = P_k \exp(i\omega t), \quad P_k = p_k \exp(i\varphi_k), \tag{22}$$

the modulus p_k and the arguments φ_k varying in course of time, slowly in comparison with the period of oscillation, but quickly in comparison with the duration of any measurement. Let us suppose that we can measure the mean intensity of an oscillation E linearly dependent on these oscillations

$$E = \sum_k C_k E_k, \quad C_k = c_k \exp(i\eta_k). \tag{23}$$

The value of this mean intensity is (the asterisk indicating the change to the complex conjugate quantity)

$$\langle EE^* \rangle_{Av} = \sum_{kl} C_k C_l^* \langle P_k P_l^* \rangle_{Av}. \tag{24}$$

The mean intensity depends on the particular oscillations involved only through the von Neumann's matrix

$$\Gamma_{kl} = \langle P_k P^*{}_l \rangle_{Av}, \tag{25}$$

the knowledge of which determines all we can know about these oscillations by such measurements. Since this matrix is hermitic, we can set

$$\Gamma_{kk} = \mu_k, \quad \Gamma_{kl} = \gamma_{kl} + i\sigma_{kl}, \quad (k \neq l) \tag{26}$$

μ_k, $\gamma_{kl}=\gamma_{lk}$, $\sigma_{kl}=-\sigma_{lk}$ being real quantities. The diagonal terms μ_k are the mean intensities of the oscillations:

$$\mu_k = \langle p_k^2 \rangle_{Av} \tag{27}$$

and the other terms give the correlations between the oscillations:

$$\begin{aligned} \gamma_{kl} &= \langle p_k p_l \cos(\varphi_k - \varphi_l) \rangle_{Av}, \\ \sigma_{kl} &= \langle p_k p_l \sin(\varphi_k - \varphi_l) \rangle_{Av}. \end{aligned} \tag{28}$$

The state of excitation of n oscillators having the same frequency is thus defined by n^2 real quantities. For instance, a vectorial vibration in space having three components must be defined by *nine* quantities (P. Soleillet),[12] and the possibilities of interference between two beams of light of the same frequency depend on *sixteen* parameters, since there are four components (two for each beam).

When the different oscillations are the components of an oscillating vector $\mathbf{P}\exp(i\omega t)$, the matrix Γ_{kl} has, for any change of the reference axes, the variance of a tensor of the second order, since its elements are the mean values of the products of the components of two vectors ($\mathbf{P}$ and $\mathbf{P}^*$).

It is easy to prove that the determinant of the matrix Γ_{kl} and all its diagonal minors are always positive or zero.

When the ratios of the P_k's are independent of time, the oscillation state of the system is said to be *pure* (complete polarization in the case of a light beam); all the diagonal minors of the matrix Γ_{kl} are then zero, and conversely. When it is not so, the state is said to be *mixed* (partial polarization). In general, any mixed state of oscillation of a system of n oscillators may be considered, in an infinite number of ways, as the superposition of n pure states without correlation (for a state to be equivalent to the superposition of less pure states, it is necessary that the determinant of the Γ_{kl} be zero).

Still more generally, it is possible, in a similar way, to find the quantities which will appear in the linear investigation of a non-harmonic system whose motion is described by n statistical func-

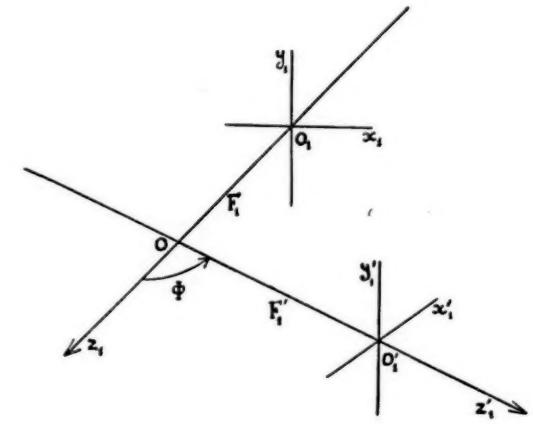

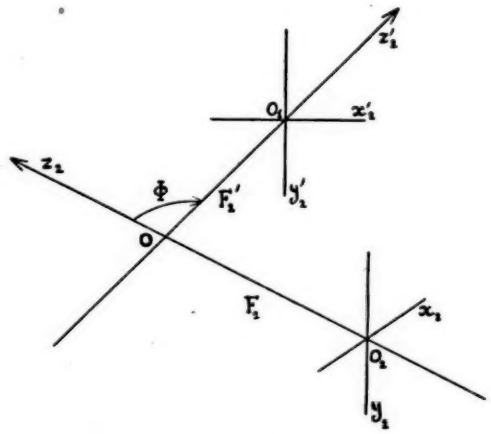

FIG. 2. (Above.) FIG. 3. (Below.)

tions of the time $E_k(t)$: These will be the *correlation functions* of M. Courtines[14] and J. Bernamont[15] defined by the relation

$$f_{kl}(\tau)=\langle E_k(t)E_l(t+\tau)\rangle_{Av}=f_{lk}(-\tau) \qquad (29)$$

or the functions corresponding to them by the Laplacian transformation

$$\Gamma_{kl}(\nu)=\int_{-\infty}^{+\infty} f_{kl}(\tau)\exp(-2\pi i\nu\tau)d\tau, \qquad (30)$$

which are the amplitudes of their representation by Fourier's integrals

$$f_{kl}(\tau)=\int_{-\infty}^{+\infty}\Gamma_{kl}(\nu)\exp(2\pi i\nu\tau)d\nu \qquad (31)$$

and verify the condition of hermiticity

$$\Gamma_{lk}(\nu)=\Gamma_{kl}(\nu)^*. \qquad (32)$$

It is thus seen that the state of motion of a system having n degrees of freedom is characterized, when linear methods of analysis are used, by n^2 continuous spectra giving, for each frequency, n spectral densities of intensity and $n(n-1)$ spectral densities of correlation.

V. THE SIXTEEN SCATTERING COEFFICIENTS OF AN ARBITRARY ISOTROPIC MEDIUM

If a monochromatic parallel beam of light F_1 is propagated along an axis O_1z_1, we consider the light scattered at a point O of this axis in a direction Oz'_1, making an angle ϕ (between 0 and π) with Oz_1. Let us specify the state of polarization of the incident beam F_1 by the values I_1, M_1, C_1, S_1 of its Stokes' parameters for the axes $O_1x_1y_1$, and that of the scattered beam F'_1 by the values I'_1, M'_1, C'_1, S'_1 of its Stokes' parameters for the axes $O'_1x'_1y'_1$. The two sets of rectangular axes $O_1x_1y_1z_1$ and $O'_1x'_1y'_1z'_1$ are right handed; the planes $O_1z_1x_1$ and $O'_1z'_1x'_1$ coincide; and the parallel axes O_1y_1 and $O'_1y'_1$ are orientated so that the rotation ϕ smaller than π which brings Oz_1 on Oz'_1 is positive around their common direction (Fig. 2).

We assume the linear character of light scattering for the superposition of non-coherent beams: If two independent light beams F and G which can be propagated along O_1z_1 give, when separate, the scattered beams F' and G' along Oz'_1, the scattered beam when the incident beams F and G are superposed without any phase relation, may be obtained by the superposition without phase relation of the two beams F' and G'. Since the Stokes' parameters are additive for the superposition of non-coherent beams, this requires that the quantities I'_1, M'_1, C'_1, S'_1 be linear homogeneous functions of the quantities I_1, M_1, C_1, S_1, i.e., that

$$\begin{aligned} I'_1&=a_{11}I_1+a_{12}M_1+a_{13}C_1+a_{14}S_1,\\ M'_1&=a_{21}I_1+a_{22}M_1+a_{23}C_1+a_{24}S_1,\\ C'_1&=a_{31}I_1+a_{32}M_1+a_{33}C_1+a_{34}S_1,\\ S'_1&=a_{41}I_1+a_{42}M_1+a_{43}C_1+a_{44}S_1. \end{aligned} \qquad (33)$$

If the scattering is produced by an isotropic medium, the sixteen *scattering coefficients* a_{ik} will

depend only, for a given medium, on the frequency of the light and on the scattering angle ϕ.

We shall see in the next sections that symmetry and reciprocity arguments prove that the number of independent scattering coefficients is actually less than sixteen.

VI. SYMMETRICAL MEDIUM

If the scattering medium is symmetrical, and consequently without any rotatory power, the plane of scattering $Oz_1z'_1$ determined by the directions of excitation and observation, is a plane of symmetry for the medium. Therefore, if the incident beam (I_1, M_1, C_1, S_1) is replaced by the symmetrical beam with respect to this plane, a beam whose parameters are (I_1, M_1, $-C_1$, $-S_1$), the new scattered beam must be symmetrical to the first scattered beam, and hence its parameters will be (I'_1, M'_1, $-C'_1$, $-S'_1$). In other words the relations (33) must hold if the sign of the parameters C_1, S_1, C'_1, S'_1 is changed whatever the values of I_1, M_1, C_1, S_1. This requires that for an isotropic symmetrical medium

$$a_{13}=a_{14}=a_{23}=a_{24}=a_{31}=a_{32}=a_{41}=a_{42}=0,$$

and consequently that for such a medium the relations (33) reduce to

$$\begin{aligned} I'_1&=a_{11}I_1+a_{12}M_1,\\ M'_1&=a_{21}I_1+a_{22}M_1,\\ C'_1&=a_{33}C_1+a_{34}S_1,\\ S'_1&=a_{43}C_1+a_{44}S_1. \end{aligned} \tag{33A}$$

For a symmetrical medium the number of scattering coefficients is only eight.

VII. RECIPROCITY

We must now apply the law of reciprocity, and for this purpose consider an incident beam being propagated along the axis Oz_2 opposite to the direction Oz'_1 of the first scattered beam, and the corresponding scattered beam F'_2 in the direction Oz'_2 opposite to the direction Oz_1 of the first incident beam (Fig. 3). We shall take as reference axes for the states of polarization of these new beams two sets of axes having, with respect to F_2 and F'_2 the same orientation as the axes previously used with respect to F_1 and F'_1: For beam F_2 the axis O_2x_2 in coincidence with $O'_1x'_1$ and the axis O_2y_2 opposite to $O'_1y'_1$, for beam F'_2 the axis $O'_2x'_2$ in coincidence with O_1x_1 and the axis $O'_2y'_2$ opposite to O_1y_1. With these reference axes the Stokes' parameters I'_2, M'_2, C'_2, S'_2 of the scattered beam F'_2 will be expressed as linear functions of the parameters I_2, M_2, C_2, S_2 of the incident beam F_2 by relations identical to the relations (33):

$$\begin{aligned} I'_2&=a_{11}I_2+a_{12}M_2+a_{13}C_2+a_{14}S_2,\\ M'_2&=a_{21}I_2+a_{22}M_2+a_{23}C_2+a_{24}S_2,\\ C'_2&=a_{31}I_2+a_{32}M_2+a_{33}C_2+a_{34}S_2,\\ S'_2&=a_{41}I_2+a_{42}M_2+a_{43}C_2+a_{44}S_2. \end{aligned} \tag{34}$$

The coefficients a_{ik} have the same values, since the scattering angle has the same value ϕ and since the medium is supposed to be isotropic.*

To be able to express reciprocity, we must introduce on the paths of the incident and scattered beams some polarizers transforming an initial beam having a fixed linear polarization into an incident beam of any elliptical polarization, and any component of the scattered beam into a final beam having, like the initial beam a fixed linear polarization.

For this purpose we may introduce on the path of the incident beam F_1: (1) a linear polarizer N with fixed orientation such that the electrical vibration of the light emerging from it is along O_1x_1, this light having thus the Stokes' parameters (1, 1, 0, 0) if its intensity is unity; (2) a crystal plate R with rotatory power turning the light vibration through an angle ψ; according to formulas (20) the Stokes' parameters of the beam after this plate will be (1, cos 2ψ, sin 2ψ, 0); (3) a birefringent crystal plate B with its axes parallel to the reference axes $O_1x_1y_1$ and producing a change in phase φ between the vibrations along O_1x_1 and O_1y_1. The incident beam thus obtained may have any complete elliptical polarization; its Stokes' parameters will be, according to Eq. (21),

$$\begin{aligned} I_1&=1,\\ M_1&=\cos 2\psi,\\ C_1&=\sin 2\psi\cos\varphi,\\ S_1&=\sin 2\psi\sin\varphi. \end{aligned} \tag{35}$$

* It is even sufficient that the direction Oz_1 and Oz_2 be equivalent in the scattering medium, which might, for instance, have only axial symmetry around the perpendicular Oy to the scattering plane.

Similarly, on the path of the scattered beam F'_1 whose Stokes' parameters I'_1, M'_1, C'_1, S'_1 will be obtained by relations (33) in which I_1, M_1, C_1, S_1 have the values given by (35), we shall introduce: (1) a birefringent crystal plate B' with its axes parallel to the axes $O'_1x'_1y'_1$ and producing a change in phase φ' between the vibrations along $O'_1x'_1$ and $O'_1y'_1$; after this plate the Stokes' parameters of the beam will be (Eq. 21)

$$\begin{aligned} &I'_1,\\ &M'_1,\\ &C'_1\cos\varphi'-S'_1\sin\varphi',\\ &C'_1\sin\varphi'+S'_1\cos\varphi';\end{aligned}$$

(2) a crystal plate R' with rotatory power turning the light vibration through an angle ψ'; after this plate the Stokes' parameters will become (Eq. 20)

$$\begin{aligned} &I'_1,\\ &M'_1\cos 2\psi'-(C'_1\cos\varphi'-S'_1\sin\varphi')\sin 2\psi',\\ &M'_1\sin 2\psi'+(C'_1\cos\varphi'-S'_1\sin\varphi')\cos 2\psi',\\ &C'_1\sin\varphi'+S'_1\cos\varphi';\end{aligned}$$

(3) a linear polarizer N' with fixed orientation selecting the electrical vibration along $O'_1x'_1$. The intensity J_1 of the light coming out of this polarizer will be equal to half the sum of the first two Stokes' parameters of the light entering it; thus

$$J_1=\tfrac{1}{2}[I'_1+M'_1\cos 2\psi'-C'_1\sin 2\psi'\cos\varphi'+S'_1\sin 2\psi'\sin\varphi']. \quad (36)$$

Let us consider now the light being propagated in the reverse direction through this arrangement, when the intensity of the beam F_2 coming out of the polarizer N' toward the scattering medium has an intensity equal to unity. The values of the Stokes' parameters are then for this beam (1, 1, 0, 0) and after the plates R' and B' they will be

$$\begin{aligned} &I_2=1,\\ &M_2=\cos 2\psi',\\ &C_2=\sin 2\psi'\cos\varphi',\\ &S_2=\sin 2\psi'\sin\varphi'.\end{aligned} \quad (37)$$

The parameters I'_2, M'_2, C'_2, S'_2 of the corresponding scattered beam will be given by Eq. (34) I_2, M_2, C_2, S_2 having the values (37), and the intensity of the light coming out of the arrangement through the polarizer N, obtained as for the first scattered beam, will be

$$J_2=\tfrac{1}{2}[I'_2+M'_2\cos 2\psi-C'_2\sin 2\psi\cos\varphi+S'_2\sin 2\psi\sin\varphi]. \quad (38)$$

Since the incident beams F_1 and F_2 have the same intensity, and the initial and final states of polarization are the same complete linear polarization, the intensities J_1 and J_2 of the emergent beams must be equal, according to the law of reciprocity, whatever crystal plates are introduced in the path of the light.

We have, consequently,

$$\begin{aligned} I'_1+M'_1\cos 2\psi'-C'_1\sin 2\psi'\cos\varphi'&\\ +S_1'\sin 2\psi'\sin\varphi'=I'_2+M'_2\cos 2\psi&\\ -C'_2\sin 2\psi\cos\varphi+S'_2\sin 2\psi\sin\varphi,&\end{aligned} \quad (39)$$

whatever the values of the angles ψ, φ, ψ', φ'. Using Eqs. (33), (34), (35), and (37), we obtain

$$\begin{aligned} &(a_{12}-a_{21})(\cos 2\psi-\cos 2\psi')\\ &+(a_{13}+a_{31})(\sin 2\psi\cos\varphi-\sin 2\psi'\cos\varphi')\\ &+(a_{14}-a_{41})(\sin 2\psi\sin\varphi-\sin 2\psi'\sin\varphi')\\ &+(a_{23}+a_{32})(\sin 2\psi\cos\varphi\cos 2\psi'\\ &\qquad-\sin 2\psi'\cos\varphi'\cos 2\psi)\\ &+(a_{24}-a_{42})(\sin 2\psi\sin\varphi\cos 2\psi'\\ &\qquad-\sin 2\psi'\sin\varphi'\cos 2\psi)\\ &-(a_{34}+a_{43})\sin(\varphi-\varphi')\sin 2\psi\sin 2\psi'=0. \end{aligned} \quad (40)$$

This identity can be maintained only if all the coefficients of the trigonometrical expressions in it are zero: For $\psi=0$, $\psi'=\pi/2$ it reduces to

$$a_{12}-a_{21}=0; \quad (41)$$

for $\psi=-\psi'=\pi/4$, $\varphi=\varphi'=0$, to

$$a_{13}+a_{31}=0; \quad (42)$$

for $\psi=-\psi'=\pi/4$, $\varphi=\varphi'=\pi/2$, to

$$a_{14}-a_{41}=0. \quad (43)$$

After the suppression of the three first terms in the identity (40), as a consequence of the zero value of their coefficients, the new identity obtained reduces, for $\psi=\pi/4$, $\psi'=\varphi=\varphi'=0$ to

$$a_{23}+a_{32}=0; \quad (44)$$

for $\psi=\pi/4$, $\psi'=0$, $\varphi=\varphi'=\pi/2$, to

$$a_{24}-a_{42}=0; \quad (45)$$

and for $\psi=\psi'=\pi/4$, $\varphi=\pi/2$, $\varphi'=0$, to

$$a_{34}+a_{43}=0. \quad (46)$$

The sixteen scattering coefficients must therefore obey six conditions of symmetry or antisymmetry, and the linear relations which give the Stokes' parameters of the scattered beam in terms of those of the incident beam, may be written

$$\begin{aligned} I' &= a_1 I + b_1 M - b_3 C + b_5 S, \\ M' &= b_1 I + a_2 M - b_4 C + b_6 S, \\ C' &= b_3 I + b_4 M + a_3 C + b_2 S, \\ S' &= b_5 I + b_6 M - b_2 C + a_4 S. \end{aligned} \tag{47}$$

The scattering of light, through a given angle, by an asymmetrical isotropic medium is characterized by ten independent coefficients.

If the scattering medium is symmetrical, and has therefore no rotatory power, the coefficients b_3, b_4, b_5, b_6 are necessarily zero, since in this case the relations (47) must have the form of the relations (33A), and the linear relations between the Stokes' parameters are reduced to

$$\begin{aligned} I' &= a_1 I + b_1 M, \\ M' &= b_1 I + a_2 M, \\ C' &= a_3 C + b_2 S, \\ S' &= -b_2 C + a_4 S. \end{aligned} \tag{47A}$$

The scattering of light, through a given angle, by a symmetrical isotropic medium is characterized by six independent coefficients.

R. S. Krishnan in his publications dated 1938[1–5] considered only incident beams with linear polarization either horizontal ($I=1$, $M=1$, $C=S=0$) or vertical ($I=1$, $M=-1$, $C=S=0$). These excitation conditions involve only the four coefficients a_{11}, a_{12}, a_{21}, a_{22}, and the relation obtained by him $H_v = V_h$ is equivalent to the first relation proved here $a_{12}=a_{21}$.

In the more general case considered in his paper of 1939, the incident beam has a linear polarization in a direction making an angle θ with the perpendicular to the scattering plane. The Stokes' parameters of the incident beam are then

$$I=1, \quad M=-2\cos 2\theta, \quad C=\sin 2\theta, \quad S=0$$

and, applying Eq. (47) we obtain

$$\rho_\theta = \frac{H_\theta}{V_\theta} = \frac{I'+M'}{I'-M'} = \frac{a_1+b_1(1-\cos 2\theta)-a_2\cos 2\theta-(b_3+b_4)\sin 2\theta}{a_1-b_1(1+\cos 2\theta)+a_2\cos 2\theta-(b_3-b_4)\sin 2\theta}.$$

When θ is 0 or $\pi/2$ this formula gives

$$\rho_v = \frac{H_v}{V_v} = \frac{a_1-a_2}{a_1+2b_1+a_2}, \quad \rho_h = \frac{V_h}{H_h} = \frac{a_1-a_2}{a_1-2b_1+a_2},$$

which shows that the expression of ρ_θ may be written

$$\rho_\theta = \frac{1+\mathrm{tg}^2\,\theta/\rho_h-2(b_3+b_4)(a_1-a_2)^{-1}\,\mathrm{tg}\,\theta}{\mathrm{tg}^2\,\theta+1/\rho_v-2(b_3-b_4)(a_1-a_2)^{-1}\,\mathrm{tg}\,\theta}.$$

This proves that Eq. (7) proposed with some doubt by R. S. Krishnan, must be true for any symmetrical medium, since then $b_3=b_4=0$ but not for an asymmetrical medium.

VIII. FORWARD AXIAL SCATTERING

The light scattered in the same direction as the incident beam cannot be distinguished from the remaining light of this beam. However, if the incident beam has a small aperture ω, it is possible to define, as a limit when $\omega\to 0$, a transmitted beam T, with axis Oz_1 and aperture ω, and a scattered beam including all rays between two cones of apertures η ($\eta>\omega$) and $\eta+d\eta$, having also Oz_1 as axis. The scattered beam F'_0 thus defined may vary with the small angle η, but whatever this angle, it will have axial symmetry around Oz_1.

The law of reciprocity applies to the transmitted beam T as well as to the axially scattered beam F'_0. If reference axes parallel to those chosen for the incident beam are used for the polarization states of these beams, the linear relations between Stokes' parameters will have in both cases, the form obtained above. Writing them for beam F'_0, we will indicate the zero value of the scattering angle ϕ by marking the coefficients with a superscript 0

$$\begin{aligned} I' &= a_1^0 I + b_1^0 M - b_3^0 C + b_5^0 S, \\ M' &= b_1^0 I + a_2^0 M - b_4^0 C + b_6^0 S, \\ C' &= b_3^0 I + b_4^0 M + a_3^0 C + b_2^0 S, \\ S' &= b_5^0 I + b_6^0 M - b_2^0 C + a_4^0 S. \end{aligned} \tag{48}$$

In this case we must also express the axial symmetry around the common direction of the incident and scattered beams: If the incident beam is turned around itself through any angle, the axially scattered beam F'_0 will simply turn around itself through the same angle. It is sufficient to consider an infinitesimal rotation

$\frac{1}{2}d\alpha$ which changes the beam (I, M, C, S) into a beam F_1 with parameters

$$\begin{aligned} I_1&=I,\\ M_1&=M-Cd\alpha,\\ C_1&=Md\alpha+C,\\ S_1&=S, \end{aligned} \tag{49}$$

and the beam $F'_0(I', M', C', S')$ into a beam F'_{01} with the parameters

$$\begin{aligned} I'_1&=I',\\ M'_1&=M'-C'd\alpha,\\ C'_1&=M'd\alpha+C',\\ S'_1&=S'. \end{aligned} \tag{50}$$

The parameters I'_1, M'_1, C'_1, S'_1 must be expressed in terms of I_1, M_1, C_1, S_1 by the relations identical to relations (48). Eliminating I, M, C, S and I', M', C', S' between the relations (48), (49), and (50), we obtain

$$\begin{aligned} I'_1&=a_1{}^0I_1+(b_1{}^0+b_3{}^0d\alpha)M_1\\ &\quad-(b_3{}^0-b_1{}^0d\alpha)C_1+b_5{}^0S_1,\\ M'_1&=(b_1{}^0-b_3{}^0d\alpha)I_1+a_2{}^0M_1\\ &\quad-[b_4{}^0+(a_3{}^0-a_2{}^0)d\alpha]C_1\\ &\quad+(b_6{}^0-b_2{}^0d\alpha)S_1,\\ C'_1&=(b_3{}^0+b_1{}^0d\alpha)I_1+(b_4{}^0-(a_3{}^0-a_2{}^0)d\alpha]M_1\\ &\quad+a_3{}^0C_1+(b_2{}^0+b_6{}^0d\alpha)S_1,\\ S_1'&=b_5{}^0I_1+(b_6{}^0+b_2{}^0d\alpha)M_1\\ &\quad-(b_2{}^0-b_6{}^0d\alpha)C_1+a_4{}^0S_1. \end{aligned} \tag{51}$$

So that this linear system be identical with system (48) it is necessary and sufficient that

$$b_1{}^0=b_2{}^0=b_3{}^0=b_6{}^0=0, \quad a_2{}^0=a_3{}^0.$$

The linear transformation for the Stokes' parameter is thus, for axial scattering:

$$\begin{aligned} I'&=a_1{}^0I+b_5{}^0S,\\ M'&=a_2{}^0M-b_4{}^0C,\\ C'&=b_4{}^0M+a_2{}^0C,\\ S'&=b_5{}^0I+a_4{}^0S. \end{aligned} \tag{53}$$

These equations apply to any asymmetrical medium. They show that forward axial scattering involves in general *five* independent coefficients.

For a symmetrical medium $b_4{}^0$ and $b_5{}^0$ are necessarily zero; therefore, the linear transformation is reduced to

$$\begin{aligned} I'&=a_1{}^0I,\\ M'&=a_2{}^0M,\\ C'&=a_2{}^0C,\\ S'&=a_4{}^0S. \end{aligned} \tag{53A}$$

The forward axial scattering involves in this case only *three* independent coefficients.

For the transmitted beam T the linear transformation will have also the form (53) or (53A) but with other values of the coefficients, which will in this case correspond to simple classical properties: The quantity

$$1-a_1{}^0$$

will measure the absorption for natural light; the quantity

$$b_4{}^0 : a_2{}^0$$

the tangent of the rotation (rotatory power); the quantity

$$1-(a_2{}^{02}+b_4{}^{02}+b_5{}^{02})^{\frac{1}{2}} : a_1{}^0$$

the depolarization for linear light; the quantity

$$1-a_4{}^0 : a_1{}^0$$

the depolarization for circular light; and the quantity

$$b_5{}^0 : a_1{}^0$$

the circular dichroism.

IX. BACKWARD AXIAL SCATTERING

A similar argument may be applied to the scattering in the direction opposite to that of the incident beam, since there is also in this case axial symmetry. But then any rotation of the incident beam around its direction must produce an *inverse* rotation of the same magnitude of the scattered beam around its direction.

Marking with a superscript π the coefficients of the linear transformation (47) for the value $\phi=\pi$ which correspond to backward scattering, the invariance for an infinitesimal rotation leads to the conditions

$$b_1{}^\pi=b_2{}^\pi=b_3{}^\pi=b_4{}^\pi=b_6{}^\pi=0, \quad a_2{}^\pi=-a_3{}^\pi \tag{54}$$

and the linear transformation is

$$\begin{aligned} I'&=a_1{}^\pi I+b_5{}^\pi S,\\ M'&=a_2{}^\pi M,\\ C'&=-a_2{}^\pi C,\\ S'&=b_5{}^\pi I+a_4{}^\pi S. \end{aligned} \tag{55}$$

The backward scattering by an asymmetrical medium involves only *four* independent coefficients.

For a symmetrical medium b_5^π must be zero, so that the linear transformation is

$$\begin{aligned} I' &= a_1^\pi I, \\ M' &= a_2^\pi M, \\ C' &= -a_2^\pi C, \\ S' &= a_4^\pi S. \end{aligned} \tag{55A}$$

The backward scattering involves then *three* independent coefficients, like the forward scattering.

X. SCATTERING BY PARTICLES HAVING SPHERICAL SYMMETRY

When the incident light is completely polarized, the light scattered by one particle of any shape is completely polarized. Any depolarization of the light scattered by an isotropic distribution of similar particles is the result of the difference in polarization of light waves scattered by particles of different orientation; but if the scattering is caused by identical particles having spherical symmetry, the polarization will be the same for all the partial waves, and there will be no depolarization, if we suppose the emulsion sufficiently diluted, so that double scattering be negligible.

Thus, for such a diluted emulsion of identical spherical particles, whenever the incident light is completely polarized, the scattered light must be also completely polarized; consequently, whenever the Stokes' parameters of the incident beam verify the condition

$$I^2-M^2-C^2-S^2=0$$

the Stokes' parameters of the scattered beam must verify the similar condition

$$I'^2-M'^2-C'^2-S'^2=0.$$

In other words, the linear transformation (47) on the Stokes' parameters must correspond in this case to a rotation and a similarity in a Minkowsky four-dimensional space. Expressing this we obtain the relations

$$\begin{aligned} a_1b_1-a_2b_1-b_3b_4-b_5b_6&=0, \\ -a_1b_3+b_1b_4-a_3b_3+b_2b_5&=0, \\ a_1b_5-b_1b_6-b_2b_3-a_4b_5&=0, \\ -b_1b_3+a_2b_4-a_3b_4+b_2b_6&=0, \\ b_1b_5-a_2b_6-b_2b_4-a_4b_6&=0, \\ -b_3b_5+b_4b_6-a_3b_2+a_4b_2&=0, \end{aligned} \tag{56}$$

and

$$\begin{aligned} a_1^2&=a_2^2+b_3^2+b_4^2+b_5^2+b_6^2, \\ a_1^2&=a_3^2+b_1^2+b_2^2+b_4^2+b_5^2, \\ a_1^2&=a_4^2+b_1^2+b_2^2+b_3^2+b_6^2. \end{aligned} \tag{57}$$

The three relations (57) are a consequence of the six relations (56), which are linear with respect to the four quantities a_1, a_2, a_3, a_4 and are coherent if *

$$b_2b_3b_4+b_2b_5b_6+b_1b_4b_6-b_1b_3b_5=0. \tag{58}$$

They give then

$$\begin{aligned} 2a_1&=\frac{b_3b_4+b_5b_6}{b_1}+\frac{b_2b_5+b_1b_4}{b_3}+\frac{b_2b_3+b_1b_6}{b_5}, \\ 2a_2&=-\frac{b_3b_4+b_5b_6}{b_1}+\frac{b_2b_5+b_1b_4}{b_3}+\frac{b_2b_3+b_1b_6}{b_5}, \\ 2a_3&=-\frac{b_3b_4+b_5b_6}{b_1}+\frac{b_2b_5+b_1b_4}{b_3}-\frac{b_2b_3+b_1b_6}{b_5}, \\ 2a_4&=\frac{b_3b_4+b_5b_6}{b_1}+\frac{b_2b_5+b_1b_4}{b_3}-\frac{b_2b_3+b_1b_6}{b_5}, \end{aligned} \tag{59}$$

from which follows a linear relation between the a's

$$a_1-a_2+a_3-a_4=0. \tag{60}$$

There are thus only five independent parameters in the scattering by identical spherical particles without mirror symmetry.

In the case of an emulsion containing spherical particles differing in magnitude or optical properties, each scattering coefficient will be the sum of the corresponding coefficients for the various types of spherical particles in the mixture. The only relation between the scattering coefficients which will hold after this adding process, will be the linear relation (60), which is thus characteristic of scattering by any mixture of spherical particles without mirror symmetry.

For identical spherical particles with mirror symmetry we must have $b_3=b_4=b_5=b_6=0$ and the general solution of Eqs. (56), (57) gives

$$a_1=a_2, \quad a_3=a_4 \tag{60A}$$

and

$$a_1^2=a_3^2+b_1^2+b_2^2. \tag{61}$$

The two relations (60A) being linear will remain true for a mixture of different spherical particles

* It is also possible to solve the Eqs. (56) when the b's obey the two conditions

$$b_1b_2=b_3b_6=b_4b_5,$$

but the singular solutions then obtained do not correspond to scattering by spherical particles.

with mirror symmetry: There are then four independent scattering coefficients.

The first of the relations (60A) is equivalent to the relation $H_v = V_h = 0$ resulting, in the case of homogeneous symmetrical spheres, from the theory of G. Mie.[7]

XI. COMPARISON WITH DIPOLAR SCATTERING

The general polarization properties of dipolar secondary light emission have been determined by P. Soleillet.[12] His theory results in the fact that the linear relations between the Stokes' parameters of the incident and scattered beams, must be in the case of dipolar scattering

$$\begin{aligned} I' &= (a - b\sin^2\phi)I - b\sin^2\phi M, \\ M' &= -b\sin^2\phi I + b(1+\cos^2\phi)M, \\ C' &= 2b\cos\phi C, \\ S' &= 2c\cos\phi S, \end{aligned} \tag{62}$$

in which a, b, c are independent of the angle of scattering ϕ. There is then no distinction between symmetrical and asymmetrical media.

For any angle of scattering, dipolar scattering is qualitatively characterized by the condition

$$b_2 = 0, \tag{63}$$

which expresses the non-existence of any ellipticity in the scattered light when there is no ellipticity in the polarization of the incident light ($S' = 0$ when $S = 0$).

For transverse dipolar scattering ($\phi = \pi/2$) we have, moreover,

$$a_3(\pi/2) = a_4(\pi/2) = 0 \tag{64}$$

and

$$b_1(\pi/2) + a_2(\pi/2) = 0, \tag{65}$$

which proves that whatever the polarization of the incident light, there is then neither obliquity of polarization ($C' = 0$) nor ellipticity ($S' = 0$), and that for an incident beam polarized in the plane of scattering ($I = M$, $C = S = 0$) the scattered light is not at all polarized ($M' = C' = S' = 0$).

This last test was used by R. S. Krishnan to prove the multipolar character of light scattering by some media, particularly by liquid mixtures in the neighborhood of the critical state. But this proof has been criticized,[16, 23] because convergence in the incident beam or secondary scattering is, at least qualitatively, a possible cause of the observed polarizations.

The existence of some ellipticity in the scattered light for an incident beam linearly obliquely polarized ($C \neq 0$, $S = 0$) which would prove that the coefficient b_2 is not zero, would be a much more sure test of the multipolar character of the scattering, and consequently, of the non-negligible magnitude, in comparison with the wave-length, of the elements of heterogeneity of the scattering medium.

LITERATURE

(1) R. S. Krishnan, Proc. Ind. Acad. Sci. **fA**, 21 (1938).
(2) R. S. Krishnan, Proc. Ind. Acad. Sci. **fA**, 91 (1938).
(3) R. S. Krishnan, Proc. Ind. Acad. Sci. **fA**, 98 (1938).
(4) R. S. Krishnan, Kolloid. Zeits. **84**, 2 (1938).
(5) R. S. Krishnan, Kolloid. Zeits. **84**, 18 (1938).
(6) Lord Rayleigh, Phil. Mag. **35**, 373 (1918).
(7) G. Mie, Ann. d. Physik **25**, 377 (1908).
(8) R. S. Krishnan, Proc. Ind. Acad. Sci. **A10**, 395 (1939).
(9) Lord Rayleigh, *Theory of Sound* (edition 1877). volume 1, §109, p. 93.
(10) Lord Rayleigh, Phil. Mag. **49**, 324 (1900).
(11) G. G. Stokes, Trans. Camb. Phil. Soc. **9**, 399 (1852).
(12) P. Soleillet, Ann. de physique **12**, 23 (1929).
(13) J. von Neumann, *Mathematische Grundlagen der Quantenmechanik* (Berlin, 1932).
(14) M. Courtines, Congrès international d'Électricité **2**, 545 (Paris, 1932).
(15) J. Bernamont, Ann. de physique **7**, 71 (1937).
(16) B. K. Mookerjee, Ind. J. Phys. **12**, 15 (1938).
(17) Lord Rayleigh, Phil. Mag. **47**, 375 (1899).
(18) R. Gans, Ann. d. Physik **37**, 881 (1912).
(19) R. Gans, Ann. d. Physik **62**, 331 (1920).
(20) Y. Rocard, Ann. de physique **10**, 116 (1928).
(21) Lord Rayleigh, Proc. Roy. Soc. **A84**, 25 (1910).
(22) Francis Perrin, J. de Chimie physique **36**, 234 (1939).
(23) S. Parthsarathy, Phil. Mag. **29**, 148 (1940).
(24) R. S. Krishnan, Phil. Mag. **29**, 515 (1940).

Energy Levels and Thermodynamic Functions for Molecules with Internal Rotation

I. Rigid Frame with Attached Tops

KENNETH S. PITZER AND WILLIAM D. GWINN
Department of Chemistry, University of California, Berkeley, California

(Received April 18, 1942)

A general treatment of internal rotation is given for molecules whose moments of inertia for over-all rotation are independent of internal rotational coordinates. Tables are presented for the various thermodynamic functions which are accurate for molecules with one internal rotation and for the potential energy $(V/2)(1-\cos n\phi)$. The tables are shown to be a good approximation for molecules with several internal rotational coordinates, provided the potential energy can be expressed as a sum of terms of this type. Methods are suggested for treating problems where cross terms involving more than one internal coordinate are present in the potential energy. The energy level expressions are developed for the more general case with the potential energy expressed by a Fourier series. Although a few specific cases were worked out with different shape potential barriers, it appears that the simple form assumed above will be satisfactory for many purposes.

ALTHOUGH a number of papers have already been published concerning the energy levels and thermodynamic functions of internal rotational degrees of freedom,[1–11] all of them have either treated highly specialized cases or have made approximations which need further examination. The treatment that follows applies to any molecule which can be regarded as a rigid frame with attached symmetrical tops; or in other words, any molecule whose moments of inertia for over-all rotation are independent of the coordinates of internal rotation.[12] (For example, *iso*butane and acetone fall within this class while *n*-butane and sym. dichloroethane do not.) Furthermore, in the present treatment all approximations that are made for convenience or necessity in calculation will be carefully examined and their range of validity defined.

In comparison with previous work it may be stated that the tables published by one of us[7] are probably a satisfactory approximation for the cases to which they have been applied. The formulas developed by Crawford[9] and recommended by Wilson[8b] as more accurate than these tables are actually less accurate insofar as the two differ significantly. The present results reduce exactly to those of Koehler and Dennison[10] who considered the special case of methyl alcohol.

The only formula which appears to be sufficiently general and useful to justify tabulation of the results for the full range of the variables leads to the same tables that were published previously. These have been recalculated, however, and now have an accuracy far beyond that of the present experimental thermodynamic data. (See Tables I–VI.)

THERMODYNAMIC RESULTS FOR THE SIMPLER CASES

We shall first present the thermodynamic results in the simple form which is accurate for all molecules with one symmetrical top and for the simple potential barrier $\frac{1}{2}V(1-\cos n\phi)$. In many cases this will be quite accurate for molecules with several tops. The proof, methods of computing the tables, and the more general formulas

[1] H. H. Nielsen, Phys. Rev. **40**, 445 (1932).
[2] J. E. Mayer, S. Brunauer, and M. G. Mayer, J. Am. Chem. Soc. **55**, 37 (1933).
[3] E. Teller and K. Weigert, Nachr. Ges. Wiss. Göttingen, Math. physik. Klasse, 218 (1933).
[4] L. J. B. La Coste, Phys. Rev. **46**, 718 (1934).
[5] M. L. Edinoff and J. G. Aston, J. Chem. Phys. **3**, 379 (1935).
[6] L. S. Kassel, J. Chem. Phys. (a) **3**, 115 (1935); (b) **3**, 326 (1935); (c) **4**, 276 (1936); (d) **4**, 435 (1936).
[7] K. S. Pitzer, J. Chem. Phys. **5**, 469 (1937).
[8] E. B. Wilson, Jr., (a) J. Chem. Phys. **6**, 740 (1938); (b) Chem. Rev. **27**, 17 (1940).
[9] B. L. Crawford, Jr., J. Chem. Phys. **8**, 273 (1940).
[10] J. S. Koehler and D. M. Dennison, Phys. Rev. **57**, 1006 (1940).
[11] D. Price, J. Chem. Phys. **9**, 807 (1941).
[12] It was originally planned to present at this time a second paper dealing with molecules not falling within this class. The pressure of other work makes this impossible. Two methods applicable to different types of molecules may be mentioned, however. For relatively heavy molecules the method used by one of us for the *n*-paraffin series is applicable (K. S. Pitzer, J. Chem. Phys. **8**, 711 (1940)). If the moments of inertia for over-all rotation change only slightly with internal rotation, the methods of this paper offer a satisfactory approximation.

TABLE I. Free energy, $-F/T$ (cal. per degree mole).

V/RT \ $1/Q_f$	0.25	0.30	0.35	0.40	0.45	0.50	0.55	0.60	0.65	0.70	0.75	0.80
0.0	2.754	2.392	2.086	1.821	1.587	1.377	1.188					
.2	2.710	2.359	2.061	1.803	1.574	1.368	1.182					
.4	2.623	2.296	2.014	1.765	1.543	1.342	1.160					
.6	2.518	2.208	1.944	1.708	1.498	1.309	1.134					
.8	2.406	2.106	1.856	1.636	1.442	1.266	1.100					
1.0	2.296	2.004	1.764	1.559	1.379	1.214	1.059					
1.5	2.040	1.770	1.548	1.370	1.210	1.069	.938					
2.0	1.819	1.563	1.360	1.193	1.052	.927	.817					
2.5	1.630	1.389	1.197	1.043	.912	.802	.709					
3.0	1.473	1.240	1.059	.914	.793	.695	.612	.53				
3.5	1.340	1.117	.943	.802	.694	.603	.528	.46				
4.0	1.225	1.013	.847	.713	.613	.527	.456	.40	.34			
4.5	1.133	.925	.764	.637	.543	.463	.397	.35	.29			
5.0	1.053	.849	.696	.577	.483	.408	.347	.30	.25	.22		
6	.919	.728	.586	.477	.393	.325	.272	.23	.19	.16	.14	
7	.819	.636	.503	.402	.325	.267	.218	.183	.15	.12	.10	.08
8	.735	.564	.440	.346	.275	.221	.178	.146	.119	.10	.08	.06
9	.667	.504	.388	.300	.235	.186	.149	.119	.096	.079	.06	.05
10	.610	.456	.345	.264	.203	.159	.125	.099	.079	.064	.051	.04
12	.521	.380	.280	.209	.157	.120	.092	.071	.055	.043	.033	.027
14	.452	.321	.232	.169	.124	.092	.069	.052	.038	.030	.022	.018
16	.396	.276	.195	.139	.100	.072	.053	.039	.028	.021	.016	.012
18	.351	.240	.166	.117	.082	.058	.042	.030	.022	.016	.012	.009
20	.315	.211	.144	.098	.068	.047	.033	.024	.017	.012	.009	.006

TABLE II. Free energy increase from free rotation, $(F-F_f)/T$ (cal. per mole degree)
$-F/T=-F_f/T-(F-F_f)/T=R\ln Q_f-(F-F_f)/T$.

V/RT \ $1/Q_f$	0	0.05	0.10	0.15	0.20	0.25	0.30	0.35	0.40	0.45	0.50	0.55
0.0	0.0000	0.000	0.000	0.000	0.000	0.000	0.000	0.000	0.000	0.000	0.000	0.000
0.2	.1937	.154	.117	.085	.061	.044	.033	.025	.018	.013	.009	.005
0.4	.3776	.326	.274	.225	.176	.131	.096	.072	.056	.044	.035	.026
0.6	.5516	.489	.424	.361	.298	.236	.184	.142	.113	.089	.068	.054
0.8	.7161	.640	.566	.493	.420	.348	.286	.230	.185	.145	.111	.088
1.0	.8711	.784	.699	.617	.537	.461	.389	.322	.262	.208	.163	.129
1.5	1.2200	1.114	1.010	.909	.809	.714	.622	.538	.451	.375	.308	.250
2.0	1.5182	1.395	1.276	1.159	1.045	.935	.829	.726	.628	.535	.450	.371
2.5	1.7724	1.635	1.501	1.371	1.246	1.124	1.004	.889	.778	.675	.575	.479
3.0	1.9893	1.839	1.693	1.552	1.415	1.282	1.152	1.027	.907	.794	.682	.576
3.5	2.1756	2.013	1.856	1.704	1.557	1.414	1.275	1.143	1.019	.893	.774	.660
4.0	2.3366	2.163	1.996	1.833	1.676	1.525	1.379	1.239	1.108	.974	.850	.732
4.5	2.4772	2.293	2.117	1.945	1.780	1.621	1.467	1.322	1.184	1.044	.914	.791
5.0	2.6012	2.408	2.221	2.042	1.868	1.703	1.543	1.392	1.244	1.104	.969	.841
6.0	2.8108	2.599	2.396	2.202	2.015	1.836	1.664	1.500	1.344	1.194	1.052	.916
7.0	2.9833	2.755	2.537	2.328	2.129	1.936	1.757	1.583	1.418	1.262	1.111	.971
8.0	3.1294	2.886	2.653	2.432	2.220	2.020	1.828	1.646	1.474	1.312	1.157	1.011
9.0	3.2563	2.998	2.753	2.520	2.298	2.087	1.888	1.698	1.520	1.351	1.192	1.039
10.0	3.3686	3.097	2.839	2.594	2.362	2.144	1.936	1.741	1.557	1.383	1.219	1.063
12.0	3.5602	3.263	2.982	2.718	2.468	2.233	2.013	1.806	1.612	1.429	1.258	1.096
14.0	3.7205	3.400	3.099	2.816	2.551	2.303	2.071	1.854	1.651	1.462	1.285	1.119
16.0	3.8584	3.517	3.197	2.897	2.618	2.358	2.116	1.891	1.682	1.486	1.305	1.135
18.0	3.9793	3.618	3.280	2.965	2.674	2.403	2.152	1.920	1.704	1.505	1.319	1.146
20.0	4.0872	3.707	3.353	3.024	2.720	2.440	2.181	1.942	1.722	1.519	1.331	1.155

for molecules with several tops or different potential barriers will be given in later sections.

The quantities entering in the formulas are:

I_1, I_2, I_3 the three principal moments of inertia of the rigid molecule (internal rotation frozen).

V_m the height of the potential barrier for the mth top.

n_m the number of potential minima per revolu-

TABLE III. Entropy, S (cal. per degree mole).

V/RT \ $1/Q_f$	0.25	0.30	0.35	0.40	0.45	0.50	0.55	0.60	0.65	0.70	0.75	0.80
0.0	3.748	3.386	3.079	2.814	2.580	2.371	2.181					
0.2	3.743	3.382	3.076	2.811	2.578	2.369	2.179					
0.4	3.730	3.370	3.065	2.801	2.568	2.359	2.171					
0.6	3.709	3.347	3.043	2.780	2.547	2.340	2.153					
0.8	3.679	3.318	3.013	2.750	2.519	2.315	2.128					
1.0	3.638	3.279	2.974	2.714	2.485	2.279	2.095					
1.5	3.512	3.156	2.854	2.600	2.376	2.173	1.992					
2.0	3.355	3.004	2.709	2.458	2.241	2.048	1.873					
2.5	3.180	2.836	2.548	2.303	2.091	1.907	1.741					
3.0	3.008	2.667	2.380	2.138	1.933	1.756	1.600	1.45				
3.5	2.838	2.500	2.218	1.978	1.782	1.610	1.459	1.34				
4.0	2.678	2.343	2.069	1.834	1.643	1.475	1.326	1.22	1.10			
4.5	2.528	2.199	1.926	1.698	1.511	1.348	1.204	1.10	1.00			
5.0	2.396	2.068	1.798	1.579	1.392	1.233	1.095	.97	.88	.81		
6.0	2.166	1.844	1.585	1.370	1.192	1.040	.913	.79	.70	.63	.56	
7.0	1.983	1.665	1.411	1.204	1.033	.891	.770	.665	.57	.50	.44	.39
8.0	1.830	1.519	1.272	1.071	.906	.770	.656	.564	.482	.41	.36	.31
9.0	1.703	1.397	1.156	.962	.804	.674	.569	.482	.411	.348	.29	.25
10.0	1.593	1.295	1.060	.872	.719	.596	.495	.418	.352	.295	.245	.21
12.0	1.417	1.125	.904	.728	.588	.476	.388	.315	.258	.212	.173	.143
14.0	1.275	.994	.783	.620	.492	.388	.309	.247	.196	.158	.126	.102
16.0	1.157	.890	.688	.533	.414	.322	.251	.196	.155	.120	.094	.075
18.0	1.058	.801	.609	.464	.353	.270	.205	.158	.121	.093	.072	.056
20.0	.975	.727	.542	.405	.303	.228	.170	.129	.097	.073	.056	.042

TABLE IV. Entropy decrease from free rotation, $(S_f - S)$ (cal. per mole degree)
$S = S_f - (S_f - S) = R(\frac{1}{2} + \ln Q_f) - (S_f - S)$.

V/RT \ $1/Q_f$	0.0	0.05	0.10	0.15	0.20	0.25	0.30	0.35	0.40	0.45	0.50	0.55
0.0	0.0000	0.000	0.000	0.000	0.000	0.000	0.000	0.000	0.000	0.000	0.000	0.000
0.2	.0049	.005	.004	.004	.004	.004	.004	.003	.003	.002	.002	.002
0.4	.0198	.020	.018	.018	.018	.018	.016	.014	.013	.012	.012	.010
0.6	.0440	.044	.043	.043	.040	.039	.039	.036	.034	.033	.031	.028
0.8	.0771	.077	.077	.075	.072	.069	.068	.066	.064	.061	.056	.053
1.0	.1185	.118	.117	.115	.112	.110	.107	.105	.100	.095	.092	.086
1.5	.2527	.252	.250	.248	.242	.236	.230	.225	.214	.204	.198	.189
2.0	.4182	.417	.415	.410	.402	.393	.382	.370	.356	.339	.323	.308
2.5	.6001	.599	.594	.585	.577	.568	.550	.531	.511	.489	.464	.440
3.0	.7856	.783	.777	.768	.757	.740	.719	.699	.676	.647	.615	.581
3.5	.9660	.964	.957	.944	.929	.910	.886	.861	.836	.798	.761	.722
4.0	1.1356	1.133	1.126	1.111	1.094	1.070	1.043	1.011	.980	.937	.896	.855
4.5	1.2918	1.289	1.280	1.265	1.244	1.220	1.187	1.153	1.116	1.069	1.023	.977
5.0	1.4339	1.431	1.421	1.404	1.380	1.352	1.318	1.281	1.235	1.188	1.138	1.086
6.0	1.6781	1.674	1.662	1.643	1.616	1.582	1.542	1.494	1.444	1.388	1.331	1.268
7.0	1.8783	1.874	1.860	1.837	1.807	1.765	1.721	1.668	1.610	1.547	1.480	1.411
8.0	2.0447	2.040	2.024	1.998	1.962	1.918	1.867	1.807	1.743	1.674	1.601	1.525
9.0	2.1864	2.180	2.163	2.134	2.095	2.045	1.989	1.923	1.852	1.776	1.697	1.612
10.0	2.3095	2.303	2.284	2.252	2.208	2.155	2.091	2.019	1.942	1.861	1.775	1.686
12.0	2.5155	2.508	2.485	2.447	2.394	2.331	2.261	2.175	2.086	1.992	1.895	1.793
14.0	2.6847	2.676	2.650	2.607	2.547	2.473	2.392	2.296	2.194	2.088	1.983	1.872
16.0	2.8289	2.819	2.788	2.740	2.674	2.591	2.496	2.391	2.281	2.166	2.049	1.930
18.0	2.9545	2.943	2.910	2.855	2.781	2.690	2.585	2.470	2.350	2.227	2.101	1.976
20.0	3.0659	3.054	3.017	2.956	2.872	2.773	2.659	2.537	2.409	2.277	2.143	2.011

tion; also the symmetry number of the internal rotation.

I_m the reduced moment of inertia for the rotation of the mth top. Only I_m needs further discussion; it is given by the equation:

$$I_m = A_m(1 - \sum_{i=1}^{3} A_m \lambda^2_{mi}/I_i), \qquad (1a)$$

TABLE V. Heat content, $(H_T-H_0)/T$ (cal. per degree mole).

V/RT \ $1/Q_f$	0.0	0.05	0.10	0.15	0.20	0.25	0.30	0.35	0.40	0.45	0.50	0.55	0.60	0.65	0.70	0.75	0.80
0.0	0.9934	0.993	0.993	0.993	0.993	0.993	0.993	0.993	0.993	0.993	0.993	0.993					
0.2	1.1822	1.142	1.106	1.074	1.050	1.032	1.022	1.015	1.008	1.004	1.000	.997					
0.4	1.3513	1.300	1.249	1.200	1.151	1.106	1.073	1.051	1.036	1.025	1.015	1.009					
0.6	1.5011	1.437	1.374	1.311	1.251	1.190	1.138	1.099	1.072	1.049	1.030	1.019					
0.8	1.6324	1.556	1.482	1.411	1.340	1.272	1.211	1.157	1.114	1.077	1.048	1.028					
1.0	1.7460	1.660	1.576	1.495	1.418	1.344	1.275	1.211	1.155	1.106	1.065	1.037					
1.5	1.9607	1.856	1.753	1.654	1.561	1.472	1.385	1.306	1.230	1.164	1.103	1.054					
2.0	2.0934	1.971	1.854	1.742	1.636	1.536	1.440	1.350	1.265	1.190	1.120	1.056					
2.5	2.1657	2.031	1.900	1.779	1.662	1.550	1.448	1.351	1.260	1.179	1.104	1.032					
3.0	2.1971	2.049	1.909	1.777	1.651	1.535	1.426	1.321	1.224	1.140	1.060	.988	.92				
3.5	2.2030	2.043	1.893	1.753	1.621	1.497	1.382	1.275	1.176	1.088	1.006	.931	.88				
4.0	2.1944	2.024	1.864	1.715	1.577	1.448	1.329	1.221	1.121	1.030	.947	.870	.82	.77			
4.5	2.1788	1.998	1.829	1.673	1.529	1.394	1.273	1.162	1.061	.968	.884	.807	.75	.71			
5.0	2.1607	1.971	1.794	1.631	1.481	1.344	1.218	1.104	1.002	.909	.824	.748	.67	.63	.59		
6.0	2.1261	1.918	1.727	1.552	1.392	1.247	1.115	.999	.893	.799	.714	.641	.56	.51	.47	.42	
7.0	2.0984	1.875	1.670	1.484	1.315	1.164	1.029	.908	.802	.708	.624	.553	.482	.42	.38	.34	.31
8.0	2.0781	1.840	1.623	1.427	1.251	1.095	.955	.833	.725	.631	.549	.479	.418	.363	.31	.28	.25
9.0	2.0634	1.811	1.583	1.379	1.196	1.035	.892	.768	.661	.569	.488	.420	.363	.315	.269	.23	.20
10.0	2.0526	1.787	1.548	1.335	1.147	.982	.838	.715	.608	.515	.437	.371	.319	.273	.231	.194	.17
12.0	2.0382	1.749	1.492	1.264	1.067	.896	.745	.624	.519	.431	.356	.296	.244	.203	.169	.140	.116
14.0	2.0292	1.717	1.441	1.202	.997	.823	.672	.551	.450	.367	.295	.240	.195	.158	.128	.104	.084
16.0	2.0229	1.690	1.401	1.150	.937	.760	.613	.493	.394	.314	.249	.198	.157	.127	.099	.078	.063
18.0	2.0182	1.666	1.363	1.102	.886	.707	.561	.443	.347	.271	.211	.164	.128	.099	.077	.060	.047
20.0	2.0147	1.646	1.329	1.061	.841	.660	.515	.399	.307	.236	.181	.138	.105	.080	.061	.047	.036

TABLE VI. Heat capacity, C (cal. per degree mole).

V/RT \ $1/Q$	0.0	0.05	0.10	0.15	0.20	0.25	0.30	0.35	0.40	0.45	0.50	0.55	0.60	0.65	0.70	0.75	0.80
0.0	.9934	.993	.993	.993	.993	.993	.993	.993	.993	.993	.99	.99					
0.2	1.0033	1.003	1.003	1.002	1.001	1.000	.999	.998	.998	.998	1.00	1.00					
0.4	1.0326	1.033	1.032	1.030	1.028	1.025	1.024	1.021	1.019	1.017	1.02	1.01					
0.6	1.0799	1.080	1.079	1.076	1.073	1.068	1.065	1.060	1.056	1.051	1.05	1.04					
0.8	1.1433	1.143	1.141	1.138	1.133	1.128	1.121	1.114	1.106	1.099	1.09	1.08					
1.0	1.2201	1.219	1.217	1.212	1.206	1.199	1.190	1.180	1.169	1.157	1.14	1.13					
1.5	1.4506	1.449	1.444	1.435	1.423	1.408	1.391	1.370	1.348	1.324	1.30	1.27					
2.0	1.6975	1.695	1.687	1.673	1.655	1.632	1.606	1.574	1.541	1.505	1.469	1.43					
2.5	1.9211	1.917	1.908	1.888	1.866	1.840	1.801	1.756	1.717	1.670	1.623	1.58					
3.0	2.0986	2.095	2.082	2.062	2.033	1.996	1.952	1.900	1.846	1.794	1.738	1.68	1.7				
3.5	2.2223	2.218	2.204	2.180	2.146	2.106	2.054	1.995	1.934	1.869	1.803	1.74	1.7				
4.0	2.2986	2.294	2.276	2.249	2.213	2.168	2.110	2.048	1.980	1.907	1.834	1.76	1.69	1.6			
4.5	2.3354	2.330	2.312	2.280	2.238	2.190	2.129	2.062	1.990	1.911	1.832	1.75	1.67	1.6			
5.0	2.3443	2.338	2.318	2.285	2.241	2.186	2.120	2.056	1.972	1.890	1.808	1.719	1.62	1.55	1.4		
6.0	2.3155	2.307	2.283	2.245	2.192	2.130	2.059	1.979	1.893	1.803	1.711	1.616	1.51	1.43	1.33	1.2	
7.0	2.2647	2.256	2.228	2.185	2.126	2.055	1.973	1.883	1.787	1.688	1.588	1.491	1.394	1.30	1.21	1.12	1.0
8.0	2.2157	2.205	2.174	2.125	2.058	1.979	1.888	1.788	1.684	1.576	1.468	1.362	1.260	1.159	1.07	.99	.91
9.0	2.1759	2.164	2.130	2.074	1.999	1.909	1.808	1.699	1.587	1.474	1.362	1.252	1.149	1.049	.955	.86	.79
10.0	2.1454	2.133	2.094	2.033	1.951	1.854	1.745	1.630	1.507	1.382	1.262	1.151	1.047	.949	.853	.762	.68
12.0	2.1050	2.089	2.043	1.972	1.877	1.763	1.636	1.502	1.365	1.233	1.107	.989	.877	.774	.683	.600	.519
14.0	2.0810	2.063	2.009	1.923	1.814	1.686	1.546	1.400	1.254	1.112	.978	.855	.744	.644	.555	.476	.408
16.0	2.0654	2.044	1.983	1.887	1.764	1.622	1.468	1.311	1.156	1.009	.873	.749	.639	.542	.457	.384	.321
18.0	2.0544	2.031	1.961	1.853	1.717	1.562	1.397	1.232	1.070	.919	.780	.657	.549	.456	.378	.312	.256
20.0	2.0462	2.020	1.944	1.827	1.678	1.510	1.333	1.158	.991	.837	.701	.580	.477	.389	.316	.256	.207

which is exact for a single top and probably a satisfactory approximation for molecules with several tops. Here A_m is the moment of inertia of the mth top itself, λ_{mi} is the direction cosine between the axis of the mth top and the ith principal axis of the whole molecule, and I_i is the moment of inertia of the whole molecule about this axis.

For molecules with several tops the next approximation to I_m is:

$$I_m = I^0{}_m - (\tfrac{1}{2}) \sum_{m' \neq m}{}' \Lambda^2{}_{mm'}/I^0{}_{m'}, \qquad (1b)$$

where $I^0{}_m$ is the value given in Eq. (1a) and

$$\Lambda_{mm'} = A_m A_{m'} \sum_{i=1}^{3} \lambda_{mi}\lambda_{m'i}/I_i. \qquad (1c)$$

The essential criterion of accuracy of the simple formulas and tables for molecules with several tops is whether the potential can be expressed as:

$$V_{(\phi_1, \phi_2 \cdots \phi_N)} = \sum_{m=1}^{N} \tfrac{1}{2} V_m (1 - \cos n_m \phi_m). \qquad (2)$$

This expression should suffice where the rotating groups are far apart and are not coupled by long

range forces. For example, Eq. (2) should suffice for *para*-xylene and *trans*-2-butene but possibly not for *ortho*-xylene, *cis*-2-butene, or propane.

The well-known formulas for translation and over-all rotation may be written as follows:

$$(H^0_0-F^0_T)/T=R[\tfrac{3}{2}\ln M+4\ln T-\ln P+\tfrac{1}{2}\ln(I_1I_2I_3\times10^{117})-\ln\sigma]-10.237, \quad (3)$$

$$(H^0_T-H^0_0)/T=C_p=4R=7.948,$$

$$S^0_T=(H^0_0-F^0_T)/T+(H^0_T-H^0_0)/T.$$

Here M is the molecular weight, P is the pressure in atmos., and σ is the symmetry number for over-all rotation. Physical constants have been taken from the *International Critical Tables* since these values are standard for this type of work. However, the only physical constant which enters the tables is the gas constant, $R=1.9869$ cal. per degree mole. This constant is a factor in all entries and in the very improbable circumstance that it is appreciably in error an appropriate factor can be applied.

The two variables for the tables were selected as the dimensionless ratios (V/RT) and $(1/Q_f)=hn/(8\pi^3IkT)^{\frac{1}{2}}$. The latter is the reciprocal of the partition function for free rotation which also appears as $R\ln Q_f$. In terms of I in g cm^2 and T°K one obtains:

$$Q_f=2.815(10^{38}IT)^{\frac{1}{2}}/n. \quad (4)$$

The use of the physical constants recently compiled by Birge[13] gives 2.7934 for the numerical constant in Eq. (4). These variables have the additional advantages of permitting a very compact form for the tables and in having the potential barrier in only one variable.

The accuracy of each entry in the tables is indicated by the number of significant figures given. Ordinarily linear interpolation will give values accurate to 0.01 cal. per degree. Graphical interpolations are recommended if the maximum accuracy is desired.

ENERGY LEVELS

Having stated the thermodynamic results for the case of greatest practical interest, let us proceed to the quantum mechanical analysis. In this section we will avoid all but one of the assumptions of the preceding section, discussing the still more general case below. The notation will be the same except for the use of T for kinetic energy instead of temperature.

Beginning with the kinetic energy we use the expression of Kassel[6c] and Crawford[9] as follows:

$$2T=\sum_{i=1}^{3}I_i(\omega'_i)^2+2\sum_{i=1}^{3}\sum_{m=1}^{N}A_m\lambda_{mi}\dot{\phi}_m\omega'_i+\sum_{m=1}^{N}A_m\dot{\phi}_m^2, \quad (5)$$

where ω'_i is the instantaneous angular velocity of the rigid frame about the ith principal axis, and $\dot{\phi}_m$ is the angular velocity of the mth top with respect to the rigid frame. Now introduce the transformation:

$$\omega_i=\omega'_i+\sum_{m=1}^{N}A_m\lambda_{mi}\dot{\phi}_m/I_i, \quad (6)$$

then

$$2T=\sum_i I_i\omega_i^2+\sum_m A_m\dot{\phi}_m^2-\sum_m\sum_{m'}\Lambda_{mm'}\dot{\phi}_m\dot{\phi}_{m'}. \quad (7)$$

The ω's are now weighted average angular velocities of the whole molecule. The Λ's were defined in Eq. (1c). This transformation has separated the terms for over-all rotation from those for internal rotation. It should also be noticed that since the A's will be usually much smaller than the I_i's, the Λ's will be much smaller than the A_m's.

Now introducing momenta:

$$P_i=\partial T/\partial\omega_i, \quad P_m=\partial T/\partial\dot{\phi}_m$$

one obtains

$$2T=\sum_i P_i^2/I_i+\sum_m\sum_{m'}\beta_{mm'}P_mP_{m'}. \quad (8)$$

Here the P_i's are the net angular momenta of the whole molecule, and $(\beta_{mm'})$ is the inverse matrix of the matrix $(A_m\delta_{mm'}-\Lambda_{m,m'})$ of Eq. (7). In order to separate variables it is desirable to remove all terms in the second sum with $m\neq m'$ and to regard them as a perturbation. This is justifiable because it is found that their coefficients $(\sim\Lambda_{mm'}/A_mA_{m'})$ are of a smaller order of magnitude than those with $m=m'$. While the exact expression for β_{mm} has been defined above in terms of matrix algebra, an approximate expression

[13] R. T. Birge, Rev. Mod. Phys. **13**, 233 (1941).

would seem to be much more useful. We then find for the kinetic energy the expression:

$$2T=\sum_i P_i^2/I_i+\sum_m P_m^2/I_m, \tag{9}$$

where I_m was defined in Eq. (1a) or more accurately in (1b) omitting the factor $(\frac{1}{2})$ before the sum. This expression is exact for one top since no $P_mP_{m'}$ terms are possible there.

For the potential energy we assume a form more general than that of the preceding section, namely:

$$V=\sum_{m=1}^{N} V_m(\varphi_m), \tag{10}$$

where for each value of m

$$V_{m(\varphi m)}=\sum_{k=1}^{\infty}\tfrac{1}{2}V_{mk}(1-\cos kn_m\varphi_m). \tag{11}$$

This form really involves two assumptions. The first is the absence of terms involving more than one φ_m which, as stated above, will probably be a good approximation in some cases and a poor one in others. The second assumption is the absence of sine terms in the Fourier series expansion of V_m. This may be justified by symmetry considerations in many cases. Both assumptions will be examined further.

Turning now to quantum mechanics, since the coefficients of the P's are constants in Eq. (9), one may write at once the separated wave equations:

$$(\textstyle\sum_i \mathbf{P}_i^2/2I_i)\psi_{OR}=W_{OR}\psi_{OR}, \tag{12}$$

$$(\mathbf{P}_m^2/2I_m)\psi_m+\textstyle\sum_k\tfrac{1}{2}V_{mk}(1-\cos kn_m\phi_m)\psi_m = W_m\psi_m \quad m=1, 2, \cdots, N, \tag{13}$$

where $\mathbf{P}_m^2=(h/2\pi i)^2\partial^2/\partial\phi_m^2$ and the $\mathbf{P}_i$'s are the operators studied by Klein.[14]

The transformation of Eq. (6) introduces some additional complexity into the representation of the $\mathbf{P}_i$ operators in terms of the Eulerian angles of the rigid frame but does not affect their essential relationships.

$$\begin{aligned}\mathbf{P}_x\mathbf{P}_y-\mathbf{P}_y\mathbf{P}_x&=(h/2\pi i)\mathbf{P}_z,\\ \mathbf{P}_y\mathbf{P}_z-\mathbf{P}_z\mathbf{P}_y&=(h/2\pi i)\mathbf{P}_x,\\ \mathbf{P}_z\mathbf{P}_x-\mathbf{P}_x\mathbf{P}_z&=(h/2\pi i)\mathbf{P}_y.\end{aligned} \tag{14}$$

[14] O. Klein, Zeits. f. Physik **58**, 730 (1929).

The energy levels for over-all rotation, W_{OR}, are therefore just those of the rigid molecule of moments of inertia I_1, I_2, I_3 as given by Klein and others.

Each wave Eq. (13) for internal rotation may be converted into the Hill differential equation by the following substitutions:

$$\begin{aligned}&2x=n\phi, \quad \theta_k=8\pi^2IV_k/n^2h^2,\\ &W-\tfrac{1}{2}\textstyle\sum_k V_k=n^2h^2\theta_0/32\pi^2I,\\ &M''(x)+(\theta_0+2\textstyle\sum_{k=1}^{\infty}\theta_k\cos 2kx)M(x)=0,\end{aligned} \tag{15}$$

where the subscript m has been omitted throughout. In general, the boundary conditions on $M(x)$ are very complicated since the requirement is

$$\begin{aligned}&\psi_{OR}(\varphi_m)M_m(n\varphi_m/2)\\ &\quad=\psi_{OR}(\varphi_m+2\pi)M_m((n/2)(\varphi_m+2\pi)),\end{aligned} \tag{16}$$

where the wave function for over-all rotation ψ_{OR} depends on ϕ_m in addition to the Eulerian angles of the rigid frame. The dependence of ψ_{OR} on ϕ_m cannot be stated simply. Nevertheless, it is apparent that Eq. (16) cannot be satisfied unless $M_m(x)$ remains finite even when x approaches either positive or negative infinity. We shall proceed to consider all solutions of the Hill equation which satisfy this very general boundary condition and to show that for thermodynamic calculations further analysis is not necessary at this point.

We shall follow the solution offered by Hill.[15] A general solution is

$$M(x)=e^{\mu x}\sum_{k=-\infty}^{+\infty} b_k e^{2kix}, \tag{17}$$

where the sum is evidently a purely periodic function. Ordinarily the second solution is given by $M(-x)$. In the special case $\mu=\pm 0, \pm i$ these two solutions become identical. If $M(x)$ is to remain finite for all x, it is seen that μ must be a pure imaginary number or zero. Otherwise $M(x)$ will contain a real exponential factor that will approach infinity either as x increases indefinitely in a positive direction or else as it increases

[15] G. W. Hill, Acta Math. **8**, (1886), or Whittaker and Watson, *Modern Analysis* (Cambridge University Press, 1935), pp. 413–417.

negatively. In the special case $\mu = \pm i, 0$ these two solutions become identical. By other methods a second, different solution may be obtained in this case, but it does not remain finite and therefore is not acceptable.

Now μ is given by the transcendental equation

$$\sin^2(\tfrac{1}{2}\pi i\mu) = \Delta(\theta_0\theta_1\cdots)\sin^2(\tfrac{1}{2}\pi\theta_0^{\frac{1}{2}}) = F(\theta_0\theta_1\cdots), \quad (18)$$

where $\Delta(\theta)$ is the convergent, infinite determinant

$$\Delta(\theta_1\theta_1\cdots) = \begin{vmatrix} \cdots & \cdots & \cdots & \cdots & \cdots & \cdots & \cdots & \cdots & \cdots \\ \cdots & 1 & \frac{\theta_1}{\theta_0-6^2} & \frac{\theta_2}{\theta_0-6^2} & \frac{\theta_3}{\theta_0-6^2} & \frac{\theta_4}{\theta_0-6^2} & \frac{\theta_5}{\theta_0-6^2} & \frac{\theta_6}{\theta_0-6^2} & \cdots \\ \cdots & \frac{\theta_1}{\theta_0-4^2} & 1 & \frac{\theta_1}{\theta_0-4^2} & \frac{\theta_2}{\theta_0-4^2} & \frac{\theta_3}{\theta_0-4^2} & \frac{\theta_4}{\theta_0-4^2} & \frac{\theta_5}{\theta_0-4^2} & \cdots \\ \cdots & \frac{\theta_2}{\theta_0-2^2} & \frac{\theta_1}{\theta_0-2^2} & 1 & \frac{\theta_1}{\theta_0-2^2} & \frac{\theta_2}{\theta_0-2^2} & \frac{\theta_3}{\theta_0-2^2} & \frac{\theta_4}{\theta_0-2^2} & \cdots \\ \cdots & \frac{\theta_3}{\theta_0} & \frac{\theta_2}{\theta_0} & \frac{\theta_1}{\theta_0} & 1 & \frac{\theta_1}{\theta_0} & \frac{\theta_2}{\theta_0} & \frac{\theta_3}{\theta_0} & \cdots \\ \cdots & \frac{\theta_4}{\theta_0-2^2} & \frac{\theta_3}{\theta_0-2^2} & \frac{\theta_2}{\theta_0-2^2} & \frac{\theta_1}{\theta_0-2^2} & 1 & \frac{\theta_1}{\theta_0-2^2} & \frac{\theta_2}{\theta_0-2^2} & \cdots \\ \cdots & \frac{\theta_5}{\theta_0-4^2} & \frac{\theta_4}{\theta_0-4^2} & \frac{\theta_3}{\theta_0-4^2} & \frac{\theta_2}{\theta_0-4^2} & \frac{\theta_1}{\theta_0-4^2} & 1 & \frac{\theta_1}{\theta_0-4^2} & \cdots \\ \cdots & \frac{\theta_6}{\theta_0-6^2} & \frac{\theta_5}{\theta_0-6^2} & \frac{\theta_4}{\theta_0-6^2} & \frac{\theta_3}{\theta_0-6^2} & \frac{\theta_2}{\theta_0-6^2} & \frac{\theta_1}{\theta_0-6^2} & 1 & \cdots \\ \cdots & \cdots & \cdots & \cdots & \cdots & \cdots & \cdots & \cdots & \cdots \end{vmatrix}. \quad (19)$$

$\Delta(\theta)$ has singularities at $\theta_0 = 0, 2^2, 4^2\cdots$; however, $\sin^2(\frac{1}{2}\pi\theta_0^{\frac{1}{2}})$ approaches zero in an exactly compensating manner so that $F(\theta)$ is a continuous, single valued function for all θ_0, θ_1, etc. Figure 1 shows $F(\theta)$ as a function of θ_0 for several discrete values of θ_1 and θ_2, with $\theta_3 = \theta_4\cdots = 0$.

The region of acceptable solutions (μ to be a pure imaginary) is given by $0 \leqslant F(\theta) \leqslant 1$ as can be easily seen from (18). In the special case $\theta_1 = \theta_2 = \cdots = 0$, $\Delta = 1$ all positive values and no negative values of θ_0 are in the acceptable region. Otherwise for θ_0 sufficiently negative Δ will always become positive and approach $+1$. Then F remains negative and no acceptable solutions are found. For positive or small negative values of θ_0, regions of acceptable solutions are obtained and between these are regions where no acceptable solutions exist.

We may now examine the completeness of our solution. For given values of θ_0, θ_1, etc., a linear combination of two independent solutions is a complete solution. By Eq. (18) the positive and negative values of μ correspond to the same values of θ_0, θ_1, etc., and, excepting the special case already mentioned, they give independent solutions. Thus we do have a complete solution.

We now return to the topic of boundary conditions in order to define the number of energy levels and so far as possible their exact energies. We shall not discuss the wave functions here; they are readily obtained in terms of the boundary conditions and the cited analysis of the Hill equation.[15] By symmetrical tops we mean tops whose moments of inertia perpendicular to the top axis are equal. Ordinarily this equality of moments of inertia will arise (as in CH_3) from identical atoms symmetrically placed. We shall call such tops "identically" symmetrical tops. It

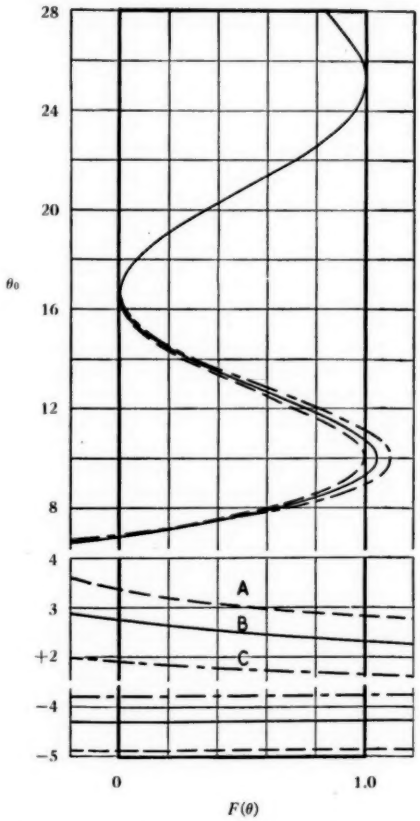

FIG. 1. $F(\theta_0, \theta_1, \theta_2 \cdots)$ as a function of θ_0 with $\theta_1=4$, $\theta_2=+0.8$ for A; $\theta_1=4$, $\theta_2=0$ for B; $\theta_1=4$, $\theta_2=-0.8$ for C; in all cases $\theta_3=\theta_4=\cdots=0$.

is possible, however, for a symmetrical top to consist of various different atoms so placed as to make the moments equal. We shall call these "accidentally" symmetrical tops.

Let us now consider a molecule made up of one n fold identically symmetrical top, and one accidentally symmetrical top. Group theoretical methods give the general boundary condition on the internal rotation to be:

$$\psi_{OR}\left(\varphi_m+\frac{2\pi}{n}\right)M_m\left(\frac{n}{2}\left(\varphi_m+\frac{2\pi}{n}\right)\right)$$

$$=e^{i(2\pi/n)k}\psi_{OR}(\phi_m)M_m\left(\frac{n}{2}\phi_m\right), \quad (20)$$

where the value of k, an integer, depends on the statistics obeyed by the identical atoms, their relative nuclear spin orientations, the symmetry of the vibrational state, and possibly other factors. For a molecule in a given state with respect to other factors one and only one value of k is allowed. Thus if the totally symmetric state for internal rotation is desired, k is zero.

Now using the results of Nielsen[1] for two coaxial tops we obtain

$$M[(n/2)(\phi+2\pi/n)]$$

$$=\exp\{i(2\pi/n)[k+K(A/I_3)]\}M[(n/2)\phi], \quad (21)$$

where A is the moment of inertia of the identically symmetrical top, I_3 is the moment of inertia of the whole molecule about the axis of the tops, and K is the quantum number for over-all rotation giving the angular momentum about the axis of the tops. This leads to an equation for μ (in Eq. (17)):

$$\mu=i(2/n)[k+K(A/I_3)]. \quad (22)$$

Thus for any given set of other conditions on this molecule, a single energy level for internal rotation is obtained in each of the acceptable regions discussed above.

We were unable to obtain any reasonably simple expression for μ in the more general case of a symmetric top attached to an unsymmetrical frame. However, since such a molecule must be related adiabatically (by a series of infinitesimal perturbations) to the case discussed above, the same number of energy levels must be present. Thus we may conclude for the general case of an identically symmetrical top attached to a rigid frame of any symmetry that there will be one energy level in each acceptable region for any given set of other quantum numbers or other specifying conditions.

Two special cases may be mentioned. If two coaxial tops have different symmetries the internal rotation may have an even higher symmetry. The molecules nitromethane and toluene exemplify this with two- and threefold symmetries combined in each case. The second case arises when the potential barrier has a higher symmetry, $n=ab$, (possibly only approximate) than the rotating groups, $n=b$. Then there will be a energy levels in each acceptable region if the value $n=ab$ is used in Eq. (15). This increases S and $-F/T$ by $R \ln a$ but does not change H or C. If $n=b$ is used in Eq. (15) then the case ceases to be a special one—only one energy level per region

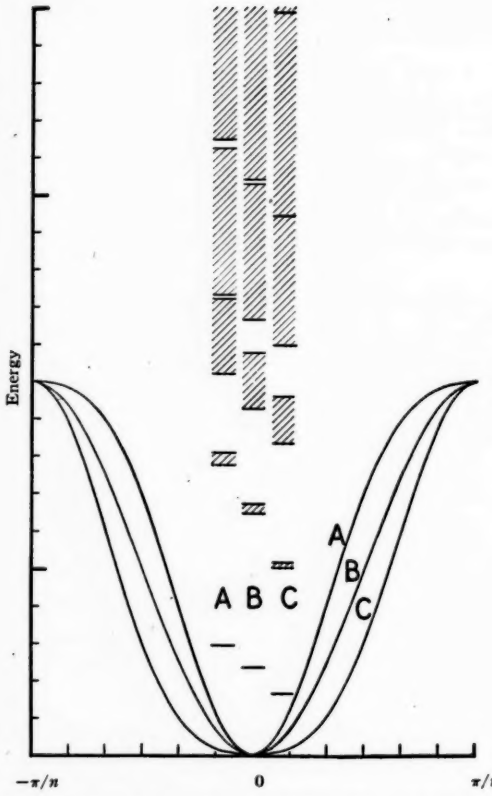

FIG. 2. Potential curves and regions where energy levels may lie. *A*, *B*, and *C* are the same as in Fig. 1.

is allowed, but the expansion of the potential energy, Eq. (11), will have only those terms where k is a multiple of a. This may complicate calculations and make the first method desirable.

There remain to be considered in this section the two energy terms which were dropped above and which we may now treat as perturbations. First are the cross terms in the kinetic energy of the type $\beta_{mm'}\mathbf{P}_m\mathbf{P}_{m'}$. The effect of these terms is somewhat similar to that of the coriolis perturbation or vibration-rotation angular momentum interaction in polyatomic molecules. The perturbation energies will be small but appreciable. However, since angular momenta are as likely to be positive as negative, as many energy levels will be raised as will be lowered. The effect on the partition function or thermodynamic properties will, therefore, be of a much smaller order of magnitude and probably negligible in all practical cases. For comparisons with spectroscopic data these terms will need to be considered, except of course in molecules with only one top where they are absent. However, in view of the lack of application at present and the extreme complexity of equations for the general case as compared to special cases, it does not seem worthwhile to pursue this subject further.

The second set of energy terms that was dropped is the portion of the Fourier series expansion of the potential energy involving sines:

$$V'=\sum_{k=1}^{\infty} S_k \sin kn\phi,$$

where in order that $\phi=0$ shall be a minimum in the potential curve it is necessary that:

$$\left(\frac{\partial V'}{\partial \phi}\right)_{\phi=0} = n\sum_{k=1}^{\infty} kS_k = 0.$$

Thus the S_k's must vary the sign tending to cancel one another in effect. For many special cases (two coaxial tops, for example) it is possible to prove that the first-order perturbation energy will be exactly zero. In general this is not possible but then the situation is like that discussed above, i.e., some energy levels are raised and others lowered. Thus it seems certain that these terms will not affect the thermodynamic functions appreciably although they may perturb individual energy levels somewhat. In many cases the sine terms are eliminated completely by symmetry considerations.

PARTITION FUNCTION

We shall now calculate the partition function for the reasonably general case considered in the preceding section. Holding all other quantum

TABLE VII. The effect of μ on the thermodynamic functions.

$\sin^2 \frac{1}{2}i\pi\mu$	$-F/T$	H/T	C
$(V/RT)=4$		$(1/Q)=0.5642$	
0.0	0.436	0.851	1.737
.2	.436	.851	1.735
.4	.436	.851	1.733
.6	.436	.852	1.728
.8	.436	.852	1.725
1.0	.436	.853	1.724
$(V/RT)=6$		$(1/Q)=0.6910$	
0.0	0.167	0.475	1.378
.2	.166	.477	1.367
.4	.165	.481	1.358
.6	.165	.484	1.344
.8	.164	.488	1.340
1.0	.164	.492	1.334

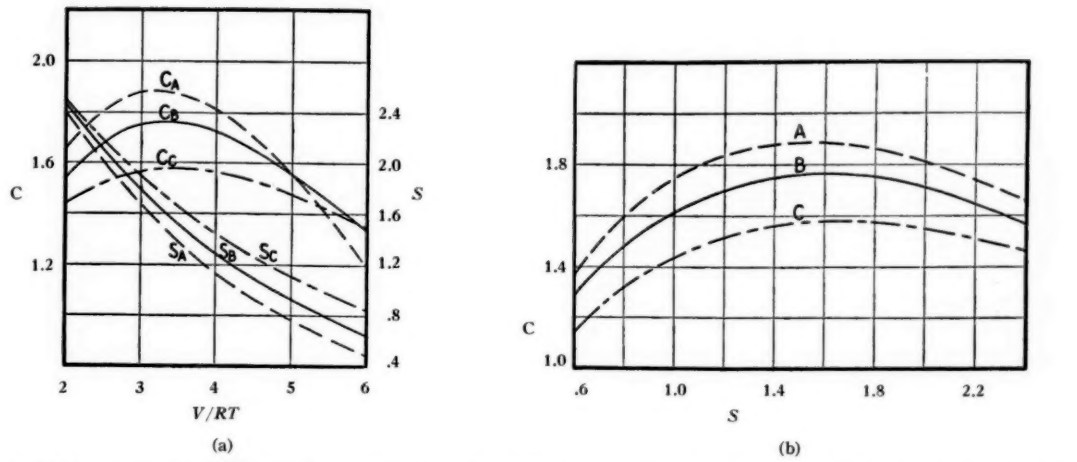

FIG. 3. (a) Heat capacity and entropy as a function of temperature for the potential curves of Figs. 1 and 2. (b) Heat capacity as a function of entropy for the same potential curves. This shows the possibility of determining the shape of potential curve from thermodynamic data alone. It is apparent that the experimental error would have to be less than one-tenth cal. per degree to distinguish definitely *A* or *C* from *B*.

numbers or conditions constant, and therefore μ constant, one may write for the mth internal rotation

$$Q_m(\mu)=\sum_{l=0}^{\infty}\exp\left[-(W_{m,l}(\mu)-W_{m,0})/kT\right], \quad (23)$$

where l is simply an index numbering off the acceptable regions of energy levels, and W_0 is the energy of the lowest real state. Numerical evaluation of typical cases for various values of μ showed that the partition function was a smooth and nearly linear function of μ between its limits of 0 and i. Two examples are listed in Table VII. In other words, if the partition function is summed for the two cases $\mu=0$, $i(F(\theta)=0, 1)$ and the two values are essentially the same, then this value may be taken as a good approximation for all μ.

The tables given above were evaluated by this method. If only the first term is taken in the potential energy expression, $\theta_2=\theta_3\cdots=0$ in Eqs. (15) and (19), then the Hill Eq. (15) reduces to the Mathieu equation. Ince[16] has given the characteristic values, and hence the energy levels, for the cases $\mu=0$, i (ordinary Mathieu functions) over a range of values of θ_1, the potential barrier height. Additional energy levels were calculated by Ince's methods as needed.

The equations for the thermodynamic functions are the usual ones:

$$\begin{aligned}
-F/T&=R\ln Q,\\
H/T&=R(Q'/Q),\\
S&=H/T-F/T=R(\ln Q+Q'/Q),\\
C&=R[Q''/Q-(Q'/Q)^2],\\
Q'&=\sum_{l=0}^{\infty}\left[(W_l-W_0)/kT\right]e^{-(W_l-W_0)/kT},\\
Q''&=\sum_{l=0}^{\infty}\left[(W_l-W_0)/kT\right]^2e^{-(W_l-W_0)/kT}.
\end{aligned} \quad (24)$$

Wherever the sums for $\mu=0$, i differed appreciably the resulting values were rounded off to limit uncertainty to the last significant figure. The directly summed values were carefully interpolated by graphical methods and the use of deviation functions to the even points desired in the tables. Use was made of the classical or limiting function:

$$Q=\frac{(2\pi IkT)^{\frac{1}{2}}}{h}\int_0^{2\pi/n}e^{-(V/2kT)(1-\cos n\phi)}d\phi, \quad (25)$$

which is closely related to certain Bessel functions. In these terms the thermodynamic functions take the following form:

$$\begin{aligned}
(F-F_f)/T&=R[y-\ln J_0(iy)],\\
H/T&=R[\tfrac{1}{2}+y+yiJ_1(iy)/J_0(iy)],\\
C&=R[\tfrac{1}{2}+y^2-yiJ_1(iy)/J_0(iy)\\
&\qquad-\{yiJ_1(iy)/J_0(iy)\}^2],\\
y&=\tfrac{1}{2}(V/RT).
\end{aligned} \quad (26)$$

[16] E. L. Ince, Proc. Roy. Soc. Edinburgh **52**, 355 (1931).

These results apply, of course, in the limit $(1/Q)$ zero.

In addition to these results which comprise the tables of the first section, a few calculations were made for different shapes of potential barrier by the direct evaluation of Hill's determinant. Figure 2 shows the potential curves and energy levels while Fig. 3 shows the thermodynamic functions. The entropy-heat capacity curves indicate that precise thermodynamic data would be needed to distinguish clearly even these extreme variations of shape. Spectroscopic data would seem more promising in this regard. Thus for most practical thermodynamic work the use of the simple cosine potential barrier should be satisfactory.

A USEFUL APPROXIMATION

Before proceeding to still more complex cases, a generally useful approximation will be described. Any potential function, $V_{(\phi_1 \cdots \phi_N)}$ can be expanded in a power series about a point of equilibrium.

$$V = \tfrac{1}{2} \sum_m \sum_{m'} b_{mm'} \phi_m \phi_{m'} + \frac{1}{3!} \sum_m \sum_{m'} \sum_{m''} c_{mm'm''} \phi_m \phi_{m'} \phi_{m''} + \cdots, \quad (27)$$

$$b_{mm'} = (\partial^2 V / \partial \phi_m \partial \phi_{m'})_e,$$

$$c_{mm'm''} = (\partial^3 V / \partial \phi_m \partial \phi_{m'} \partial \phi_{m''})_e, \quad \text{etc.}$$

The origins of the ϕ_m's are now of course at the equilibrium positions where the derivatives are evaluated. If only the first sum is used, the usual harmonic oscillator treatment is obtained. For internal rotation problems this is not a very good approximation by itself, because of the large anharmonicity (importance of the other sums) which appears even in the lower energy levels. However, the following combination appears to be quite accurate:

$$Q = Q_{\text{Class}} [Q_{\text{HO Quant}} / Q_{\text{HO Class}}], \quad (28)$$

where Q_{Class} is the complete classical partition function:

$$Q_{\text{Class}} = \frac{1}{h^N} \int_{-\infty}^{+\infty} \cdots \int_{-\infty}^{+\infty} \int_0^{2\pi/n_1} \cdots \int_0^{2\pi/n_N} \times e^{-(T+V)/kT} dp_1 \cdots dp_N d\phi_1 \cdots d\phi_N, \quad (29)$$

and Q_{HO} represents an harmonic oscillator partition function of either the quantum mechanical or classical form. Since the ratio in brackets in (28) approaches unity at high temperatures, the results must be correct there. Similarly, if the two lowest energy levels are given by the harmonic oscillator treatment with reasonable accuracy, the result is necessarily a good approximation at very low temperatures because Q_{Class} and $Q_{\text{HO Class}}$ will become equal. The best test is a comparison in a case where the exact answer is known. This is presented in Table VIII where a comparison is made for the case of one top and the simple cosine potential barrier. The exact answer comes of course from the earlier part of this paper.

TABLE VIII. Comparison of approximate (Eq. (28)) and exact partition functions in terms of heat capacity and entropy.

	V/RT \ $1/Q_f$	0.10	0.20	0.40
δC	0	0.000	0.000	0.000
approx.	1	− .002	− .007	− .030
− exact	4	+ .001	+ .004	+ .016
(cal./degree)	9	.000	− .000	− .017
	16	+ .001	− .001	− .020
δS	0	0.000	0.000	0.000
approx.	1	+ .001	+ .004	+ .022
− exact	4	.000	− .001	− .002
(cal./degree)	9	.000	.000	+ .002
	16	.000	+ .003	+ .007

FURTHER STUDY OF MOLECULES WITH SEVERAL TOPS

We shall now proceed to apply the approximate method just described to molecules with several attached tops, where the potential energy is not separable according to Eq. (10). By the procedure of Eqs. (5) to (7) the kinetic energy of external rotation was separated and we have for internal rotation the exact expression

$$2T = \sum_m A_m \dot{\phi}_m^2 - \sum_m \sum_{m'} \Lambda_{mm'} \dot{\phi}_m \dot{\phi}_{m'}. \quad (30)$$

First let us consider the exact classical partition function (29). By the interesting theorem of Eidinoff and Aston[5] this becomes

$$Q_{\text{Class}} = (2\pi kT/h^2)^{N/2} [D]^{\frac{1}{2}} \times \int_0^{2\pi/n_1} \cdots \int_0^{2\pi/n_N} e^{-V/kT} d\varphi_1 \cdots d\phi_N, \quad (31)$$

where

$$[D]=\begin{vmatrix} A_1-\Lambda_{11} & -\Lambda_{12} & \cdots & -\Lambda_{1N} \\ -\Lambda_{21} & A_2-\Lambda_{22} & \cdots & -\Lambda_{2N} \\ \cdot & \cdot & \cdots & \cdot \\ \cdot & \cdot & \cdots & \cdot \\ \cdot & \cdot & \cdots & \cdot \\ -\Lambda_{N1} & -\Lambda_{N2} & \cdots & A_N-\Lambda_{NN} \end{vmatrix} = \prod_{m=1}^{N} I_m. \tag{32}$$

I_m is given approximately by Eq. (1a) and more accurately by (1b). Using the latter values of I_m the second equality in (32) is accurate to terms of order Λ^2 which will be sufficient for all practical purposes.

Turning now to the harmonic oscillator approximation, we have for the potential energy from (27):

$$2V=\sum_m \sum_{m'} b_{mm'}\phi_m\phi_{m'}, \qquad b_{mm'}=(\partial^2 V/\partial\phi_m\partial\phi_{m'})_e. \tag{33}$$

We now follow the usual normal coordinate analysis which is given in greater detail in many books. In the lth normal mode of frequency ν_l the equation of motion will be

$$\phi_m=A_{ml}\sin(2\pi\nu_l t+\delta_l). \tag{34}$$

By the usual Lagrangian methods we find

$$-4\pi^2\nu_l^2(I_mA_{ml}-\sum_{m'\neq m}{}' \Lambda_{mm'}A_{m'l})+\sum_{m'} b_{mm'}A_{m'l}=0, \tag{35}$$

which leads to the determinantal equation

$$\begin{vmatrix} b_{11}-4\pi^2\nu^2 I_1 & b_{12}+4\pi^2\nu^2\Lambda_{12} & \cdots & b_{1N}+4\pi^2\nu^2\Lambda_{1N} \\ b_{21}+4\pi^2\nu^2\Lambda_{21} & b_{22}-4\pi^2\nu^2 I_2 & \cdots & b_{2N}+4\pi^2\nu^2\Lambda_{2N} \\ \cdot & \cdot & \cdots & \cdot \\ \cdot & \cdot & \cdots & \cdot \\ \cdot & \cdot & \cdots & \cdot \\ \cdot & \cdot & \cdots & \cdot \\ b_{N1}+4\pi^2\nu^2\Lambda_{N1} & b_{N2}+4\pi^2\nu^2\Lambda_{N2} & \cdots & b_{NN}-4\pi^2\nu^2 I_N \end{vmatrix} = 0. \tag{36}$$

This equation has N roots $\nu_1\cdots\nu_N$ which may be obtained by suitable calculations.

The quantum mechanical energy levels corresponding to this approximation are

$$W=\sum_{l=1}^{N}(v_l+\tfrac{1}{2})h\nu_l, \tag{37}$$

and the partition function

$$Q_{\text{HO Quant}}=\prod_{l=1}^{N}[1/(1-e^{-h\nu_l/kT})]. \tag{38}$$

The classical or high temperature limit approached by this function is

$$Q_{\text{HO Class}}=(kT/h)^N/(\prod_l \nu_l). \tag{39}$$

We have now the factors necessary for the approximate partition function, Eq. (28).

It is possible to expand the exponentials in Eq. (38) to a form more convenient for most calculations. They will be satisfactory provided $(h\nu/kT)$ is not much greater than one.

Let $h\nu/kT=a$:

$$-F/T=R\{\ln Q_{\text{Class}}+\sum_{l=1}^{N}(a_l/2-a_l^2/24+a_l^4/2880\cdots)\},$$

$$H/T=R\{N/2+P'/P+\sum_{l=1}^{N}(-a_l/2+a_l^2/12-a_l^4/720\cdots)\},$$

$$S=R\{\ln Q_{\text{Class}}+N/2+P'/P+\sum_{l=1}^{N}(a_l^2/24-a_l^4/960\cdots)\},$$

$$C=R\{N/2+P''/P-(P'/P)^2+\sum_{l=1}^{N}(-a_l^2/12+a_l^4/240\cdots)\}, \tag{40}$$

$$Q_{\text{Class}}=P_{\text{Class}}(2\pi kT/h^2)^{N/2}\prod_{m=1}^{N} I_m^{\frac{1}{2}},$$

$$P_{\text{Class}}=\int_0^{2\pi/n_1}\cdots\int_0^{2\pi/n_N} e^{-V/kT}d\phi_1\cdots d\phi_N,$$

$$P'_{\text{Class}}=\int_0^{2\pi/n_1}\cdots\int_0^{2\pi/n_N}(V/kT)\times e^{-V/kT}d\phi_1\cdots d\phi_N,$$

$$P''_{\text{Class}}=\int_0^{2\pi/n_1}\cdots\int_0^{2\pi/n_N}(V/kT)^2\times e^{-V/kT}d\phi_1\cdots d\phi_N.$$

The potential energy, V, may or may not be expressible in simple form. If the various integrals (P, P', P'') cannot be handled directly, graphical or other numerical methods should be feasible. Satisfactory results may be obtained using Simpson's rule with points spaced at surprisingly large intervals.

This approximate method may even prove worthwhile in cases where the solution of the infinite determinant, Eq. (19), would lead to exact results but is too laborious. The two methods complement one another; that of this section is convenient and accurate for large moments of inertia and high temperatures while the exact quantum mechanical methods are necessary and not too difficult with small moments of inertia and moderate temperatures.

We have enjoyed discussions of certain phases of this work with Dr. Bryce L. Crawford.

JULY, 1942 JOURNAL OF CHEMICAL PHYSICS VOLUME 10

The Effect of Intermittent Light on a Chain Reaction with Bimolecular and Unimolecular Chain-Breaking Steps

O. K. RICE
University of North Carolina, Chapel Hill, North Carolina
(Received April 6, 1942)

The effect of intermittent light, as produced by a rotating sector, has been considered for a chain reaction having the following mechanism:

$$A_2+h\nu\rightarrow 2A,$$
$$A+B\rightarrow C+A,$$
$$2A\rightarrow \text{stable products},$$
$$A\rightarrow \text{stable products}.$$

It has been shown how to calculate the reaction rate as a function of the sector speed for different values of a certain parameter which depends on the individual rate constants and the light intensity and gives, essentially, the relative importance of the bimolecular and unimolecular chain-breaking steps. The relationships have been exhibited graphically for the case in which one-fourth of the sector passes the light beam. These relationships may be reversed, making it possible to obtain the rate constants of the intermediate reactions from measurements with intermittent light.

WHEN a photochemical reaction proceeds by a chain mechanism it is frequently found that the rate is not directly proportional to I_{abs}, but depends on some more complicated function of I_{abs}, very commonly $I_{abs}^{\frac{1}{2}}$. Whenever this is the case we may find a valuable aid in the study of the reaction in intermittent light, produced by means of a rotating sector. Now let us suppose the $I_{abs}^{\frac{1}{2}}$ law holds. If the sector is run very slowly, this is equivalent to illuminating the system a fraction f of the total time, and the rate of reaction (per unit of the *total* time elapsed), will be proportional to $I_{abs}^{\frac{1}{2}}f$. On the other hand, using a very fast sector is equivalent to cutting down the light intensity to the fraction f, and the rate will be proportional to $I_{abs}^{\frac{1}{2}}f^{\frac{1}{2}}$, which, since f is less than 1, is larger than the rate for slow sector speed. The sector speed at which the change takes place is an indication of the duration in time of the chain τ, or, what amounts to the same thing, the average lifetime of the chain-carrying radical or atom.

When using a rotating sector, it is convenient to have a sector with fixed sector fraction and to vary the speed of the sector. We are then interested in finding the rate of reaction in terms of the sector speed and the rate constants of the intermediate steps. The theoretical solution of

this problem has been completely worked out by Dickinson[1] for the following reaction scheme

(1) $A_2+h\nu\rightarrow 2A$,

(2) $A+B\rightarrow C+A$,

(3) $2A\rightarrow$stable products.

In this scheme A is a free radical or atom which carries the chain. A reacts with B to give the final product, or products, symbolized by C, in a reaction (which may take place in two or more steps) in which A is regenerated. Reaction (3) is the chain-breaking step. Variations of this scheme are readily handled. For example, A_2 may be the same as B, and if different radicals are formed, only one of which takes part in the chain, this is also easily taken care of.

TABLE I. Notation.

A, B, C, symbols for chemical substances
A, B, C, concentrations of A, B, C
$\bar{A}$, $\bar{A}_l$, $\bar{A}_d$, average value of A, average during illuminated period, average during dark period, respectively
A_s', see Eq. (9)
b, see Eq. (15) (b_0, see Eq. (4))
f, "sector fraction" (fraction of the sector permitting light to pass)
I_{abs}, light absorbed per unit volume per unit time
K, over-all rate constant of the reacting substance; is the average of $-(dB/dt)/B$, averaged over total time run has gone on, including any unilluminated periods
k_1, probability that absorption of photon results in production of free radicals
k_2, k_3, etc., rate constants of similarly numbered reactions
t_l, time of illumination per flash
t_d, time of darkness between flashes
γ, see Eq. (8)
δ, see Eq. (11)
ρ, see Eq. (14) (ρ_0, see Eq. (6))
ρ_∞, value of ρ for very fast sector
τ, "chain-time" (average lifetime of chain carrying radicals)
Subscripts on A, K, τ, ρ:
s, refers to steady state conditions under continuous illumination (lack of subscript indicates quantity is a function of sector speed)
0, refers to reaction scheme consisting of reactions (1), (2), (3) [lack of subscript indicates quantity refers to scheme consisting of reactions (1), (2), (3), (4)]

[1] R. G. Dickinson, Stanford Photochemistry Conference, 1938. See W. A. Noyes, Jr., and P. A. Leighton, *The Photochemistry of Gases* (Reinhold Publishing Company, New York, 1941), pp. 202 ff.

Application of the steady state method gives in the case of *continuous* illumination, for the schemes consisting of reactions (1)–(3), the following expression for the concentration of A

$$A_{s,0}=(k_1I_{abs}/k_3)^{\frac{1}{2}} \quad (1)$$

with the over-all rate constant of the reacting substance B (calculated as for a unimolecular reaction) given by

$$K_{s,0}=-(dB/dt)/B=k_2A_{s,0}=k_2(k_1I_{abs}/k_3)^{\frac{1}{2}}. \quad (2)$$

The rate of destruction of A is $2k_3A^2$, so that the chance of destruction of a particular A per unit time is $2k_3A$, and the average lifetime (i.e., the chain-time) at the steady state with continuous irradiation is given by

$$\tau_0=(2k_3A_{s,0})^{-1}=\tfrac{1}{2}(k_1k_3I_{abs})^{-\frac{1}{2}}. \quad (3)$$

It is found that with given sector fraction the over-all rate constant in intermittent light K_0 is a function of only one parameter, which gives essentially the sector speed, namely,

$$b_0=t_l/\tau_0=2t_lk_3A_{s,0}=2t_l(k_1k_3I_{abs})^{\frac{1}{2}}. \quad (4)$$

We can refer to Eq. (2) and write this in the form

$$b_0=2t_lK_{s,0}(k_3^{\frac{1}{2}}/k_2)k_3^{\frac{1}{2}}, \quad (5)$$

where $k_3^{\frac{1}{2}}/k_2$ can be considered known, having been experimentally determined from Eq. (2) (assuming k_1 is known or can be estimated). It is then convenient to plot the ratio

$$\rho_0=2K_0/K_{s,0}, \quad (6)$$

against $\log(t_lK_{s,0}k_3^{\frac{1}{2}}/k_2)$. The shape of this curve should theoretically be definitely fixed. Since ρ_0 is, theoretically, a known function of b_0, the curve can be used to find the value of b_0 for which $t_lK_{s,0}k_3^{\frac{1}{2}}/k_2$ has a given value. Equation (5) can then be used to find k_3; this possibility of the determination of the individual rate constants is the great advantage of the use of the rotating sector.

However, the results of experiments on acetaldehyde performed recently in our laboratory indicate that the square-root law for the intensity, as expressed by Eq. (2), does not hold precisely, and it appears necessary to consider at least one other chain-breaking step, namely

a unimolecular one.

(4) A→stable products.

The differential equations for this more complicated type of mechanism have been considered by Briers and Chapman[2] but their calculations are not cast into a form which is readily applicable to our experimental results. It, therefore, seemed that it would be worthwhile to consider this case, following the method outlined by Dickinson, and to present the results in a form which can be readily applied, not only to our own experimental work, but to those of any investigators who, in the future, carry out measurements along these lines.

The introduction of reaction (4) results in a new equation for the steady state value of A, which is obtained by setting

$$dA/dt = 2k_1 I_{\text{abs}} - 2k_3 A^2 - k_4 A = 0.$$

Solution of this equation gives

$$A_s = -\frac{k_4}{4k_3} + \left[\left(\frac{k_4}{4k_3}\right)^2 + \frac{k_1}{k_3} I_{\text{abs}}\right]^{\frac{1}{2}}, \tag{7}$$

which reduces to Eq. (1) if $k_4 = 0$. It is now found convenient to set

$$\gamma = k_4/4k_3 \tag{8}$$

and

$$A'_s = (\gamma^2 + A_{s,0}^2)^{\frac{1}{2}}, \tag{9}$$

which gives

$$A_s = A'_s - \gamma. \tag{10}$$

Further setting

$$\delta = \gamma/A_s' = (1 + A_{s,0}^2/\gamma^2)^{-\frac{1}{2}} \tag{11}$$

we have

$$A_s = \gamma(\delta^{-1} - 1) \tag{12a}$$

with the over-all rate constant given by

$$K_s = k_2 A_s = k_2\gamma(\delta^{-1} - 1). \tag{12b}$$

Of interest, also, is the equation

$$K_s/K_{s,0} = (1-\delta)^{\frac{1}{2}}/(1+\delta)^{\frac{1}{2}} \tag{13}$$

derived from Eqs. (11), (12b), and (2).

The quantity δ is the parameter which determines the relative importance of the unimolecular and bimolecular chain-breaking steps. If γ is not too large compared to $A_{s,0}$, then, from Eq. (9), $A'_s = A_{s,0}$ (correct to terms containing γ, but not terms containing γ^2), whence we get from Eqs. (11) and (8), $2\delta \leqq k_4/2k_3 A_{s,0}$; that is, in words, 2δ is equal to the ratio of the rate of chain breaking by reaction (4) to the rate of chain breaking by reaction (3) if reaction (4) did not occur. At the same time, however, the rate of chain breaking by reaction (3) decreases, since $A_s \leqq A_{s,0} - \gamma$. The decrease in the rate of chain breaking by reaction (3) is obviously in the ratio $\gamma/A_{s,0} \leqq \delta$ to the original rate of chain breaking, and hence $2\delta - \delta = \delta$ gives the net relative increase in the rate of chain breaking, and the chain time will be decreased in the ratio $1/(1+\delta)$, that is $\tau \leqq \tau_0(1+\delta)^{-1}$.

If we fix f, the sector factor, then it may be shown that for each possible value of δ from 0 to 1 (δ goes from 0 to 1 as γ goes from 0 to ∞) there is a relation, analogous to that between ρ_0 and b_0, giving the ratio in this case,

$$\rho = 2K/K_s, \tag{14}$$

as a function of a parameter which depends on the sector speed. In this case the parameter used is

$$b = 2t_l k_3 A'_s = 2t_l k_3 (A_s + \gamma). \tag{15}$$

It is clear from the remarks following Eq. (13) that b continues to be equal to t_l/τ_0 if γ is small.

The shape of the curves in this case is obtained in a way which is quite analogous to the method used by Dickinson in dealing with the simpler mechanism. We note that during the light period

$$dA/dt = 2k_1 I_{\text{abs}} - 2k_3 A^2 - k_4 A, \tag{16}$$

while during the dark period

$$dA/dt = -2k_3 A^2 - k_4 A. \tag{17}$$

Integration of these equations gives, after some rearrangement, for the light period

$$A = -\gamma + A'_s \tanh (2k_3 t A'_s + C_l) \tag{18}$$

and for the dark period

$$A = 2\gamma(\exp(k_4 t + C_d) - 1)^{-1}, \tag{19}$$

where C_l and C_d are integration constants.[3] We

[2] F. Briers and D. L. Chapman, J. Chem. Soc., p. 1802 (1928).

[3] Equation (18) is obtained from Eq. (16) by use of B. O. Peirce, *A Short Table of Integrals* (Ginn and Company), formulas No. 67 and 654, afterwards solving for A. Similarly, Eq. (19) follows from Eq. (17) using Peirce, No. 34.

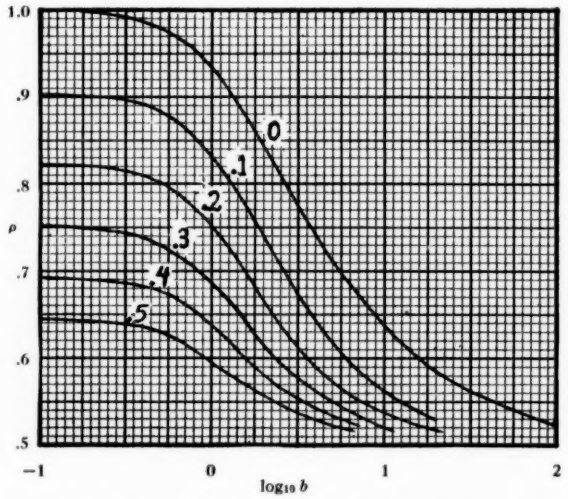

FIG. 1. The numbers on the curves indicate values of δ.

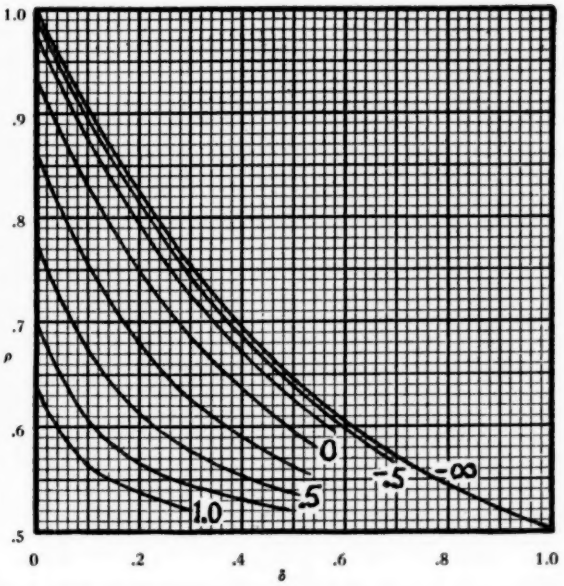

FIG. 2. The numbers on the curves indicate values of $\log_{10} b$.

do not, of course, have a steady state, but the system will quickly reach a quasi-steady state in which the sequence of events through a light and a dark period is repeated in each cycle. In this situation the constants C_l and C_d can be eliminated by use of the fact that A at the end of a light (dark) period is equal to A at the beginning of a dark (light) period. One can then by integration through the light and dark periods, respectively, evaluate the average values, $\bar{A}_l$ and $\bar{A}_d$. Now the apparent over-all rate of reaction will be proportional to

$$\bar{A}=(t_l\bar{A}_l+t_d\bar{A}_d)(t_l+t_d)^{-1}. \tag{20}$$

By evaluating $\bar{A}$ the value of ρ is readily found as a function of b for any value of f. The mathematical details are given in the Appendix.

Experimentally it has proved very convenient to let $f=\frac{1}{4}$, and in Fig. 1, we show ρ as a function of b for various values of δ with $f=\frac{1}{4}$. Curves for intermediate values of δ may be found by interpolation, and to facilitate this we give in Fig. 2 curves for ρ as a function of δ with various fixed values of b.

The limiting value of ρ when K corresponds to a very fast sector speed depends, with fixed f, only on δ. This limiting value may be found by using the proportionality of K to $\bar{A}$ and writing

$$\rho=2\bar{A}/A_s. \tag{21}$$

A_s may be evaluated by using Eq. (7) and $\bar{A}$, for a very rapidly rotating sector, may be obtained by replacing I_{abs} in Eq. (7) by fI_{abs}. Expressing the k's in terms of γ and $A_{s,0}$ we get for ρ in this case

$$\rho_\infty=\frac{2(\gamma^2+fA_{s,0}^2)^{\frac{1}{2}}-2\gamma}{(\gamma^2+A_{s,0}^2)^{\frac{1}{2}}-\gamma}=\frac{2(f\delta^{-2}+1-f)^{\frac{1}{2}}-2}{\delta^{-1}-1}. \tag{22}$$

Equation (22) may be used to determine δ for any given conditions of illumination (δ, of course, depends on I_{abs}) by performing a continuous run and a run with a rapidly rotating sector under as nearly as possible identical experimental conditions. In doing this, one will naturally determine K_s, and then, knowing δ from Eq. (22) (or Fig. 2), $k_2\gamma$ may be determined from Eq. (12b). $k_2\gamma$, it should be noted, is a quantity depending only upon the reaction constants and the temperature. The quantity $k_3^{\frac{1}{2}}/k_2$ can clearly be obtained from Eq. (7) once $K_s=k_2A_s$ has been measured, if $k_2\gamma$ is known, if I_{abs} has been determined, and if k_1 is known or can be estimated. Having $k_2\gamma$ and $k_3^{\frac{1}{2}}/k_2$, the value of k_3 itself may be obtained by experiments at various sector speeds, much as in the case of the simpler reaction mechanism. After k_3 is thus determined, k_2 and k_4 may, of course, also be found.

It is again convenient to express b in terms of the observed steady state reaction rate K_s. From Eq. (15), remembering $K_s=k_2A_s$, we have

$$b=2t_l(K_s+\gamma k_2)(k_3^{\frac{1}{2}}/k_2)k_3^{\frac{1}{2}}. \tag{23}$$

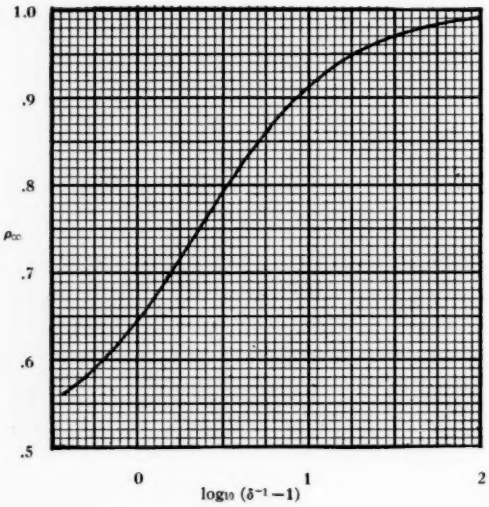

FIG. 3.

The procedure now is to plot ρ against $\log[t_l(K_s+\gamma k_2)(k_3^{\frac{1}{2}}/k_2)]$. Knowing ρ as a function of b, we find the value of b which corresponds to some particular value of $t_l(K_s+\gamma k_2)(k_3^{\frac{1}{2}}/k_2)$. Then we immediately find k_3 from Eq. (23). This, of course, assumes that δ is fixed and known. But δ does depend upon the light intensity, and it is sometimes difficult to keep the light intensity constant when experiments are performed over some interval of time. However, once $k_2\gamma$ is known δ can be readily found directly from the measured value of K_s by Eq. (12b). If the values of δ in a series of runs vary only slightly they may readily be reduced to a single value of δ by means of a set of curves such as is shown in Fig. 2.

It may be noted in closing that it may be worth while in studying a reaction to check the validity of the mechanism consisting of reactions (1)–(4) by making measurements with a very fast sector over a range of light intensities, thus varying δ. According to Eq. (22) ρ_∞ for fixed f depends only on δ. Therefore, we see from Eq. (12b) that the curve obtained by plotting $\log K_s$ against ρ_∞ should have a definite shape which can readily be calculated. It is given, for $f=\frac{1}{4}$, in Fig. 3.

APPENDIX—EVALUATION OF ρ AS A FUNCTION OF b

In using Eqs. (18) and (19) to evaluate A_l and A_d, we shall assume that $t=0$ at the beginning of a light period, and that C_l and C_d are evaluated accordingly. Then we have

$$\bar{A}_l = t_l^{-1}\int_0^{t_l} A\,dt \tag{24}$$

and

$$\bar{A}_d = t_d^{-1}\int_{-t_d}^{0} A\,dt. \tag{25}$$

Inserting Eq. (18) in Eq. (24) and using Peirce No. 448 we get

$$\bar{A}_l = -\gamma + \frac{1}{2k_3t_l}\ln\frac{\cosh\,(2k_3t_lA'_s+C_l)}{\cosh\,C_l}. \tag{26}$$

Expanding the cosh term in the numerator as the hyperbolic cosine of the sum of two arguments (Peirce No. 661) we get (using also Peirce No. 654 and noting Eq. (15))

$$\bar{A}_l = -\gamma + (2k_3t_l)^{-1}\ln[\cosh b(1+\tanh b\,\tanh C_l)]. \tag{27}$$

Now let us set $y=A/A'_s$ at $t=0$ and $x=A/A'_s$ at $t=t_l$ or $t=-t_d$ (A is the same at t_l and $-t_d$ in the quasi-stationary state). By setting $t=0$ in Eq. (18) we see, using Eq. (11), that $\tanh C_l=y+\delta$, while from Eqs. (11) and (15) we see that $2k_3t_l=b\delta/\gamma$. Equation (27) becomes

$$\bar{A}_l = -\gamma + (\gamma/b\delta)\ln\{\cosh b[1+(y+\delta)\tanh b]\}. \tag{28}$$

Evaluating $\bar{A}_d$ from Eqs. (25) and (19), using Peirce No. 410, we get

$$\begin{aligned}\bar{A}_d &= -2\gamma + (2\gamma/k_4t_d)\ln(x/y)\\ &= -2\gamma + (\gamma/b\delta)(t_l/t_d)\ln(x/y)\\ &= -2\gamma + (\gamma/b\delta)f(1-f)^{-1}\ln(x/y).\end{aligned} \tag{29}$$

$\bar{A}_l$ and $\bar{A}_d$ can be evaluated from Eqs. (28) and (29) if x and y can be found. The integration of Eqs. (16) and (17), which ultimately gives Eqs. (18) and (19), results, in the intermediate steps, in the following relations, which have been transformed with the aid of Eqs. (8), (11), and (15).

$$\tanh^{-1}(AA'^{-1}_s+\delta) = bt/t_l + C_l, \tag{30}$$

$$\ln[(A+2\gamma)/A] = k_4t + C_d. \tag{31}$$

Evaluating Eq. (30) at $t=t_l$ and at $t=0$ and subtracting the latter from the former

$$\tanh^{-1}(x+\delta) = b + \tanh^{-1}(y+\delta). \tag{32}$$

Taking the hyperbolic tangent of both sides of Eq. (32),

$$x+\delta = \frac{\tanh b + y + \delta}{1+(y+\delta)\tanh b}. \tag{33}$$

Similarly, evaluating Eq. (31) at $t=0$ and $t=-t_d$, and subtracting the latter from the former, noticing at the same time that $k_4t_d = 2b\delta t_d/t_l = 2b\delta(f^{-1}-1)$

$$\ln\frac{(y+2\delta)x}{y(x+2\delta)} = 2b\delta(f^{-1}-1), \tag{34}$$

or

$$\frac{(y+2\delta)x}{y(x+2\delta)} = \exp[2b\delta(f^{-1}-1)]. \tag{35}$$

Simultaneous solution of Eqs. (33) and (35) gives x and y. These may now be used to evaluate $\bar{A}_l$ and $\bar{A}_d$, and hence $\bar{A}$, which, together with Eq. (12a) gives ρ (Eq. (21)). It will be noticed that the factor γ appears both in $\bar{A}$ and A_s. It will cancel out when the expression for ρ is formed, and so, for given f, the ratio ρ depends solely on δ and b.

The Chain Photolysis of Acetaldehyde in Intermittent Light[1]

W. L. HADEN, JR.,[2] AND O. K. RICE
University of North Carolina, Chapel Hill, North Carolina

(Received April 6, 1942)

(1) By comparison of the data on the photochemical decomposition and the azomethane-induced decomposition of acetaldehyde vapor, it has been concluded that the chain-carrying steps in the two cases are different. For the photolysis the following mechanism is suggested:

(1) $CH_3CHO+h\nu\rightarrow CH_3+CHO$,
(2) $CHO+CH_3CHO\rightarrow CH_4+CO+CHO$,
(3) $CHO+CH_3\rightarrow$stable products (chain-ending),
(4) $CHO\rightarrow$stable products (chain-ending).

(There are possibly other chain-ending steps similar to reaction (3)). (2) Experiments have been performed using intermittent light at 200° and 300°. As a result of these experiments, estimates have been made for the individual rate constants, k_2, k_3, and k_4, and it has been found that the activation energies are 2.6, 11.3, and 7.8 kcal., respectively. (3) It has been found that k_2 and k_3 check closely with the collision number multiplied by the appropriate Arrhenius factor. There is little or no evidence of necessity for mutual orientation of the molecules. The significance of this has been discussed. Reaction (4) probably takes place at the walls, and the value of k_4 is of the same order of magnitude as the fraction of the molecules hitting the walls per second, times the appropriate Arrhenius factor. (4) The extent of and effect of diffusion of radicals beyond the illuminated region have been considered.

SOME years ago it was suggested to one of us by Dr. D. V. Sickman that the use of intermittent light, obtained by means of a rotating sector, would yield valuable additional information on the photolysis of acetaldehyde.[3] It is the purpose of the present paper to present some results of this sort, the continuation of experiments recently reported in a preliminary note.[4] The theory of the effect of intermittent light, which it will be necessary to apply, has been fully set forth in the preceding article.[5]

1. MECHANISM OF THE PHOTOLYSIS

It has been found that at elevated temperatures (between about 150° and 300°C) the rate of photolysis of acetaldehyde is proportional to the square root of the light absorbed per unit volume per unit time, I_{abs}, and to the pressure of acetaldehyde.[6] Grahame and Rollefson[6b] have noted that at low light intensities there appear to be deviations from the square root law, and we shall later see that such deviations are of some importance, but as a rough approximation to the experimental facts the above statement will suffice for the present. A number of mechanisms can be, and have been, written down which reproduce this rate law. Some of them, however, can be eliminated by other considerations. It seems to be necessary to go into these matters in some detail, in order to be able to interpret the experimental results we have to present.

All the mechanisms which have been proposed conform to the general type represented by reactions (1)–(3) of the preceding article.[5] One of the most commonly suggested mechanisms is the following:

$$\begin{array}{ll} (1) & CH_3CHO+h\nu\rightarrow CH_3+CHO, \\ (2) & CH_3+CH_3CHO\rightarrow CH_4+CH_3CO, \\ (2') & CH_3CO\rightarrow CH_3+CO, \\ (3) & 2CH_3\rightarrow C_2H_6. \end{array} \qquad \text{I}$$

The CHO radical is supposed to break up as

[1] Presented in part at the Symposium on Elementary Reactions, Division of Physical and Inorganic Chemistry, American Chemical Society, Atlantic City meeting, September, 1941. We wish to acknowledge the contribution of E. P. H. Meibohm, who constructed a considerable portion of the apparatus (Master's Thesis, University of North Carolina, 1938), and G. W. Murphy, who made some of the runs at 300° and assisted in other ways.

[2] Eastman Kodak Company Fellow, 1939–1940. Present address: Columbia Chemical Division, Pittsburgh Plate Glass Company, Barberton, Ohio.

[3] For other examples of the use of the rotating sector or other methods to measure lifetimes of atoms or radicals see F. Briers and D. L. Chapman, J. Chem. Soc., p. 1802 (1928); H. W. Melville, Proc. Roy. Soc. **A163**, 511 (1937); E. A. B. Birse and H. W. Melville, *ibid.*, **A175**, 164, 187 (1940); T. T. Jones and H. W. Melville, *ibid.*, **175**, 392 (1940).

[4] W. L. Haden, Jr., E. P. H. Meibohm, and O. K. Rice, J. Chem. Phys. **8**, 998 (1940).

[5] O. K. Rice, J. Chem. Phys. **10**, 440 (1942).

[6] (a) J. A. Leermakers, J. Am. Chem. Soc. **56**, 1537 (1934); (b) D. C. Grahame and G. K. Rollefson, J. Chem. Phys. **8**, 98 (1940). References 6a and 6b, though agreeing in outline, disagree in detail. The latter gives faster rates and lower activation energy. See also (c) E. I. Akeroyd and R. G. W. Norrish, J. Chem. Soc., p. 890 (1936).

follows:

$$(4)\quad CHO \rightarrow CO + H$$

followed by

$$(5)\quad H + CH_3CHO \rightarrow H_2 + CH_3CO,$$
$$(2')\quad CH_3CO \rightarrow CH_3 + CO.$$

Thus each CHO becomes effectively converted into CH_3, which is the chain carrier. Reaction (2) is the rate determining step, but the CH_3 concentration is determined by reactions (1) and (3). The rate is given by Eq. (2) of the preceding article, B now being CH_3CHO.

The above mechanism is essentially the same as that proposed for the decomposition of acetaldehyde as induced by the admixture of a small amount of azomethane, at temperatures at which azomethane decomposes but acetaldehyde alone does not.[7]

Reaction (1) is replaced by the following:

$$(1)\quad CH_3NNCH_3 \rightarrow N_2 + 2CH_3. \qquad \text{II}$$

Reactions II (2), (2'), and (3) are the same as the corresponding reactions in scheme I, and reactions (4) and (5) are, of course, missing, since no CHO radical ever appears. This leads to the rate law

$$-d(CH_3CHO)/dt = (k_2 k_1^{\frac{1}{2}}/k_3^{\frac{1}{2}})(CH_3CHO)(CH_3NNCH_3)^{\frac{1}{2}},$$

which agrees with the observations. If we are correct, as is almost certainly the case,[8] in assuming that the decomposition of azomethane produces methyl radicals, then it is difficult to imagine any other mechanism which will conform to a rate law of this type and at the same time give CO and CH_4 as the principal products of the decomposition.

If we accept this conclusion, however, it at once becomes apparent from a comparison of Leermakers' data on the photochemical decomposition and Allen and Sickman's on the azomethane-induced decomposition, that mechanism I for the photochemical decomposition is hardly tenable.

Before attempting to discuss this matter, however, it will be well to consider the value of k_1 for the photochemical reaction. Experiments by Gorin[9] showed that it is possible to remove radicals formed by light if a small pressure of iodine vapor is present. Methyl radicals combine with iodine to give CH_3I, and formyl radicals apparently react with each other to give H_2CO and CO. The iodine atoms released apparently recombine without further action. From analyses of the products formed in such experiments, Gorin found that about 0.7 of the molecules which absorbed light at 3130A, formed radicals (i.e., $k_1 = 0.7$). These experiments have been repeated by Blacet, Heldman, and Loeffler,[10] who found $k_1 = 0.20$, which does not agree well with the value of Gorin. Their results also disagree in some other respects from those of Gorin.* We shall, however, use Gorin's value. For k_1 for the azomethane-induced reaction we take Ramsperger's[11] value for the rate constant of azomethane at 300°, namely, 3×10^{-4} sec.$^{-1}$. The data of Leermakers and Allen and Sickman, then, indicate that $k_2/k_3^{\frac{1}{2}}$ is almost 3 times as great for the photochemical reaction as for the induced reaction. This means that, if the acetaldehyde pressure and the rates of production of free radicals are the same in the two cases, the photochemical reaction goes almost 3 times as fast, and this factor is about doubled at 200°. It appears probable from Grahame and Rollefson's and Gorin's data that the results would be practically unchanged for the photochemical decomposition at shorter wave-lengths (2500–2700A). If Grahame and Rollefson's data had been used throughout instead of Leermakers' data, however, the photochemical reaction would have appeared relatively even faster; use of Blacet, Heldman, and Loeffler's data to dedetermine k_1 would also have made the value of $k_2/k_3^{\frac{1}{2}}$, for the photochemical reaction relatively still larger both at 3130A and 2650A, though if we use their values of k_1 the resulting values of $k_2/k_3^{\frac{1}{2}}$ show considerable discrepancy as between

[7] A. O. Allen and D. V. Sickman, J. Am. Chem. Soc. **56**, 2031 (1934).

[8] T. W. Davis, F. P. Jahn, and M. Burton, J. Am. Chem. Soc. **60**, 10 (1938).

[9] E. Gorin, Acta Physicochimica **9**, 681 (1938).

[10] F. E. Blacet, J. Heldman, and D. Loeffler, paper presented to Division of Physical and Inorganic Chemistry of the American Chemical Society, Atlantic City, September 1941 (J. Am. Chem. Soc. **64**, 889, 893 (1942)).

* In particular they believe CHO to react with I_2. In view of our conclusions below, and the fact that I_2 seems to stop any chain, this may seem to be a more probable disposition of the formyl radicals.

[11] H. C. Ramsperger, J. Am. Chem. Soc. **49**, 912 (1927).

the two wave-lengths, a situation which is difficult to understand. In any event, it seems fairly certain that, under similar conditions, the photochemical reaction goes considerably faster than the azomethane-induced reaction, which is the point which we wish to establish at this time, and from which we shall shortly draw certain conclusions concerning the reaction mechanism.[12]

The values of $E_2-\frac{1}{2}E_3$ [where E_2 and E_3 are the energies of activation for reactions (2) and (3)] are, for the photochemical reaction and induced reaction, approximately 10 and 14 kcal. per mole, respectively. The slower reaction thus has the higher activation energy, as is to be expected. The Arrhenius factor $\exp[-(E_2-\frac{1}{2}E_3)/RT]$ is about 30 times as small at 300°C for the induced reaction as for the photochemical reaction, so that the difference in the reaction rates is considerably less than would be expected from the activation energies.

It has been recognized that the difference in activation energies indicates that the two chain mechanisms must differ in some respect. It has been suggested that the presence of the formyl radicals in the photochemical reaction gives a chain-breaking step involving the reaction or recombination of a methyl radical with a formyl radical, which cannot occur in the induced reaction. That this happens is altogether probable, but it is clear that the introduction of a new chain-breaking step can hardly make the photochemical reaction go *faster*. This can be explained only by a new chain-carrying mechanism.

Although it has been frequently supposed that reaction I (4) takes place very readily, evidence has been presented by Burton[13] that CHO radicals are stable up to 100°, and it seems quite likely that they will be stable up to higher temperatures. This suggests the possibility that the new chain-carrying step in the photochemical reaction involves the formyl radicals. If they react with the acetaldehyde faster than the CH_3's, then, as has already been suggested by one of us,[14] the CHO radical will be the principal chain carrier when it is present. The following mechanism appears probable:

$$\text{(1)}\quad CH_3CHO+h\nu\rightarrow CH_3+CHO,$$

$$\text{(2)}\quad CHO+CH_3CHO\rightarrow CH_4+CO+CHO,$$

$$\text{(3)}\quad CHO+CH_3\rightarrow \text{stable products,}\qquad \text{III}$$

$$\text{(3')}\quad 2CHO\rightarrow \text{stable products,}$$

$$\text{(3'')}\quad 2CH_3\rightarrow \text{stable products.}$$

The exact method by which reaction (2) proceeds is not important for the kinetic analysis of this mechanism, as long as a new CHO is always produced. It may occur in steps, and the following sequence is a possibility:

$$CH_3CHO+CHO\rightarrow CH_3-\underset{\displaystyle O}{\overset{\displaystyle H}{\overset{|}{\underset{|}{C}}}}-CHO,$$

$$CH_3-\underset{\displaystyle O}{\overset{\displaystyle H}{\overset{|}{\underset{|}{C}}}}-CHO\rightarrow CH_4+-\underset{\displaystyle O}{\overset{}{\overset{\|}{C}}}-CHO,$$

$$-\underset{\displaystyle O}{\overset{}{\overset{\|}{C}}}-CHO\rightarrow CO+CHO.$$

It may also be possible, as suggested in a private communication by Dr. M. Burton, that the CHO radical, because of its magnetic moment, induces a predissociation in an excited acetaldehyde molecule. He believes that this may be an example of a rather large class of reactions, in which the chain carrier may be a free radical or other molecule with a magnetic moment (e.g., NO or O_2).[15]

We shall assume in dealing with the photolysis of acetaldehyde that the mechanism is represented in its essential features by III, though it is not possible to assert unequivocally that all other conceivable mechanisms are excluded. It has been suggested, for example, that hydrogen atoms may take part in the chain. But if this is the case, it is difficult to find a suitable chain-

[12] Our calculation may be compared with the calculation of M. Burton, H. A. Taylor, and T. W. Davis, J. Chem. Phys. **10**, 146 (1942), which is for 2650A, is based on earlier work of G. K. Rollefson and D. C. Grahame, J. Chem. Phys. **7**, 775 (1939), and is for a value of $k_1=0.184$.

[13] M. Burton, J. Am. Chem. Soc. **60**, 212 (1938).

[14] See p. 1540 of reference 6a.

[15] See H. A. Taylor and M. Burton, J. Chem. Phys. **7**, 417 (1939).

breaking step. Such a chain-breaking step as

$$H+CH_3 \rightarrow CH_4$$

would be allowable in this case, but it appears most likely that this would require a third body. If this third body is an acetaldehyde molecule, as it would have to be, the rate of reaction would be proportional to $I_{abs}^{\frac{1}{2}}(CH_3CHO)^{\frac{1}{2}}$ instead of $I_{abs}^{\frac{1}{2}}(CH_3CHO)$ as observed. Burton[13] has given evidence that hydrogen atoms do not appear in the primary step.

There thus seem to be reasons to consider that mechanism III is the actual mechanism in the photochemical case. We may, however, anticipate at this point, and note that the results of our experiments indicate that this mechanism does still need some modification, which is unimportant at 200°C and high light intensities, but fairly appreciable at low light intensities and at 300°. What is indicated is the presence, also, of an unimolecular chain-breaking step. This is anticipated by the remark of Grahame and Rollefson to the effect that at low light intensities the rate appears to fall below the expected value. They attributed this effect to a chain-ending process at the walls, and the considerations of Section 6 below make it appear quite probable that this interpretation is correct. Though the CHO radical may be fairly stable, it would not be at all surprising if, to a limited extent and especially at the walls, it did undergo direct decomposition according to the reaction

$$(4)\quad CHO \rightarrow CO+H. \qquad \text{III}$$

This was postulated in mechanism I. There it was supposed that the hydrogen atoms reacted in such a way as to produce eventually a methyl radical. Since it appears that CH_3 reacts much more slowly with acetaldehyde than CHO, this would mean that reaction (4) would be essentially a chain-breaking step. However, if reaction (4) takes place at the walls, it is more than likely that the hydrogen atoms are adsorbed, later to appear as hydrogen molecules.

It is, of course, not possible to decide definitely between the various chain-breaking steps suggested in mechanism III. For the purpose of discussion, we shall assume reaction III (3) to be the principal one, with reaction III (4) playing a subsidiary but rather important role. We shall also assume that the concentrations of CH_3 and CHO are equal, which can only be strictly true, of course, under conditions such that III (4) is negligible, unless the methyls also disappear at the wall to the same extent as the formyls. Otherwise, there would be a tendency for CH_3 to accumulate until finally reaction III (3″) occurred to a sufficient extent to stop further accumulation. An increase in concentration of CH_3, if neglected in the calculations, would show up in an apparent increase in k_3. The extent and accuracy of our results, however, do not warrant the attempt to iron out all minor inconsistencies in the mechanism, and the assumptions we choose apparently make up a reasonably good working hypothesis.

It is to be noted that reaction III (1) produces but one CHO radical and reaction III (3) destroys but one. In this way they differ from reactions (1) and (3) of the preceding paper. This will be corrected for if in all formulas we substitute $k_1/2$ for k_1 and $k_3/2$ for k_3. In particular we have

$$b=t_l(K_s+k_2\gamma)(k_3^{\frac{1}{2}}/k_2)k_3^{\frac{1}{2}} \qquad (1a)$$

and

$$\gamma=k_4/2k_3. \qquad (1b)$$

2. EXPERIMENTAL PART

Preparation of Acetaldehyde

The acetaldehyde used was prepared from Eastman paraldehyde which had been fractionated through a long vacuum jacketed silver column. The paraldehyde was depolymerized by the addition of a few drops of dilute sulfuric acid, and the operation was carried out in the kettle of the same fractionating column. Thus the acetaldehyde was fractionated as it was formed. Because of the low boiling point (20.2°) of acetaldehyde, it was necessary to run ice water through the condenser, and to cool the portion of the reflux system not enclosed in the vacuum jacket to prevent superheating of the vapor. The latter operation was satisfactorily done by wrapping with cloth and saturating the cloth occasionally with acetone, thus cooling by evaporation.

The acetaldehyde was collected in a reservoir, which was sealed to a vacuum line after cooling the acetaldehyde to a safe point. It was then distilled back and forth between traps on the line, in order to remove any dissolved air and was occasionally distilled later to remove any polymer which might have formed.

According to Letort[16] the thermal decomposition of acetaldehyde is very sensitive to traces of air. It is probable

[16] M. Letort, J. Chim. Phys. **34**, 265 (1937).

that this is true of the photochemical reaction, also. We believe, however, that in the experiments reported any effect of traces of air has been eliminated. Our procedure was to make several runs with the same sample of acetaldehyde, and the total amount of decomposition was never over a few percent. Between runs the acetaldehyde was frozen out in a liquid-air trap and all permanent gases were pumped off. The results obtained in such a series of experiments were generally quite consistent, except for the first one, which was likely to be high. We attributed this to a trace of air remaining in the acetaldehyde and always discarded this preliminary run, at least in the later series of experiments.

The Reaction System

The reaction system consisted of a quartz cell 9.9 cm long and 2.43 cm in diameter, which was connected to the rest of the system by a Pyrex quartz seal. The acetaldehyde reservoir was connected to the reaction cell through a mercury cut-off. On the other side of the reaction cell was a manometer, a trap for freezing out the acetaldehyde, and another mercury cut-off. Beyond the second cut-off was the analytical apparatus, which has been described elsewhere.[17] The cell was placed in the center of a fairly large furnace, the temperature of which was controlled by automatic regulation. The temperature was measured by an iron-constantan thermocouple which was calibrated from the cooling curve of tin. The temperatures given are probably correct to within $\pm 2°$, but the variation of temperature during a run, or between runs made close together, was almost always considerably less than 1°.

The Optical System

The source of ultraviolet light was a capillary high pressure mercury arc of the type described by Daniels and Heidt.[18] This was enclosed in a water-cooling jacket made of Pyrex tubing, and the leads from the arc were passed through a rubber stopper at the top of the tube. The water was introduced at the bottom of the tube, and there was a large outlet near the top. A small heating coil, consisting of about six turns of No. 24 Chromel wire was placed at the lower end of the arc to heat the mercury and start the arc, and the cooling water was turned on as soon as the arc flashed. In order to allow free transmission of the 3130A line, a small hemisphere about 1 cm in diameter was blown on the Pyrex jacket opposite the arc. This acts both as a thin glass window and as a lens when the water is run through, focusing the light to a considerable extent. The light was further collimated by a fused quartz lens which rendered it nearly parallel or only slightly divergent at the reaction cell. The light was then passed through 1.55 cm of a 0.001 *M* solution of K_2CrO_4 in 0.05 *M* KOH and a Corex red-purple A filter 3 mm in thickness. This combination gives fairly good purity of radiation near 3130A, but transmits a small amount of visible light, which does not affect the acetaldehyde.

The light then entered the reaction cell, which had plane fused quartz windows. Over the window near the light source was placed a diaphragm with an opening 1.35 cm in diameter to prevent light striking the sides of the cell.

The measurement of light intensity was carried out by means of a Weston photronic cell, type 2, with a quartz window. The photo-cell was used only as a qualitative indicator of light intensity, and to maintain the intensity constant over a series of runs. Absolute intensities were calculated, by comparison with Grahame and Rollefson's results, from the rate of reaction in continuous light.

The rotating sector consisted of a cardboard disk from which a section of 90° was cut. From another sector four symmetrical sections of 22.5° each were cut. The disk was mounted on a ball-bearing shaft and was driven by a belt from a friction drive stirring motor. The speed could be varied by adjusting the friction disk on the motor, or by use of a rheostat in series with the motor. The speed was measured stroboscopically.[19]

Experimental Procedure and Errors

After the lamp had been lit and had come to a steady condition, and the optical system had been adjusted, a photo-cell reading was made, the light beam was intercepted by a shutter, and the acetaldehyde was admitted to the reaction cell. When the acetaldehyde was in the cell, the shutter was removed from the light path, and the cell was illuminated. Generally this illumination lasted between one and ten minutes. At the end of the run the light beam was interrupted, liquid air was placed on the trap, and the gas drawn through the trap to the analytical apparatus,[17] after which another photo-cell reading was made. The gas was first brought into contact with a pellet of moist KOH to remove any traces of acetaldehyde which might have escaped through the liquid-air trap. The pressure of the remaining permanent gas, consisting chiefly of CO and CH_4, was then measured in a previously calibrated volume, and the room temperature was noted.

The runs were always made in pairs, and a run with intermittent illumination was compared with an immediately following or preceding run with continuous light (or the average of both), performed under conditions as nearly similar as possible. In any given series of runs in which the optical set-up remained unchanged, the results were generally very reproducible. When it became necessary to replace a lamp, necessitating refocusing, the same deflection on the galvanometer attached to the photo-cell as previously used resulted frequently in a different rate of reaction. The reproducibility in this respect seemed less good at 300° than at 200°, and at 300° variations in rate amounting in the extreme to 25 or 30 percent were found. On one occasion at 300°, when the experiments were running quite smoothly, it was found that a new sample of acetaldehyde gave a 25 percent increase in rate without any change in the optical system, but, unfortunately, the lamp stopped

[17] W. L. Haden, Jr., and E. S. Luttrupp, Ind. Eng. Chem., Anal. Ed., **13**, 571 (1941).

[18] F. Daniels and L. J. Heidt, J. Am. Chem. Soc. **54**, 2381 (1932).

[19] See A. Farkas and H. W. Melville, *Experimental Methods in Gas Reactions* (Macmillan, 1939), p. 241.

after one preliminary (discarded) run, one continuous run, and one intermittent run were made, so this could not be further checked. In spite of these variations in individual rates, the ratio of the rate in intermittent light to that in continuous light was extremely reproducible.

If one seeks possible causes for the lack of reproducibility observed, he finds it rather difficult to understand. It is true that if the light is somewhat differently focused from time to time the illuminated volume will vary. If a given total amount of light falls on the system, an increase in the illuminated volume will decrease the light intensity as much as it increases the amount of gas illuminated. However, with the rate depending approximately on the square root of the light intensity, it is seen that the decrease in intensity is not as important as the increase in volume of gas reached. Now our optical system was by no means ideal as regards the matter of having a known and constant illuminated volume, but an increase in rate of 25 percent would require an effective increase in illuminated volume of more than 50 percent, and this amount of variation we believe to be considerably larger than could have occurred. Furthermore, our results indicate that the chain lasted long enough for free radicals to diffuse to an appreciable extent toward the wall, which effect would tend to equalize the effective volumes. If the cell were completely filled with radicals it would not matter where they were formed, and the situation would be equivalent to illuminating the entire cell with light of lower intensity. Unfortunately, this ideal condition could not be realized, either, in the most important series of experiments.

On the other hand, if we are to refer the observed error to the photo-cell, it must be noted that to explain a 25 percent variation in rate, again a 50 percent variation in intensity is necessary. That the photo-cell should vary in sensitivity by such a factor because of slight changes in the position of the light beam also seems unlikely.

In general, resetting of the optical system was accompanied by the introduction of a new sample of acetaldehyde. It seems difficult to believe that our acetaldehyde could have varied sufficiently to give 25 percent difference in rates, although it may be sensitive to such things as small amounts of polymer which might be present. As stated before, we believe we eliminated any oxygen.

In handling the results, our procedure has been to assume that the observed rate is a better measure of the intensity than the photo-cell readings. Whether or not this is justifiable, it leads to excellent correlation of the data.

3. RESULTS AT HIGH SECTOR SPEEDS WITH VARYING LIGHT INTENSITY

We shall first consider results obtained with very fast sector speeds (60 light flashes per sec. is sufficient—see Section 4), at 200° and an acetaldehyde pressure of 10 cm. Towards the end of the preceding paper[5] it was suggested that we should plot $\log K_s$ against ρ_∞ and compare with the theoretical curve. (Here

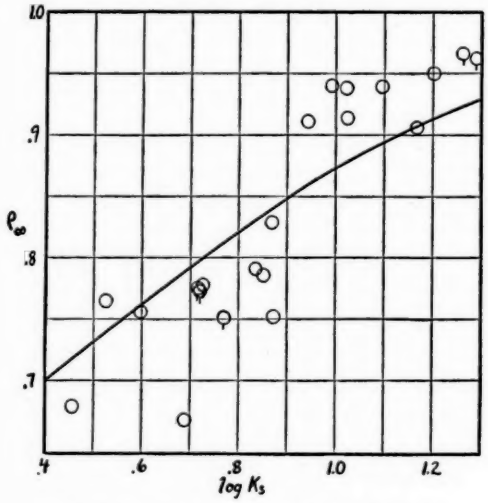

FIG. 1. Experiments at high sector speed.

$K = -(CH_3CHO)^{-1}d(CH_3CHO)/dt$ with the subscript s referring to the case of continuous illumination, and ρ is defined by Eq. (14) of the preceding article. ρ_∞ refers to rapid sector speed.) Essentially this has been done in Fig. 1. However, on account of the possible doubt expressed above, as to the effective volume of the reaction cell, we have preferred to use a special set of units for K_s, so that it may be closely related to the experimental data. We have, therefore, used the pressure in cm of non-condensible product gases, (essentially $CO+CH_4$) measured dry at 25°C, in a calibrated volume of 0.100 cc, (or corrected to the equivalent thereof) produced by 1 minute of continuous irradiation of acetaldehyde at 10.0 cm pressure and 200°C. This, of course, assumes that the illuminated volume is constant, though unknown, and does not eliminate errors caused by variation in the illuminated volume. The gases were actually measured wet, so a correction was made for water vapor pressure, as well as corrections for slight changes in conditions, as room temperature and pressure of acetaldehyde (which was always within 2 or 3 percent of 10.0 cm). Most of these runs (plain circles) are from a single series which was performed within a limited time using 120 flashes per second and varying the light intensity. The circles with tails represent runs done at various times in the course of the research—some of these were at 60 flashes per second. All runs performed after December 1,

1940, at 10 cm and 60 or 120 flashes per second are included, except a few which were spoiled.

The theoretical curve, from Fig. 3 of the preceding paper, is shown in Fig. 1 for comparison with the experimental points. Only the shape of it is important; since the actual rate constants are not yet known, the theoretical curve may, for comparison, be shifted arbitrarily along the axis of abscissas, thus determining $k_2\gamma$ (see Eq. (12b) of the preceding article). The curve shown corresponds to a value of $k_2\gamma = 1.58$, in the units described above.

It is probably true that the experimental points fit the theoretical curve within the limits of accuracy; however, there seems to be a trend in the experimental points toward a more rapid decrease than is anticipated theoretically in ρ_∞ as K_s decreases, and this may well be real. If K_s were proportional to $I_{abs}^{\frac{1}{2}}$ throughout the range, ρ_∞ would remain at 1. The fact that ρ_∞ falls off from 1 indicates that at low values of K_s, i.e., at low I_{abs} values, K_s is beginning to deviate in the direction of proportionality to I_{abs} instead of $I_{abs}^{\frac{1}{2}}$; this means that at these low intensities K_s decreases more rapidly than $I_{abs}^{\frac{1}{2}}$. The trend in the experimental results means that the onset of this effect comes in more suddenly than mechanism III would lead one to expect. A probable explanation of this is that reaction (4), which probably occurs at the walls, increases in importance at the lower light intensities. The chain time, of course, increases as the light intensity decreases. From the calculation in the Appendix, it may be inferred that the rate of diffusion of radicals is such that probably only a moderate number of them get to the wall at the highest intensities used by us, but that they begin to reach the walls in large numbers at only slightly lower intensities. The result is an effective increase in k_4 at the low intensities. If the choice of chain-breaking step, made at the end of Section 1, is correct, we might also expect an apparent increase in k_3 under these conditions, which would also contribute to the discrepancy observed. On the other hand, the greater diffusion which takes place at low light intensities has a tendency to lower the concentration of free radicals, which would then be expected to have a relatively longer life period, thus causing K_s to decrease abnormally slowly rather than abnormally rapidly. However, this would probably only partially counterbalance the effect of the changes in k_4 and k_3.

4. RESULTS WITH VARYING SECTOR SPEEDS

A large number of runs were made at 10 cm and 200°C, with varying sector speeds and at a number of different light intensities. With the exception of a few which were done at odd light intensities and those known to be spoiled, all done after December 1, 1940 are presented in Table I. K_s is expressed as described in the preceding section. The value of K_s is always taken from a continuous run just preceding or just following the intermittent run (or it is the average of such runs). The conditions for the continuous run were always kept as near as possible to those of the intermittent run. Slight variations in conditions were corrected for; in particular, slight variations in light intensity, as recorded by the photo-cell, were corrected for by assuming the rate to be proportional to the square root of the intensity, and this was sufficiently good for the small corrections involved. The corrections were always applied to the continuous run. The value of δ, which is the parameter determining the relative importance of the chain-breaking steps III (3) and III (4), was obtained from K_s by means of Eq. (12b) of

TABLE I. Experiments at 200° and 10 cm. $k_2\gamma = 1.585$.

K_s	Flashes per sec.	ρ	δ	δ(corr.)	ρ(corr.)	$l/(K_s+k_2\gamma)$
3.30	½	0.540	0.325	0.35	0.537	2.44
3.30	1	.570	.325		.563	1.220
2.78	2	.668	.3635		.675	.545
2.97	½	.535	.348		.534	2.275
2.86	1	.592	.356		.595	1.110
2.74	2	.612	.366		.619	.540
2.69	4	.682	.370		.694	.267
2.72	8	.666	.368		.675	.1343
7.96	1	.652	.1659	.17	.650	2.385
7.41	4	.804	.1760		.809	.562
7.59	15	.766	.1730		.768	.1528
19.52	120	.962	.0750	.075	.962	.0440
18.28	60	.966	.0799		.970	.0828
18.54	32	.901	.0788		.904	.1572
18.75	16	.953	.0779		.955	.318
20.20	32	.945	.0728		.943	.1702
20.24	2	.710	.0725		.708	2.73
20.32	4	.787	.0723		.785	1.369
21.00	8	.886	.0702		.882	.706
20.73	1	.601	.0710		.598	5.58
19.95	½	.576	.0736		.575	10.76
28.47	8	.884	.0527	.050	.886	.939
30.20	4	.773	.0498		.773	1.986

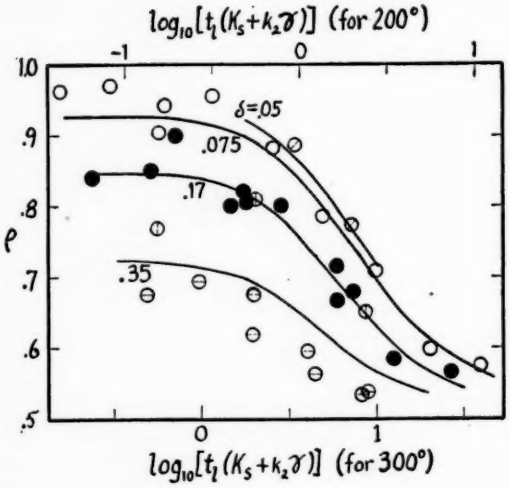

FIG. 2. Experiments at 10 cm, varying sector speeds. Open circles, 200°, with values of δ as follows: ⊘, 0.05; ○, 0.075; ⊕, 0.17; ⊖, 0.35. Black circles, 300°, $\delta=0.17$.

the preceding article,[5] using $k_2\gamma=1.58$, as determined in Section 3. It will be noted that in Table I the runs occur in groups, clustering around certain values of δ. To get a basis of comparison all the runs in a group were corrected to a definite value of δ, as shown in the table. These corrections were made holding $t_l(K_s+k_2\gamma)$ constant (which is equivalent to holding b, of the preceding article, constant) and determining from Fig. 2 of the preceding article, how much ρ should be changed to correspond to the indicated change in δ.

A similar set of results at 300° and 12.1-cm pressure (same concentration as 10-cm pressure at 200°) is shown in Table II. The value of $k_2\gamma=16.9$ was obtained directly from the runs at 60 and 120 flashes per second. It was assumed that in these runs $\rho=\rho_\infty$, the value of δ then being obtained from the uppermost curve of Fig. 2 of the preceding article. $k_2\gamma$ was then obtained directly from Eq. (12b) of the preceding article, and the average taken for the two runs noted. The non-condensible gas produced was measured in a larger calibrated volume, but the results are corrected to 0.100 cc, so the units are the same as in Table I. The last five runs of Table II were made by Mr. G. W. Murphy; they were the last five made by him. Some runs made before these, which were very erratic, were discarded on the grounds that this operator had not yet become familiar with the technique.

Since the selection of the value of $k_2/k_3^{\frac{1}{2}}$ from the data of previous investigators needs some discussion, and since K_s is in special units, it seemed advisable to plot ρ against log $[t_l(K_s+k_2\gamma)]$ in this instance, a slight deviation from the procedure recommended in the preceding article. $t_l(K_s+k_2\gamma)$ is proportional to b at any temperature, and results at different temperatures can be compared on the same graph by displacing the origins of abscissas with respect to each other. This has been done in Fig. 2, where a comparison of all the data with theoretical curves is given. It is seen that the agreement is as good throughout as could be expected from Fig. 1.

Since the deviation in Fig. 1 is probably real, however, it seems more reasonable, when attempting to calculate rate constants and consider temperature coefficients, to use the value of $k_2\gamma$ actually corresponding to the curve for the particular value of δ. Thus if we calculate $k_2\gamma$ for the set of runs with $\delta=0.075$ in Table I in a way similar to that used to calculate $k_2\gamma$ for Table II, we find, approximately, $k_2\gamma=0.79$. If now we recalculate δ on this basis, we find the values cluster about 0.04 rather 0.075. The results thus obtained were corrected as before and are shown in Fig. 3, which includes, also, the results at 300°, but only the one set of results at 200°. The latter were (save for two runs) the most recent runs made at 200°, and are, we believe, the most reliable. Furthermore, the conditions as to light intensity were closely comparable to those at 300°. We shall, therefore, use Fig. 3 as a basis for the calculation of rate constants and temperature coefficients.

TABLE II. Experiments at 300° and 12.1 cm. $k_2\gamma=16.9$, δ(corr.)$=0.17$.

K_s	Flashes per sec.	ρ	δ	ρ(corr.)	$t_l(K_s+k_2\gamma)$
74.0	8	0.788	0.186	0.800	2.84
76.8	4	.708	.180	.715	5.86
75.8	16	.791	.182	.801	1.449
69.0	30	.879	.197	.900	.715
83.6	2	.586	.168	.585	12.58
78.7	4	.662	.177	.666	5.97
99.4	16	.826	.146	.805	1.819
100.0	4	.696	.145	.678	7.30
104.2	60	.875	.140	.850	.505
97.9	120	.859	.148	.840	.239
92.0	16	.831	.155	.820	1.701
89.1	1	.570	.159	.566	26.5

5. CALCULATION OF THE RATE CONSTANTS

In order to evaluate K_s in absolute terms, it is necessary to know the effective volume in which the reaction occurs. This will necessarily depend upon the diffusion of the free radicals, for if the radicals can diffuse out of the light path to any appreciable extent, the effect becomes that of a less intense beam illuminating a larger volume. An approximate treatment is given in the Appendix. The effective volume in our experimental set-up is estimated to be 35 cc, which enables us to convert K_s to sec.$^{-1}$. The conversion factor for 200°C is

$$0.100/35\times0.50\times473/298\times1/60\times1/10 = 3.78\times10^{-6}.$$

The first fraction converts from the calibrated volume to 35 cc, the second term relates the number of molecules of acetaldehyde decomposed to the number of permanent gas molecules formed, the third factor corrects the temperature to the furnace temperature, the fourth converts min.$^{-1}$ to sec.$^{-1}$, and the denominator of the last factor is the pressure of the acetaldehyde. For 300°C the conversion factor is the same, since the pressure is 12.1 cm, which compensates the change in temperature.

Since we made no determination of the absolute intensity of our light source, it is necessary to evaluate $k_2/k_3^{\frac{1}{2}}$ from the work of previous investigators. On account of the wide light beam used, it may be shown that the diffusion in Grahame and Rollefson's experiments[6] at high intensities is not important. Since they based their calculations on the actual illuminated volumes, and since their intensity was high at 200° and 3130A, it seems reasonable to use their value of $k_1^{\frac{1}{2}}k_2/k_3^{\frac{1}{2}}$ of 40 Einsteins$^{-\frac{1}{2}}$ cc$^{\frac{1}{2}}$ sec.$^{-\frac{1}{2}}$. With a value of k_1 of 0.7, following Gorin,[9] we then get $k_2/k_3^{\frac{1}{2}}=48$.

However, because their light intensity at 300° was considerably lower, and since the unimolecular chain-breaking step seems to be much more important at 300°, we do not believe we should use their temperature coefficient. Rather, for this purpose, we turn to the work of Leermakers,[6] since his light intensity was considerably higher. The difference between Grahame and Rollefson's and Leermakers' results at 200° undoubtedly rests largely on the fact that the former based their calculations on the actual illuminated volume, while Leermakers assumed his radicals diffused uniformly through the cell. In this assumption, Leermakers was, with his high light intensities, undoubtedly wrong. If we assume Grahame and Rollefson's constants to be correct, we find that Leermakers' effective volume must have been 15 cc. With a cell of 41-cc capacity, and his set-up, this is not unreasonable, though perhaps slightly low. Using 15 cc, the value of I_{abs} in most of Leermakers' experiments at about 10-cm pressure was about 10^{-10} Einstein per cc per sec., while for their highest intensity, at around 10 cm, Grahame and Rollefson's I_{abs} was about 10^{-11} Einstein per cc per sec. Leermakers' very high light intensity should make the diffusion fairly small, and should assure that a correct value of the activation energy $E_2-\frac{1}{2}E_3$ of $k_2/k_3^{\frac{1}{2}}$ will be obtained from the results. We, therefore, adopt his value of 10 kcal. per mole.[20] We feel that this is a very

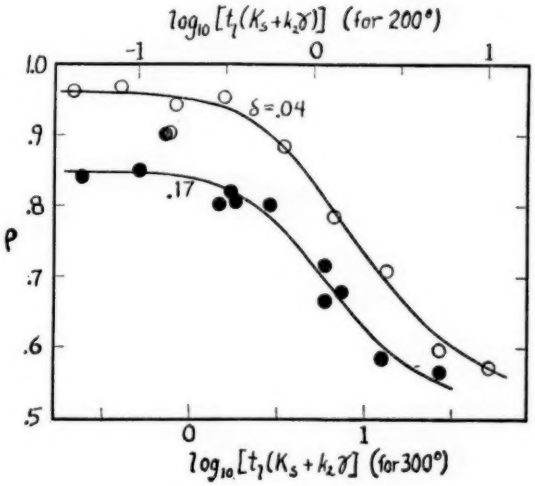

FIG. 3. Experiments at 10 cm, varying sector speeds. Open circles, 200°, $\delta=0.04$. Black circles, 300°, $\delta=0.17$.

[20] If we compared runs at equal deflections of the galvanometer, we found a temperature coefficient not higher than Grahame and Rollefson's. As stated, however, we do not believe our intensity measurements are comparable unless the optical system is left practically unchanged. A few runs, made later by Mr. G. W. Murphy, during which the optical system was kept as constant as possible, gave a very consistent set of results, though their absolute rates appeared much higher than we expected for the galvanometer deflections obtained. These checked Leermakers' temperature coefficient almost exactly.

TABLE III. Summary of rate constants.

Symbol	Units	Expt. rate constants At 200°	Expt. rate constants At 300°	Act. energies Cal. per mole reaction	Collision numbers At 200°	Collision numbers At 300°
$k_2/k_3^{\frac{1}{2}}$	$mole^{-\frac{1}{2}}$ $cc^{\frac{1}{2}}$ $sec.^{-\frac{1}{2}}$	48	306	10,000		
k_3	$mole^{-1}$ cc $sec.^{-1}$	4.0×10^{14}	6.6×10^{14}	2,600	1.9×10^{14} 0.21×10^{14}*	2.1×10^{14} 0.34×10^{14}*
k_2	$mole^{-1}$ cc $sec.^{-1}$	9.7×10^{8}	7.8×10^{9}	11,300	1.5×10^{9}*	1.2×10^{10}*
k_4	$sec.^{-1}$	2.5	10.8	7,800	12*	49*

* These collision numbers have been multiplied by the appropriate Arrhenius factor.

reasonable solution of the difficulty regarding the temperature coefficients, though the fact that in our experiments the reproducibility as regards the rate of reaction observed for a given current from the photo-cell appears to be less good at 300° than at 200°, together with the fact that the unimolecular chain-breaking reaction appears to be more important at 300°, suggests the possibility that an unreproducible wall reaction at 300° may affect the results. This matter obviously needs further investigation.

With K_s known in absolute units, and with $k_3^{\frac{1}{2}}/k_2$ evaluated, it is a simple matter to find k_3 itself. Comparison of Fig. 3, in which the abscissa is given in terms of the experimental value $t_l(K_s+k_2\gamma)$, with the theoretical curve in which the abscissa is the log of the defined quantity $b=t_l(K_s+k_2\gamma)(k_3^{\frac{1}{2}}/k_2)k_3^{\frac{1}{2}}$ (see Eq. (1a)) tells us what value of $t_l(K_s+k_2\gamma)$ corresponds to a given value of b, thus enabling us to solve for k_3. Knowing k_3 and $k_3^{\frac{1}{2}}/k_2$ we find k_2; knowing k_2, k_3, and $k_2\gamma=k_2k_4/2k_3$ (see Eq. (1b)) we find k_4. The results are given for 200° and 300° in Table III. The corresponding activation energies are also given. Included also, for comparison, are certain theoretically calculated quantities, which will be discussed below.

The values in Table III are not to be considered as highly accurate, but the orders of magnitude are undoubtedly correct. An idea of the possible errors involved may be obtained by calculating k_3 for 200° from Fig. 2 instead of Fig. 3, using the same set of runs. If we do this we find $k_3=2.1\times10^{14}$, differing by an almost twofold factor from the value tabulated. Further, there is some uncertainty in $k_2/k_3^{\frac{1}{2}}$ itself, due in greatest measure to uncertainty in k_1. The value of k_3 given is, then, certainly a rough approximation; but it is of great interest, nevertheless, and is correct to within the same order of accuracy as it is generally possible to determine the frequency factor of the rate constant of a chemical reaction. k_2 is probably about twice as accurate as k_3 (outside of possible error from k_1) since it is calculated from a relation involving $k_3^{\frac{1}{2}}$. k_4 at 200°, calculated from Fig. 2, is about 50 percent greater than calculated from Fig. 3. It is quite possible, however, that the errors in k_4 are larger than this would indicate. Since, as seen from Fig. 1, the theoretical equation for the rapidly moving sector is not exactly obeyed, the significance of k_4, found by applying this equation, is in some doubt, and the number of runs at 300° is small. We do not believe that these same doubts apply with anything like equal force to k_2 and k_3, at least at high intensities where the importance of the unimolecular chain-breaking step is not great. On account of the greater importance of the unimolecular reaction at 300°, they may affect the temperature coefficient of k_2 and k_3 somewhat. For example, if we should neglect the unimolecular chain-breaking reaction at both temperatures, we would get an energy of activation E_3 of over 13 kcal. This is so large as to be utterly impossible, as will be clear from the discussion in the next section. Therefore, the fact that the value of E_3 in Table III is quite reasonable lends some confidence in the validity of our calculation of k_4.

6. INTERPRETATION OF THE RESULTS

It is, of course, not absolutely certain which of the chain-breaking steps in mechanism III is the principal one. However, as a matter of fact, it is not very important for the purpose of interpreting the numerical results given in Table III, and we shall simply assume, as at the end of Section 1, that reaction III (3) is the correct one. It is then indicated that we should

compare k_3 with the collision number for CHO and CH_3 (by collision number we mean the number of collisions per cc per sec. with both substances at unit concentration). This calculated collision number (based on an effective σ^2 of 10^{-15} cm^2, σ being the collisional diameter) is given in the last columns of Table III. The effective collision number, i.e., the collision number multiplied by the Arrhenius factor $e^{-2100/RT}$ is also given.[21] It is seen that k_3 is of the same order of magnitude as the collision number. The Arrhenius factor reduces the effective collision number to the point where it is one-twentieth of k_3. In view of the various uncertainties involved, both in k_3 itself and its temperature coefficient, as well as in σ, such a factor is probably within the expectations. It would appear to indicate, however, that the value of E_3 is probably somewhat less than 2600 cal., and that we may reasonably certainly say that E_3 lies between 2600 cal. and $\frac{1}{2}RT \sim 500$ cal.

Since reaction occurs at practically every available collision, it is seen that the reaction is not slowed down to any appreciable extent by the necessity of mutual orientation of the reactants. The reaction is, therefore, a case in which the "hypothesis of exact orientation"[22] does not hold. This would be unexpected if the reaction involved transfer of an atom and formation of CH_4 and CO. It would, perhaps, seem less surprising if the collision of CH_3 and CHO resulted in the formation of a molecule of acetaldehyde.[23] There are other cases in which methyl radicals do not seem to need to be completely oriented;[22] we have had, of course, little experience with CHO radicals.

The theoretical value of k_2 is calculated in essentially the same way as k_3. k_2 is compared with the collision number for CHO with CH_3CHO (again calculated using $\sigma^2 = 10^{-15}$ cm^2) multiplied by $e^{-10,800/RT}$. It again appears that reaction occurs at practically every collision in which the necessary energy is available, showing little or no effect of orientation. This is certainly surprising if an ordinary chemical reaction, such as addition of the CHO to acetaldehyde, as suggested in Section 1 is involved. It may, perhaps, be taken as evidence in favor of the suggestion of Burton that the CHO induces a predissociation in the acetaldehyde, provided some certain degree of freedom in the latter is already at the proper energy, presumably corresponding to the crossing of a repulsive potential energy curve with an attractive one, though the predissociation must be induced with extremely high efficiency. The energy at which the crossing occurs is close to $E_2 - \frac{1}{2}RT + RT \cong 11.8$ kcal., or about half a volt, above the lowest point of the potential-energy curve of the ground state.

Although this interpretation seems most reasonable on the basis of the photochemical reaction alone, it is not entirely satisfying when one considers the azomethane-induced reaction. If the chain-carrying step of this reaction differs merely in that a methyl radical, instead of a formyl radical, induces the predissociation, one could, indeed, suppose that reaction I (2) would be slower, but one would hardly surmise that it would have a higher activation energy, since this quantity should depend entirely on the properties of the acetaldehyde. Yet Allen and Sickman's experiments on the induced reaction indicate that E_2 must be appreciably higher than is the case with the photochemical reaction. The explanation of this apparent anomaly is not clear.

In the case of k_4, the values in Table III offer rather good evidence that the unimolecular chain-breaking step does not occur in the gas phase. If it did occur in the gas phase it certainly could not be a strictly first-order reaction, but, rather, it would be an unimolecular reaction in the low pressure, second-order stage. CHO is such a small molecule that one would expect that once it attained the necessary activation energy it would decompose before the next collision. It ought to react, therefore, after every collision with acetaldehyde in which it obtains the necessary energy, and this would be the total number of collisions multiplied by the Arrhenius factor $e^{-7300/RT}$. However, it will be noted that CHO reacts with acetaldehyde in a chain-carrying step only if there is available a

[21] The energy of activation, 2600 cal., given in Table III, includes the intrinsic collisional activation, $\frac{1}{2}RT$ of collision. (See H. Gershinowitz and O. K. Rice, J. Chem. Phys. **5**, 275 (1934). The collisional activation energy has been subtracted out in calculating all Arrhenius factors.

[22] O. K. Rice and H. Gershinowitz, J. Chem. Phys. **3**, 479 (1935).

[23] See E. Gorin, Acta Physicochimica **9**, 692 (1938).

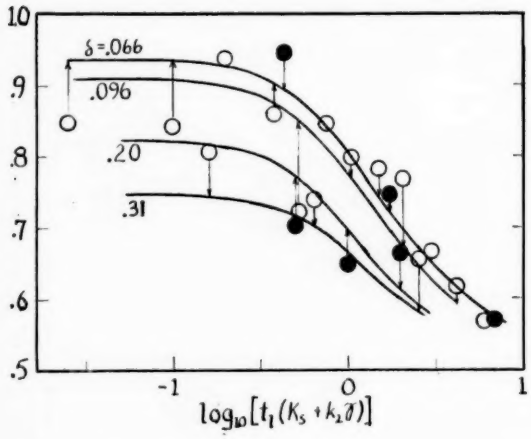

FIG. 4. Experiments at higher pressures and 200°. Open circles, 20 cm. Black circles, 40 cm. Arrows indicate the curve on which point should lie.

higher excess energy than 7300 cal. If the chain-breaking step did, therefore, go in the gas phase, it ought to go faster than the chain-carrying step, which does not happen, and would, indeed, be an impossibility. Therefore, we believe that reaction III (4) must be a wall reaction. Accordingly, we have calculated the number of collisions with the walls. The figure given in Table III is the total number of collisions with the walls, taking into account the whole surface of the reaction vessel, divided by the total number of CHO's in the reaction vessel, assuming them uniformly distributed throughout the whole vessel, multiplied by $e^{-7300/RT}$. Since the total number of collisions and the total number of radicals are both proportional to the concentration, the quantity given is independent of the concentration, and is directly comparable to k_4. Since the assumption of uniform distribution is not correct, it is certainly not surprising that the calculated values are larger than the observed.

It should be noted that the experimental k_4's given are apparent values for high light intensities. At low intensities k_4 does actually appear to increase, as we have already noted, corresponding to the expectation for a more uniform distribution of radicals. It should be emphasized, however, that in view of the uncertainties involved in the determination of k_4, no exact correspondence between experimental and calculated values could be looked for. The check in order of magnitude does seem likely to be significant.

7. RUNS AT HIGHER PRESSURES

A number of runs were made at 200° at pressures of 20 cm, and 40 cm, especially in the earlier stages of the research. The accuracy of these runs is considerably lower than that of the runs at 10 cm, and they suffer further from the rather great variation in light intensity through the reaction vessel, because of absorption of the beam as it goes through the cell. Nevertheless, it seemed worthwhile to present these runs, and they are given in Table IV and Fig. 4. Since their accuracy was not high, small corrections for room temperature, slight variations in pressure, etc., amounting to only a few percent, were not made. Furthermore, in the various series of runs, only an average K_s is given, the variation in $t_l(K_s+k_2\gamma)$ being assumed to come solely from t_l. This was a reasonably good approximation. Some of the runs listed in Table IV are really averages of several runs, the number so averaged being indicated.

We have compared these runs with the curves in Fig. 4 on the basis of the assumption that reaction III (4) occurs at the walls. If reaction III (4) occurred in the gas phase, k_4, and hence $k_2\gamma$, would be proportional to the acetaldehyde pressure. If the reaction occurs at the walls, k_4 will be unchanged provided the amount of diffusion is the same. Examination of Fig. 1 indicates that at the higher light intensities the points pretty well parallel the theoretical curve, indicating a nearly constant apparent k_4, undoubtedly caused by compensating factors already mentioned. At higher pressures, this region of constant apparent k_4 should extend to considerably lower light intensities, because the amount of diffusion is decreased. We have, accordingly, in constructing Fig. 4, used the same value of $k_2\gamma$ which was used in Fig. 3, except in one case of very low light intensity, where the value used for Fig. 2 was assumed. It is to be remembered that Figs. 2 and 3 give different values of $(k_3^{\frac{1}{2}}/k_2)k_3^{\frac{1}{2}}$, and in getting the relation between $t_l(K_s+k_2\gamma)$ and b, which is necessary in setting up the curves in Fig. 4, we

have in each case used the appropriate value of $(k_3^{\frac{1}{2}}/k_2)k_3^{\frac{1}{2}}$. Thus the position of each curve in Fig. 4 is definitely fixed by previously discussed data, and is not specially adjusted to fit the data of Table IV.

It will be observed that the experiments fit the curves in Fig. 4 about as well as could be expected, and it may also be stated that they fit better than would be the case if k_4 were assumed to be proportional to the acetaldehyde pressure. A set of such experiments of higher accuracy, and performed in a shorter reaction vessel, would be highly desirable, as would also experiments in the presence of an excess of inert gas. Similarly, experiments at 300° would also be desirable. It is barely possible that decomposition of HCO could occur in the gas phase at 300°, and that we are actually observing a surface reaction at 200°, but that this surface reaction is overwhelmed at 300° by a gas-phase reaction. If the surface reaction had an activation energy considerably less than 7800 cal. and the gas-phase reaction an activation energy considerably higher, this could produce the results we have obtained, though the correspondence between our experimental and calculated results makes it seem somewhat improbable. Experiments at high pressures or in the presence of inert gases at 300° could settle this question definitely, and experiments at higher temperatures would likewise be of interest.

We should like to close with a word of propaganda in favor of the rotating sector. We feel that the above results make it clear that the use of intermittent light is a powerful instrument for the study of the individual steps in a chain reaction, giving an insight into the mechanism which would not otherwise be possible. The rotating sector has been much exploited in the study of photosynthesis; in the study of gas-phase reactions, though some interesting work has been done,[3] its possibilities have scarcely been touched. Yet, aside from the fact that more runs are required, it adds little in the way of technical difficulties which are not already present in ordinary photochemical experiments. The use of the rotating sector should become a routine procedure in the study of chain photolyses.

APPENDIX—THE DIFFUSION OF THE FREE RADICALS

The problem of the diffusion of radicals through acetaldehyde can be handled approximately by a relatively simple application of the diffusion equation. Since our reaction vessel is a fairly long cylinder, the equation may be written in the form

$$\frac{dA}{dt}=\frac{D}{r}\frac{d}{dr}\left(r\frac{dA}{dr}\right)+k_1I_{\text{abs}}-k_3A^2-k_4A, \qquad (2)$$

where t is the time, A the concentration of free radicals, r the distance from the axis of the cylinder, and D the diffusion constant. The first term on the right-hand side of the equation is the rate of increase in concentration at any point due to diffusion; the second term is the rate of formation of radicals per cc by absorption of light (this term is zero where the cell is dark), and the last two terms give the rate of destruction of radicals by chemical action.

In the case of continuous illumination a steady state is reached in which $dA/dt=0$, and theoretically it should be possible to handle the resulting equation in r. Even if the first term on the right is replaced by the term Dd^2A/dr^2, appropriate to a one-dimensional problem, and the term k_4A is neglected, the result eventually involves an elliptic integral. Further, the boundary conditions at the point at which I_{abs} becomes zero are complicated, involving parameters whose numerical values can only be found after the equation is solved. Under these circumstances, it seems desirable to use a rougher but considerably easier method of approximation.

In the presence of an overwhelming excess of acetaldehyde, the diffusion of any given radical will depend only on the acetaldehyde, and be entirely independent of the other radicals. Since this is the case, we may consider that the light shining at any moment into the reaction

TABLE IV. Experiments at 200° and higher pressures.

Flashes per sec.	p	Number runs	Flashes per sec.	p	Number runs
$p=20$ cm $k_2\gamma=0.8$	$K_s=11.3$ $\delta=0.066$		$p=20$ cm $k_2\gamma=0.8$	$K_s=7.5$ $\delta=0.096$	
120	0.849	1	4	0.722	1
30	.843	1	2	.799	1
15	.938	2	1	.767	1
8	.860	4	½	.616	1
4	.846	4			
2	.781	4	$p=20$ cm	$K_s=3.55$	
1	.666	3	$k_2\gamma=1.6$	$\delta=0.31$	
½	.568	3			
			8	0.806	1
			2	.739	2
			½	.655	1
$p=40$ cm $k_2\gamma=0.8$	$K_s=13.0$ $\delta=0.058$		$p=40$ cm $k_2\gamma=0.8$	$K_s=3.2$ $\delta=0.20$	
8	0.945	1	2	.702	1
2	.745	1	1	.648	1
½	.570	1	½	.664	1

The pressure has been so handled that K_s is in the same units as in Tables I and II and strictly comparable thereto.

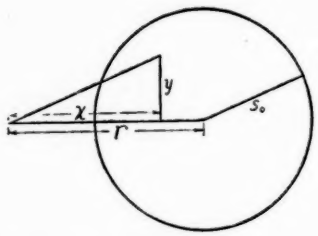

FIG. 5. Notation for Eq. (8). The circle outlines cross section of the illuminated cylinder.

vessel produces, in the case of a system with approximate cylindrical symmetry, a set of instantaneous line sources, each of which will diffuse independently of the others according to the differential equation

$$\frac{dA'}{dt}=\frac{D}{\rho}\frac{d}{d\rho}\left(\rho\frac{dA'}{d\rho}\right), \tag{3}$$

where now ρ is the radial distance to the source, and A' is the concentration due to the source. As is well known, the following solution of the equation gives A' at a distance ρ after elapse of the time t:

$$A'=at^{-1}\exp(-\rho^2/4Dt). \tag{4}$$

If the strength of the instantaneous line source is 1 radical produced per length of source, then we have

$$\int_0^\infty 2\pi\rho A'd\rho=1,$$

which gives

$$a=(4\pi D)^{-1}. \tag{5}$$

The above treatment does not consider the destruction of the radical, but is adequate to take care of the average diffusion of any radical until it is destroyed. The radical, it should be noted, may take part in the chain without being effectively destroyed, since it is almost immediately replaced by another radical.

Now the rate of destruction of radicals is, if we neglect the unimolecular term, k_3A^2. Therefore, the probability of destruction of any radical in unit time is $k_3A=1/\tau$. If A were a constant for all points in space and time (the usual steady-state assumption), out of any n_0 radicals produced at any given instant, a number n would survive after time t, given by

$$n=n_0e^{-t/\tau}. \tag{6}$$

If we have n_0 sources per unit volume produced by the light per unit time, then, if there were no diffusion, the total concentration at any point would be the sum of the concentrations left from all previous times. We should then have

$$A=\int_0^\infty ndt=n_0\tau. \tag{7}$$

We shall now make the assumption that τ is the same for all radicals. This is certainly not by any means true for the region outside the illuminated cylinder, which is just the region we are interested in; it obviously tends to underemphasize the diffusion. However, the chance that any radical will survive to reach a point outside the region of illumination depends not only on the concentration at that point, but also on the greater concentrations through which it had to travel to reach the point. Also τ is actually obtained directly from the experimental data, so that it represents an average in which the effect of diffusion is already included, though, of course, this does not completely correct for the greater lifetimes of radicals which have wandered outside the beam. As will be shown later, however, the approximations to be made in the integrations will be in the direction to nullify the error.

With the assumption of constant τ, the total concentration at any point outside the illuminated cylinder will be given by adding up the effects of all sources which have been produced in past time. The concentration due to any given source is given by Eqs. (4) and (5), so the steady state concentration is given by (for notation see Fig. 5)

$$A_s=n_0(4\pi D)^{-1}\int_0^\infty dt\int_{r-s_0}^{r+s_0}dx\int_{-y_0}^{y_0}dy \left(t^{-1}\exp\left(-\frac{x^2+y^2}{4Dt}\right)\exp\left(-\frac{t}{\tau}\right)\right), \tag{8}$$

where $y_0=(s_0^2-(r-x)^2)^{\frac{1}{2}}$. Integrating first with respect to y, we note that if y_0 is quite large we have what is essentially a complete probability integral. As y_0 decreases, corresponding to regions of x near the edge of the cylinder, the integral with respect to y also decreases, and when

$$y_0=0.5(4Dt)^{\frac{1}{2}}=(Dt)^{\frac{1}{2}} \tag{9}$$

the value of the integral is about half the value of the complete integral.[24] The complete result of integration with respect to y is a rather complex function of x, which makes integration with respect to x impossible. We shall handle this situation approximately by setting[25]

$$\int_{-y_0}^{y_0}\exp\left(-\frac{y^2}{4Dt}\right)dy=(4\pi Dt)^{\frac{1}{2}} \tag{10}$$

if $y_0\geq(Dt)^{\frac{1}{2}}$ and 0 if $y_0<(Dt)^{\frac{1}{2}}$. This is equivalent to replacing the integral with respect to y by $(4\pi Dt)^{\frac{1}{2}}$ in Eq. (8) and restricting the integration with respect to x to limits between $x=r\pm(s_0^2-Dt)^{\frac{1}{2}}$. At the upper limit $\exp(-x^2/4Dt)$ will, in the cases involving a moderate amount of diffusion which we shall encounter in practice, be so low that we may set $x=\infty$. If we replace x by $v=x/(4Dt)^{\frac{1}{2}}$ in the integral, and set $v_0=|r-(s_0^2-Dt)^{\frac{1}{2}}|/(4Dt)^{\frac{1}{2}}$ Eq. (8) becomes

$$A_s=n_0\pi^{-\frac{1}{2}}\int_0^\infty dte^{-t/\tau}\left[\int_0^\infty\exp(-v^2)dv-\int_0^{v_0}\exp(-v^2)dv\right] =\frac{n_0}{2}\int_0^\infty dte^{-t/\tau}\left[1-P\left(\frac{r-(s_0^2-Dt)^{\frac{1}{2}}}{(4Dt)^{\frac{1}{2}}}\right)\right], \tag{11}$$

where P as a function of the argument written is to be read directly out of Peirce's table of the probability integral previously referred to.

Finally, we have to consider the integration with respect to t. Since the quantity in brackets does not vary very greatly with t, it seems reasonable, as an approxima-

[24] See B. O. Peirce, *A Short Table of Integrals* (Ginn and Company), 1910, p. 116.

[25] B. O. Peirce, reference 24, p. 63.

tion, to consider the bracket a constant, with $t=\tau$. Our final result, then, is

$$A_s=(n_0\tau/2)\left[1-P\left(\frac{r-(s_0^2-D\tau)^{\frac{1}{2}}}{(4D\tau)^{\frac{1}{2}}}\right)\right]. \tag{12}$$

This expression is approximately valid for any point *outside* the illuminated cylinder in the reaction cell. We shall now find the concentration $A_s(0)$ at the *center* of the reaction cell, and this will be sufficient to enable us to plot a reasonably good curve. n_0 sources at any point at a distance ρ from the center of the cell would contribute a concentration $n_0(4\pi Dt)^{-1}\exp(-\rho^2/4Dt)$ after a time t, if no recombination took place. We thus have

$$\begin{aligned}A_s(0)&=n_0(4\pi D)^{-1}\int_0^\infty dt\int_0^{s_0}t^{-1}e^{-t/\tau}\exp(-\rho^2/4Dt)2\pi\rho d\rho\\&=n_0\int_0^\infty(1-\exp(-s_0^2/4Dt))e^{-t/\tau}dt\\&=n_0\tau(1-\exp(-s_0^2/4D\tau)).\end{aligned} \tag{13}$$

The approximation involved in the last step is legitimate in the cases to which it will be applied, since $\exp(-s_0^2/4Dt)$ is still not very different from zero when $t=\tau$.

Once we have a value of A_s as a function of r, we can find an effective volume V_e in which the reaction occurs. This is best done by comparing the number of radicals R_e destroyed per second, with the number R_i which would be destroyed if the same radicals were confined within the illuminated volume V_i. Since the number destroyed per unit volume depends upon the square of the concentration of radicals, and since R_e and R_i are taken over the whole volume, we see that

$$R_e/R_i=(A_e^2/A_i^2)V_e/V_i=V_i/V_e,$$

where $A_iV_i=A_eV_e=$total number of radicals present. But

$$R_i=k_3A_i^2V_i$$

and

$$R_e=2\pi k_3 l\int_0^\infty A_s^2 r dr$$

where l is the length of the reaction cell. Therefore

$$V_e=\frac{A_i^2V_i^2}{2\pi l\int_0^\infty A_s^2 r dr}.$$

However, since the total number of radicals is to be equa to A_iV_i we have

$$A_iV_i=2\pi l\int_0^\infty A_s r dr. \tag{14}$$

Hence

$$V_e=\frac{2\pi l\left(\int_0^\infty A_s r dr\right)^2}{\int_0^\infty A_s^2 r dr} \tag{15}$$

and if A_s can be obtained as a function of r from Eqs. (12) and (13), V_e can be evaluated.

In order to obtain A_s it is necessary to evaluate numerically the quantities in Eqs. (12) and (13). s_0 will be taken as the average radius of the beam of light in the reaction cell, which was not exactly cylindrical. This, in our experiments, was about 0.75 cm. τ and D we will evaluate specifically for the set of experiments at 200° included in Fig. 3.

τ may be evaluated directly from the experimental data. We have seen in the preceding paper that, when $b=1$, t_l is equal to the value τ_0 which the chain time would have if k_4 were zero.[26] For experiments at 200°, which are recorded in Fig. 3, we will make no great error in setting $\tau=\tau_0$. Then by direct comparison with the experimentally determined values of t_l we find $\tau=0.03$ sec.[27] This, of course, is an average value, which, as mentioned above, already includes the effect of diffusion. It is further to be noted that, both on account of the appreciable absorption of light by the acetaldehyde in the length of our cell (about 45 percent absorbed), and the spreading of the beam, τ must actually vary considerably along the cell. Our procedure, however, certainly gives a reasonably good average. The fact that the light intensity varies along the reaction cell might also be expected to affect the effective value of l to be set into Eq. (15). However, it is $I_{\text{abs}}^{\frac{1}{2}}$ which determines the amount of reaction, and the value of $I_{\text{abs}}^{\frac{1}{2}}$ near the middle of the cell is sufficiently close to the mean of its values at the two ends, so that the correction which might be expected is probably small compared to the correction due to diffusion.

D may only be estimated indirectly. It seems reasonable to suppose that the diffusion coefficient of CHO radicals in acetaldehyde will be close to the diffusion coefficient of air into ethyl alcohol, or, what is the same thing, the diffusion coefficient of ethyl alcohol into air. The latter is given as 0.1088 cm²/sec. at 9.5° and 1 atmos. by Landolt-Börnstein.[28] The diffusion coefficient varies inversely as the pressure and directly as about the 1.75 power of the absolute temperature.[29] From this we calculate $D=2.0$ at 200° and 10-cm pressure. This completes the necessary evaluation of the numerical quantities. Rather than

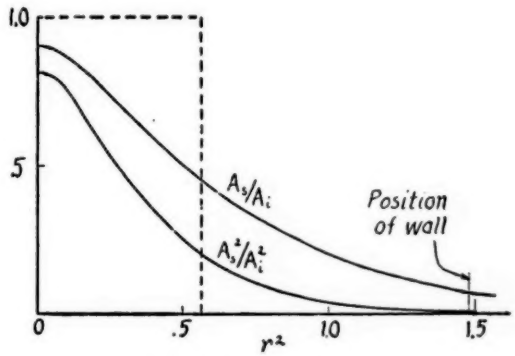

FIG. 6. Diffusion of the radicals.

[26] This is not altered in the modified mechanism we have assumed at the end of Section I.

[27] This may be compared with the value of 0.5 sec. reported in the preliminary note (reference 4). The preliminary note referred to an experiment in which the concentration of radicals was less and the chain time consequently longer, but the chief difference was due to a much rougher method of interpreting the data.

[28] Landolt-Börnstein, *Physik.-Chemische Tabellen*, Vol. 5, second edition, Supplement, p. 201.

[29] E. H. Kennard, *Kinetic Theory of Gases* (McGraw-Hill Book Company, New York, 1938), p. 198.

attempt to evaluate n, it is convenient to assume A_i to be given by Eq. (7), and calculate A_s/A_i. This quantity is given as a function of r^2 in Fig. 6 as is also $(A_s/A_i)^2$. From these curves it is easy to evaluate V_e, which turns out to be 35 cc. This corresponds to a radius of 1.06 cm, as compared to the value of s_0 of 0.75 cm.

At 300° the value of V_e may be taken as the same. D, of course, will be larger. The experiments indicate essentially the same value of τ_0, but on account of the appreciable value of k_4 in this case, τ will be smaller, and this will be almost sufficient to offset the increase in D. $D\tau$ will thus be sufficiently close, so that it is not worthwhile to make a separate calculation for 300°.

The value of V_e is, of course, extremely rough, but it may be remarked that the curves in Fig. 6 look very reasonable. The calculation of the concentration of radicals at the center of the cell should be fairly reliable, and it fits in well with the other points. By comparison of the area under the curve for A_s/A_i with that under the broken lines (which indicate the extent of the beam) it is observed that Eq. (14) does not hold exactly, since the right-hand side appears to be about 10 percent larger than the left-hand side. This is undoubtedly due to the approximate integration used to obtain Eqs. (11) and (12). In obtaining Eq. (11) we overestimated the amount of diffusion, because the true contribution of the integration with respect to y goes to zero for $x<r-(s_0^2-Dt)^{\frac{1}{2}}$ faster than it goes to 1 for $x>r-(s_0^2-Dt)^{\frac{1}{2}}$. Also, setting $t=\tau$ in the argument of the probability function in Eq. (11) in order to get Eq. (12) was probably an overestimate for the average of t, and would result in an overestimate of A_s. It is difficult to say off-hand, whether these errors would more than compensate the underestimate of the amount of diffusion arising from the assumption that τ is constant throughout the volume. The discrepancy between the right- and left-hand sides of Eq. (14) is in the direction to be expected from a decrease in τ as the radical gets outside the illuminated cylinder; that it is not more than 10 percent suggests that the errors in integration have not overcompensated the error due to calling τ constant.

JULY, 1942 JOURNAL OF CHEMICAL PHYSICS VOLUME 10

The Effect of Electrical Forces on the Stability of Colloidal Sols

W. G. EVERSOLE AND ALLEN L. HANSON
Division of Physical Chemistry, State University of Iowa, Iowa City, Iowa

(Received April 4, 1942)

It is assumed that the stabilizing potential in a sol is not the potential at a distance t from the surface of the particle, (ζ), but the potential at a distance l, (λ). l is the distance from the solid surface at which a maximum in the potential energy curve determines the rate of coagulation, and λ is a constant for a given sol in states of equal stability. The quantities $l-t$ and λ are evaluated from experimental data.

THE original concept of the relation of the ζ potential to the stability of a slightly hydrated sol was that in the stable sol the ζ potential of the particles was sufficiently high to prevent the close approach and adhesion of the particles. The addition of salt to the sol was supposed to lower the ζ potential to the critical potential, (ζ^*), and at this point coagulation of the sol would begin. It was assumed, at least by implication, that ζ^* was a constant for each sol.

However, it was soon demonstrated by data such as that of Ghosh,[1] which is given in Table I, that ζ^* was not a constant for a given sol, but in general was higher for salts having higher flocculation values. It was even observed by Kruyt and van der Willigen[2] that the addition of KCl or $K_4Fe(CN)_6$ to an arsenous sulfide sol caused the ζ potential to *increase* until ζ^* was reached and coagulation began.

Nearly all modern attempts to interpret the significance of electrostatic forces in colloidal sols involve the use of the Debye-Hückel theory. The approximations involved in this theory introduce quantitative errors into calculations re-

TABLE I. Data of Ghosh (reference 1) for isostable states of the arsenous sulfide sol. (Coagulation time = 25–30 min.)

Salt	$C^* \times 10^3$ of moles +ion/l	ζ^* mv	$\lambda^*(=\psi_{t+10})$ mv
KNO_3	70	45.8	10.8
KCl	68	43.2	10.4
$MgCl_2$	1.02	15.0	10.6
$SrCl_2$	0.98	14.6	10.6
$BaCl_2$	0.92	14.2	10.2
$AlCl_3$	0.3	15.1	11.2
$Th(NO_3)_4$	0.125	13.9	10.6

[1] B. N. Ghosh, J. Chem. Soc. p. 2693 (1929).
[2] H. R. Kruyt and P. C. Van der Willigen, Zeits. f. physik. Chemie **130**, 170 (1927).

ferring to such systems. This is particularly true at higher salt concentrations and in the immediate neighborhood of a charged wall.

A recent survey of the role of electrical forces in colloidal systems is given in an impressive collection of papers by leading authorities.[3] Therefore it is not the purpose of the present paper to give a detailed discussion of any phase of the problem, but rather to show as briefly as possible how the application of a relation derived in a recent paper[4] leads to the almost quantitative explanation of anomalous experimental data of long standing.

This relation,

$$\ln \tanh (Z'\epsilon\psi/4kT) = \ln \tanh (Z'\epsilon\psi_0/4kT) - \kappa X \quad (1)$$

involves the assumption that the thickness of the ion atmosphere is much less than the radius of curvature of the surface, but does not involve the Debye-Hückel approximations. It should therefore be most accurate at higher concentrations where $1/\kappa$ is small, and should be applicable near the charged surface. This is, of course, the region of greatest importance from the standpoint of the surface properties of the system.

Substituting numerical values into Eq. (1) for water solutions at 25° and changing to common logarithms,

$$\log \tanh (9.75Z'\psi) = \log \tanh (9.75Z'\psi_0) - 0.142Z'C^{\frac{1}{2}}X. \quad (2)$$

Z' is the valence, and C the concentration in gram moles per liter, of the ion having the opposite sign of charge to the wall. ψ^0 is the surface potential of the wall and ψ the potential in the solution at a distance X from the ψ^0 plane. Potentials are in volts and distance in angstrom units. It was assumed that the electrokinetic potential (ζ) is the potential at the distance $X=t$ and therefore,

$$\log \tanh (9.75Z'\zeta) = \log \tanh (9.75Z'\psi_0) - 0.142Z'C^{\frac{1}{2}}t. \quad (3)$$

The exact physical significance of t is open to question. It was assumed that it represents the thickness of the immobilized liquid layer at the solid wall. Bikerman[5] on the other hand, has

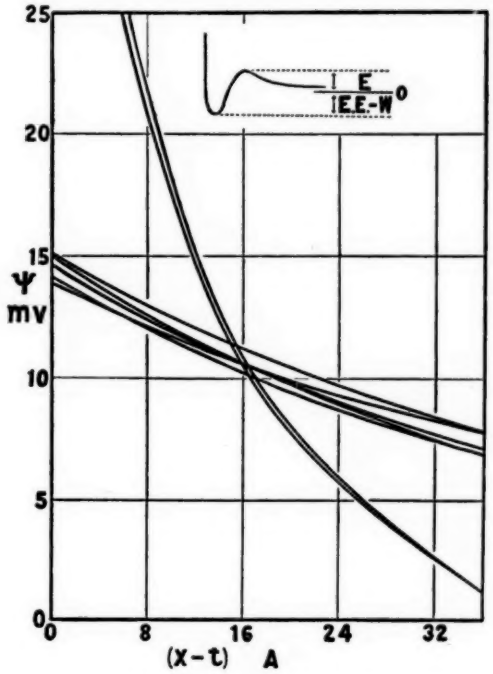

FIG. 1. Potential curves for isostable states of an As_2S_3 sol.

maintained that t measures a fictitious thickness. He holds that roughness of the solid surface rather than rigidity in the liquid structure gives rise to the immobilization of the liquid. In support of the original assumption, it has been demonstrated[6] that the value of t varies significantly for different salt solutions using the same solid wall. It seems impossible to reach a final decision on this question at the present time. However, for the discussion which follows, it will be sufficient to point out that if suitable constant values are assigned to ψ_0 and t, Eq. (2) expresses quantitatively the observed dependence of ζ on C in many cases.

Eliminating ψ_0 by subtracting Eq. (3) from Eq. (2),

$$\log \tanh (9.75Z'\psi) = \log \tanh (9.75Z'\zeta) - 0.142Z'C^{\frac{1}{2}}(X-t). \quad (4)$$

Equation (4) expresses ψ as a function of the distance, $(X-t)$, from the ζ potential plane, in terms of ζ and C, both of which are measurable quantities. Each pair of experimental values of

[3] Trans. Faraday Soc. **36**, 1–322 (1940).
[4] W. G. Eversole and P. H. Lahr, J. Chem. Phys. **9**, 530 (1941).
[5] J. J. Bikerman, J. Chem. Phys. **9**, 880 (1941).
[6] W. G. Eversole and W. W. Boardman, J. Chem. Phys. **9**, 798 (1941).

ζ and C defines one of the family of potential curves represented by the equation.

In order to compare the effects of different salts on the stability of a given sol the particular pair of values must be chosen for each salt to correspond to states of equal stability of the sol (isostable states).

Data of Ghosh[1] for isostable states of an arsenous sulfide sol are given in the first three columns of Table I. The concentration C^* for each salt has a value such that coagulation of the sol occurred in from 25 to 30 minutes after the addition of the salt. ζ^* is the critical ζ potential of the particles corresponding to this degree of stability of the sol.

Using the C^* and ζ^* values of Table I in Eq. (4), the potential curves shown in Fig. 1 have been calculated for the different salts. The salts corresponding to the different curves can be determined from the intercepts on the axis of ordinates by reference to Table I. It will be observed that the range of ψ values for the different salts is a minimum at $X-t \doteq 16A$. In fact the potential curves for three of the salts intersect in the immediate vicinity of the point, 16A, 10.6 mv, and the curves for the other four salts pass near this point on as many sides. Thus it is possible to eliminate the variation of the stabilizing potential for isostable states of the sol by postulating that the stabilizing potential is not the potential in the t plane (ζ) but the potential in the l plane (λ), where in this case $l=t+16$A and the value of the critical λ potential (λ^*) is 10.7 ± 0.5 mv. The λ^* values for the different salts are given in the last column of Table I.

The quantity l may be considered as the distance from the ψ^0 plane at which there is a maximum in the potential energy curve which characterizes the approach of two particles, or a distance slightly greater than one-half the distance of closest approach of the two surfaces.

TABLE II. Data of Powis (reference 8) for isostable states of an As_2S_3 sol. (Coagulation time = 5 hr.)

Salt	$C^*\times10^3$ of moles +ion/l	ζ^* mv	λ^* mv
KCl	40	44	22.5
$BaCl_2$	0.5	26	22.1
$AlCl_3$	0.5	25	22.8
	$l-t=9.6$A	$t_{max}=13.8$A	

Data are not at hand to calculate the value of t for the arsenous sulfide surface. However, by substituting $\psi=\infty$ in Eq. (4) and solving for $(X-t)$, the maximum possible value of t consistent with these data is obtained, since the value of t must be such that ψ^0 will be finite for all salts. For KNO_3, $t_{max}=10$A, while larger values are obtained for the other salts. Therefore it may be assumed that the value of l is between 16 and 26A. The location (l) of the maximum in the potential energy curve is defined by the point at which the surface forces of adhesion become equal to the electrical forces of repulsion.

The reason for the existence of a potential energy maximum at such a distance is obscure. However, evidence based on direct measurements[7] indicates that the distance of closest approach of two quartz surfaces in water and dilute solutions may be even greater than 100A. In general, available evidence pertaining to the state of a thin water film between solid surfaces is limited in amount and is inconclusive. Under such conditions, one is forced to infer a potential energy relation from the observed behavior of the physical system. This has been done, and the potential energy curve for the arsenous sulfide sol is represented diagrammatically in Fig. 1.

On the basis of the argument presented here, a broad qualitative picture of the energy relations in sols becomes evident. The work of adhesion (W) is opposed by kinetic energy (K.E.) which is a function of temperature, and by electrical energy (E.E.) which is a function of the potential at one-half the distance of closest approach of two surfaces. The stability (S) of a sol is measured by $S=$K.E.$+$E.E.$-W$. The condition for a stable sol is $S>0$, and for an unstable sol $S<0$. In all isothermal, isostable states of a sol, K.E. and S are constant and therefore E.E. is constant (unless the added salts affect the value of W). If $W<$K.E. the sol will be typically emulsoid in behavior and will be stable even at the isoelectric point. The condition, $S=0$ is defined by the minimum E.E. at which spontaneous peptization of the coagulated sol can occur.

A second, and perhaps more practical, criterion of isostable states of a given sol is the rate (or

[7] W. G. Eversole and P. H. Lahr, J. Chem. Phys. 9, 686 (1941).

time) of coagulation ($S<0$). From the standpoint of the kinetics of the coagulation, it may be considered that there is a potential barrier of Coulomb forces, the height (E) being a function of λ, which opposes the approach of two particles within the range of the surface forces of adhesion. The velocity constant for the coagulation process is then proportional to $\exp(-E/kT)$. If E is of the order of magnitude of kT, the rate of coagulation should be sensitively dependent on the value of λ, so that isostable states of a sol, ($S<0$), can be defined accurately in terms of equal rates (or times) of coagulation.

This view is confirmed by a comparison of the results of Ghosh[1] with those of Powis.[8] Data of Powis[8] given in Table II have been treated in the same way as those of Ghosh.[1] The value of λ^* is about twice as large as that obtained from the data of Ghosh. This is accounted for by the slower rate of coagulation used by Powis in defining his isostable states. The smaller value of $l-t$ (9.6A) can be largely accounted for by the larger value of t_{max} (13.8A), giving a value of $l_{max}=23.4$A as compared with $l_{max}=26$A obtained from the data of Ghosh. This may perhaps be taken as evidence in support of the view of Bikerman[5] in regard to the significance of t.

If $l=t$, ζ and λ become identical and ζ becomes a constant for a given sol in isostable states. This condition seems to be very nearly realized for the ferric oxide sol studied by Ghosh.[1] The values calculated from his data for this sol are, $\lambda^*=29.5\pm1.0$ mv, $l-t=1.5\pm0.25$A, and $t_{max}=11$A. Thus a shorter distance of closest approach is indicated for this sol than for the As_2S_3 sol, although t_{max} is about the same.

Using the values of $l-t$ and λ^* calculated from the data of Table I, it is possible to explain the behavior of the ζ potential of the As_2S_3 sol studied by Kruyt and Van der Willigen.[2] Introducing the values, $X-t=16$, $\psi(=\lambda^*)=0.0107$ v and $Z'=1$, into Eq. (4) and rearranging

$$\log\tanh(9.75\zeta^*)=9.0004-10+2.272C^{*\frac{1}{2}}. \quad (5)$$

This equation expresses the critical ζ potential as a function of the flocculation value for salts of univalent precipitating ions. The values of ζ^* calculated by means of this equation are plotted against the C^* values in Fig. 2. This curve divides the field into two areas. Above the curve, the coagulation time is greater than 30 minutes, while below is the region of rapid coagulation. Also plotted in Fig. 2 are the ζ potentials calculated from the cataphoretic mobilities observed by Kruyt and Van der Willigen[2] for an arsenous sulfide sol at various concentrations of KCl (lower curve) and $K_4Fe(CN)_6$ (upper curve). The ζ potentials were calculated by the classical formula using the factor 4π and the viscosity and dielectric constant of pure water. Extrapolating the experimental curves to their intersection with the ζ^* curve, the flocculation values (read from the graph) are 0.089 and 0.102 for KCl and $K_4Fe(CN)_6$, respectively. The values reported by Kruyt and van der Willigen are 0.080 and 0.130. While the agreement is only semi-quantitative, the figure shows very clearly how it is possible for a stable As_2S_3 sol to become unstable on the addition of a salt even if there is a pronounced increase in the ζ potential. For multivalent precipitating ions, the increase in ζ^* with C^* is much more rapid than with univalent ions, so that coagulation would occur at a low salt concentration even if there were a large increase in ζ potential.

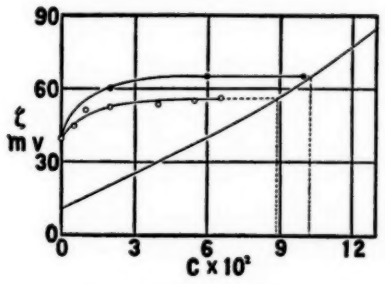

FIG. 2. Zeta-potential relations for an As_2S_3 sol.

The mechanism suggested here involves surface forces of cohesion which are effective at somewhat greater distances than is ordinarily assumed. However, it is felt that the experimental evidence lends considerable support to the assumption of their existence. It seems probable that the application of Eq. (1) rather than the Debye-Hückel equation may lead to further progress in this important field, especially in the region immediately adjacent to the solid wall.

[8] F. Powis, J. Chem. Soc. **109**, 734 (1916).

Variation of Reaction Mechanism with Surface Conditions in the Reduction of Silver Salts by Hydroxylamine*

T. H. JAMES
Kodak Research Laboratories, Eastman Kodak Company, Rochester, New York
(Received March 31, 1942)

Silver bromide oxidizes hydroxylamine at *p*H 10.2–10.8 to nitrogen and water. Under comparable conditions, silver thiocyanate yields a mixture of nitrogen and nitrous oxide as the gaseous products. By varying the surface conditions of the thiocyanate, the composition of the reaction product may be varied over a wide range. Small additions of bromide or iodide greatly decrease the nitrous oxide yield. With initial partial coverage of the precipitate surface by gelatin, the nitrous oxide yield increases to a maximum. Further gelatin additions progressively decrease the yield. Aging a fresh precipitate increases the nitrous oxide yield. The results are explained by the effects of adsorption upon the relative rates of two competing reaction mechanisms.

INTRODUCTION

ALTHOUGH the solubility product of silver thiocyanate lies close to that of silver bromide, the two salts behave quite differently in their reactions with hydroxylamine. For example, at *p*H 10.8 and in the presence of excess anion, silver bromide oxidizes hydroxylamine to nitrogen and water. Under the same general conditions, and at the same *p*Ag, silver thiocyanate may yield 70–75 percent nitrous oxide and only 30–25 percent nitrogen. Variation in the surface conditions of the thiocyanate can markedly alter the nitrous oxide yield. Adsorbed gelatin and dye molecules strongly affect the composition of the gaseous reaction product. A thin coating of bromide or iodide suffices to decrease the nitrous oxide yield to only a few percent. These results have a definite bearing on the theory of photographic development.

EXPERIMENTAL

The experimental procedure followed closely that employed in previous investigations.[1] The specific surface of silver thiocyanate could not be determined by the simple titration with 3,3′-diethyl-9-methylthiacarbocyanine which sufficed for silver chloride, because of the action of thiocyanate ion in sedimenting the dye. However, a sharp end point was obtained in the absence of excess thiocyanate ion if the precipitate was first stirred for about ten minutes with two to three times the amount of bromide ion required to cover the surface. The same procedure applied to silver chloride gave results in complete agreement with those obtained by simple titration in the presence of excess chloride ion.

In each of the subsequent experiments, one-half millimole of silver salt and two millimoles of hydroxylamine were employed. Reaction temperature was 20.03±0.03°C. Total solution volume was 60 ml. Reaction rates are expressed in terms of the slope of the reaction curve at one-third or one-half completion (the curves in general have an autocatalytic shape), and in terms of the reciprocal of the time required to yield 0.20 ml gaseous reaction product.

The *variation of specific surface with age* of the silver thiocyanate precipitate is indicated by the dye adsorption data given in Table I. The results

TABLE I. Adsorption of 3,3′-diethyl-9-methylthiacarbocyanine by AgCNS.

Age (hr.)	0	4	18	44	290
Dye (mg)	1.30	0.87	0.45	0.38	0.38

TABLE II. Effect of age of AgCNS on reaction products, *p*H 10.45.

Age (hr.)	Percent N_2	Percent N_2O
0.25	59	41
.30	58	42
.50	48	52
1.25	43	57
5.25	37	63
17	39	61
66	37.5	62.5

* Communication No. 848 from the Kodak Research Laboratories.

[1] T. H. James, (a) J. Am. Chem. Soc. **61**, 2379 (1939); (b) **62**, 536 (1940); (c) **63**, 1601 (1941); (d) **64**, 731 (1942).

are quite similar to those obtained for the aging of silver bromide[2] and silver chloride.[3,1(b)] Accompanying the decrease in specific surface with age, but not strictly paralleling it, the nitrogen yield of the hydroxylamine reaction decreases (Table II). The nitrous oxide yield correspondingly increases.

Effect of Gelatin on the Reduction of Silver Thiocyanate

The data in Table III show the effect of gelatin upon the reaction rate and nitrous oxide yield. Each precipitate was aged 17–20 hours, and then stirred with the specified amount of gelatin for one hour before use. A sharp decrease in the reaction rate is obtained by the first small additions of gelatin. Additions in excess of 2–4 mg have only a small effect. The nitrous oxide yield, on the other hand, passes through a sharp maximum corresponding to 0.2–0.4 mg of gelatin. Further additions produce a continuous decrease (Fig. 1).

Similar results were obtained by the addition of pinacyanol chloride (Table IV). A definite maximum in the nitrous oxide yield is not established in this case, but may exist. A significant decrease in the nitrous oxide yield was not observed until more than 0.5 mg of dye had been added, although the R rate had decreased ninefold. The R rate given in this case is the maximum slope of the reaction curve. These reaction curves are erratic in form, as shown in Fig. 2, and resemble those obtained in the reduction of silver chloride by hydrazine in the presence of 3,3′-diethyl-9-methylthiacarbocyanine.[4] A monomolecular layer of pinacyanol should cover the surface of this precipitate at less than 0.8 mg of dye, but no minimum reaction rate is obtained up to 5.0 mg of dye.

Much of the pinacyanol originally added was no longer present in the solution at the end of the reaction. Significant chemical destruction of the dye had not occurred, but much dye could be extracted from the silver product by means of

TABLE III. Effect of gelatin on the reaction of AgCNS with NH_2OH.

Gelatin mg	Excess CNS^- m mole	pH	$R_{1/3}$	$1/t$	N_2O
0.00	0.50	10.2	0.61	0.106	26
.10	.50	10.2	.29	.070	37
.20	.50	10.2	.12	.058	41
.40	.50	10.2	.087	.030	37
1.00	.50	10.2	—	—	22
0.00	.50	10.8	1.9	.80	63
.20	.50	10.8	0.47	.38	70
.40	.50	10.8	.37	.16	76
1.00	.50	10.8	.27	.088	70
4.00	.50	10.8	.088	.033	47
10.00	.50	10.8	.074	.024	31.5
50.00	.50	10.8	.066	.018	18
0.00	.00	10.45	3.76	4.55	64.5
.50	.00	10.45	0.76	0.62	68
50.00	.00	10.45	.035	.072	25

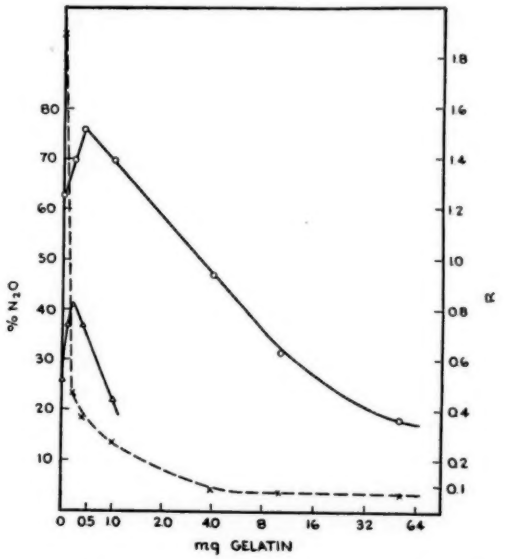

FIG. 1. Effect of gelatin on reduction of AgCNS. Triangles, N_2O at pH 10.2; circles, N_2O at pH 10.8; crosses, R at pH 10.8.

TABLE IV. Effect of pinacyanol on reaction of AgCNS with NH_2OH.

Dye mg	m moles excess CNS^-	pH	R_m	$1/t$	Percent N_2O
0.00	0.50	10.8	1.9	0.80	63
.10	.50	10.8	1.4	.50	64
.50	.50	10.8	0.22	.33	64
2.50	.50	10.8	.10	.21	60
5.00	.50	10.8	.035	.14	45
0.00	.00	10.45	3.76	4.55	64.5
.50	.00	10.45	0.36	1.66	61.5
5.00	.00	10.45	.52	1.66	53

[2] I. M. Kolthoff and A. S. O'Brien, J. Chem. Phys. **7**, 401 (1939).
[3] I. M. Kolthoff and H. C. Yutzy, J. Am. Chem. Soc. **59**, 1215 (1937).
[4] T. H. James, J. Am. Chem. Soc. **62**, 1654 (1940).

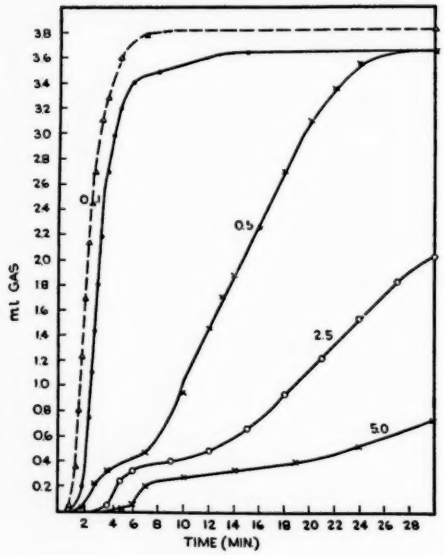

FIG. 2. Effect of pinacyanol on reduction of AgCNS a *p*H 10.8. Figures on curves give milligrams of dye.

methanol. Addition of pinacyanol to silver formed in the absence of the dye resulted in an appreciable adsorption of the dye, and the amount was substantially the same, whether the dye was added as pure aqueous solution or as 12 *M* ammonia solution. Hence, it is unlikely that the action of a silver oxide layer at the surface is involved. The silver obtained by reaction in the presence of pinacyanol was more finely divided than that obtained without addition.

Mixed Precipitates of Silver Bromide and Thiocyanate

Silver bromide and silver thiocyanate form an incomplete mixture series. Silver thiocyanate dissolves up to three percent silver bromide, and silver bromide dissolves up to ten percent thiocyanate. Intermediate precipitates are composed of the mutually saturated end solutions.[5] In the present investigation, a series of mixed precipitates was prepared by adding to 5.00 ml of 0.10 *M* silver nitrate in 15 ml total solution, 6.00 ml of 0.10 *M* mixture of potassium bromide and thiocyanate. The precipitates were aged in contact with the supernatant liquid for 17–20 hours before reaction was carried out at *p*H 10.45. In Table V, R_c is a rate value corrected for the difference in volume of gas produced by 1 mole of the silver salt mixture.

The reaction rates do not vary greatly with the change in composition of the precipitate and supernatant liquid. The composition of the gaseous product, however, exhibits a remarkable behavior. The gas remains over 90 percent nitrogen until the thiocyanate reaches 96 percent. After this, the nitrous oxide increases rapidly to the value of 51 percent for the pure thiocyanate.

Table VI gives the results obtained by addition of various amounts of excess thiocyanate, bromide, and iodide to pure, aged silver thiocyanate precipitates 15 minutes before addition of the hydroxylamine. Complete curves for a number of the experiments are given in Fig. 3. It is evident that precipitates to which excess thiocyanate has been added may give the same general reaction rates as those to which excess bromide has been added, but the nitrous oxide yield will be entirely different. There is no connection between *p*Ag and nitrous oxide yield in this case. Added bromide and iodide give identical results within the limits of experimental error.

Table VII gives results obtained when potassium bromide was added to precipitates which had been coated with gelatin or wool violet. The amounts of gelatin or dye added were two or three times those required for a single layer.

DISCUSSION

In a preceding paper,[1(d)] evidence was presented that the formation of nitrous oxide is associated with the uncatalyzed reduction of silver ions by hydroxylamine. Nitrogen is the exclusive product of the silver catalyzed reaction involving adsorption of silver ions to the catalyst. In the preceding experiments, therefore, the

TABLE V. Reaction of mixed bromide and thiocyanate precipitates.

Percent Br^-	$R_{1/2}$	R_c	$1/t$	Percent N_2O
100	0.72	0.72	0.33	0.1
80	1.08	1.08	.40	.2
20	2.05	2.08	.44	2.0
10	—	—	—	3.8
4	2.00	2.12	.52	10.0
1	2.26	2.83	.61	35.0
0	2.00	2.85	.67	51.0

[5] F. W. Kuster and A. Thiel, Zeits. f. anorg. allgem. Chemie **33**, 129 (1902).

nitrous oxide yield may be taken as a measure of the amount of uncatalyzed reaction.

The reduction of silver bromide in the *p*H range 10.2–10.8 involves exclusively, or almost so, the silver catalysis mechanism. Silver thiocyanate in the same *p*H range, however, may be reduced largely by the non-catalyzed mechanism, and the extent to which this mechanism operates varies greatly with prevailing reaction conditions. The equilibrium *p*Ag of the solution is not an important factor. The solubility product of silver thiocyanate is somewhat less than twice that of silver bromide. Thus, in Table VI, approximately the same *p*Ag would arise in solutions containing 0.1 m mole of potassium bromide or 0.2 m mole of potassium thiocyanate, yet the nitrous oxide yields are 3 percent and 54.5 percent, respectively. On the other hand, surface conditions evidently exert an important and possibly deciding influence.

The specific surface of the thiocyanate precipitates can be determined only roughly from the data at hand. The 18-hour-old precipitate prepared in the absence of excess anion adsorbs about 0.45 mg of 3,3′-diethyl-9-methylthiacarbocyanine. If the same coverage is assumed as for silver bromide,[6] this figure gives a specific surface of approximately 4000 sq. cm. If gelatin adsorption occurs on the same basis as with silver chloride, a complete protective layer should be formed by 2–3 mg gelatin.[1(b)]

TABLE VI. Effect of CNS^-, Br^-, and I^- upon reduction of AgCNS at *p*H 10.45.

Addition	Amount m moles	$R_{1/3}$	$1/t$	Percent N_2O
None	—	3.80	4.55	63.5
KCNS	0.10	2.68	0.93	57.7
KCNS	.20	1.88	.50	54.5
KCNS	.50	1.07	.19	40.5
KCNS	1.00	—	—	27.5
NaCl	0.50	—	—	62.9
KBr	.005	3.78	2.33	43.5
KBr	.010	3.76	2.33	28
KBr	.020	3.26	1.54	17
KBr	.040	—	—	7
KBr	.100	2.50	0.44	3
KBr	.200	2.00	.23	3
KI	.010	—	2.0	28
KI	.020	—	2.0	22
KI	.040	0.39	0.80	6
KBr .030 + KCNS .070		2.24	.70	19
KBr .050 + KCNS .100		1.30	.31	19.5
KBr .050 + KCNS .020		1.92	.74	11.5

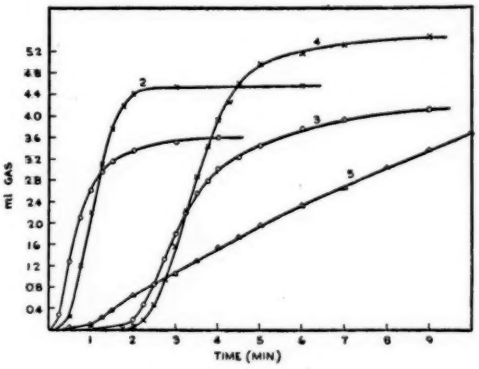

FIG. 3. Effect of excess anion on AgCNS–NH_2OH reaction curves. Curve 1, no addition; curve 2, 0.005 m mole Br^-; curve 3, 0.20 m mole CNS^-; curve 4, 0.10 m mole Br^-; curve 5, 0.04 m mole I^-.

A comparison of the nitrous oxide-gelatin curves in Fig. 1 shows that a sharp maximum is reached at both *p*H 10.2 and 10.8. This maximum lies at 0.2 mg of gelatin at the lower *p*H and 0.4 mg at the higher, both well below the requirements for a complete layer covering the surface. The rate curves show definite breaks at about the gelatin concentrations corresponding to the maximum nitrous oxide yield, but the rates decrease considerably beyond these points before they approach a minimum. The decrease in rate becomes small beyond 2–3 mg of gelatin addition.

Gelatin can reduce the reaction rate in two ways. In the first, adsorption of gelatin to the silver thiocyanate markedly decreases the rate of the direct attack of hydroxylamine upon the silver salt surface and the rate of solution. This action of the gelatin is unfavorable to the non-

TABLE VII. Reduction of coated AgCNS.

KBr added m moles	Percent N_2O from pp. coated Gelatin *p*H 10.45	Wool violet *p*H 10.8
0	46	58
0.005	28	—
.010	19	42
.050	10	4

[6] S. E. Sheppard, R. H. Lambert, and R. D. Walker, J. Chem. Phys. **7**, 265 (1939).

catalyzed reduction. In the second, adsorption of gelatin to the silver nuclei and at the salt-silver interface decreases the specific rate of the silver catalyzed reaction. The silver nuclei chiefly responsible for the start of the catalyzed reaction are probably formed at relatively unprotected spots on the silver thiocyanate surface. If the amount of gelatin present is sufficient to cover only a fraction of the surface, this may quickly impede the propagation of the catalyzed reaction as the interface reaches the sites of adsorbed gelatin. The decrease in rate of solution and of uncatalyzed attack upon the thiocyanate surface, on the other hand, should be roughly proportional to the amount of surface covered by the adsorbed gelatin. The relative decrease in rate of the catalyzed reaction will thus be greater for small surface coverage. Data previously obtained on the action of gelatin in the reduction of silver chloride by hydroxylamine support this suggestion. A maximum proportion of the uncatalyzed reaction should be reached before the surface of the precipitate is completely covered with gelatin, and further addition of gelatin should favor the catalyzed reaction. The shift in the position of the maximum towards higher amounts of gelatin with increasing *p*H is expected, since increase in *p*H relatively favors the uncatalyzed reaction.[1(d)]

The fact that increases in gelatin addition beyond that required for a complete layer produce increases in the amount of catalyzed reaction participating in the reduction shows that adsorption rates are involved. The silver formed in the attack upon the solid occupies a considerably smaller volume than the original salt. As reaction progresses, the splitting away of the nuclei from the salt along a portion of the boundary, together with disruption of the surface due to solution effects, exposes unprotected surface. Gelatin from solution, however, can act to form a new protecting layer. Thus, a kinetic competition sets in as soon as exposed surface is formed.

The same general considerations may be applied to the effect of pinacyanol upon the reduction of silver thiocyanate. The dye should differ from gelatin only in the degree to which it relatively influences the rates of the competing reactions. The action of bromide and thiocyanate ions may likewise be explained in the same general way. In this case, since excess of either ion in any amount will prove detrimental to the uncatalyzed reaction, there should be no maximum nitrous oxide yield. Actually, none was observed. The relatively much greater effect of bromide ion is of interest in connection with the observations of Lottermoser and Petersen[7] that a negative silver thiocyanate sol exhibits an essentially smaller adsorption for thiocyanate ions than a negative silver bromide sol does for bromide ions. Silver bromide in the presence of excess bromide ion reacts with hydroxylamine almost exclusively by way of the catalytic mechanism. A relatively small amount of excess bromide ion, added to the thiocyanate precipitate, converts the reaction of that substance largely to the catalytic mechanism. A much larger excess of thiocyanate ion is required to produce a comparable effect. When the solution contains both excess thiocyanate and bromide, the effect of the ions is not additive, but rather competitive. The last three experiments recorded in Table VII show a definite action of the thiocyanate in partially counteracting the effect of the bromide. This suggests that more than mere adsorption of bromide to silver ions is involved. Probably an actual interchange of bromide and thiocyanate ions occurs, resulting in the formation, or partial formation, of a thin layer of silver bromide coating the thiocyanate.

The decrease in specific surface of silver thiocyanate on aging, as indicated by the change in dye adsorption, should have in itself but slight effect upon the product of the reaction with hydroxylamine. The marked increase in nitrous oxide actually observed shows that another more important change has occurred on aging. This may be a sharp decrease in the ability of the aged surface[8] to adsorb thiocyanate ion, or a sharp decrease in the number of active spots at which catalysis centers may be formed.

---

[7] A. Lottermoser and W. Petersen, Zeits. f. physik. Chemie **133**, 69 (1928).

[8] J. H. de Boer, *Electron Emission and Adsorption Phenomena* (Cambridge University Press, 1935).

Efficiency of the Electrolytic Separation of Chlorine Isotopes

HERRICK L. JOHNSTON AND DWIGHT A. HUTCHISON
Department of Chemistry, The Ohio State University, Columbus, Ohio

(Received April 28, 1942)

The electrolytic separation coefficient α has been determined for the chlorine isotope separation in the electrolysis of sodium chloride solutions at a platinum anode. Flotation of purified NaCl crystals in ethylene dibromide was employed as the analytical procedure in determining the isotopic composition of samples. Densities of the ethylene dibromide as a function of temperature were separately determined. The electrolytic separation factor for Cl isotopes was found to be 1.0060 ± 0.0005 for the temperature range 25° to 40°C. No significant dependence on either temperature or current density was observed. The coefficient on platinum (1.0060 ± 0.0005) agrees with the value on Acheson graphite (1.0068 ± 0.0014) which may be computed from the data of Yacouban.

A RECENT paper from this laboratory[1] dealt with the accurate determination of the isotopic separation factor α in the electrolytic separation of lithium isotopes at a mercury cathode. Flotation of LiF crystals in a suitably chosen organic medium was employed to follow accurately the change in isotopic composition of the lithium. We have completed a similar investigation on the efficiency of chlorine isotope separation at a platinum anode. Although the separation efficiency is ten times smaller than with lithium we have obtained a reliable value of its constant. Flotation of NaCl crystals in ethylene dibromide proved a satisfactory method of making accurate isotopic analyses of chlorine.

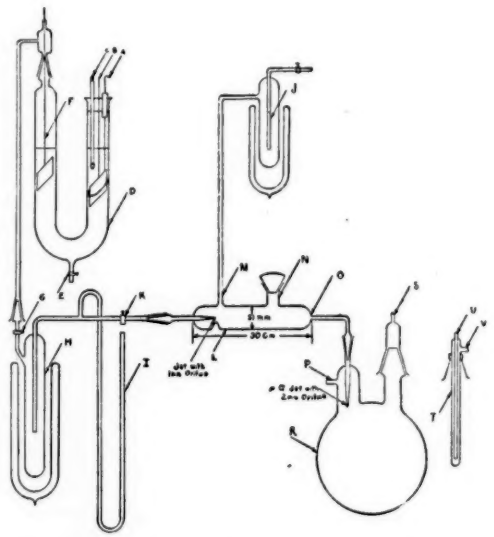

FIG. 1. Diagram of apparatus for electrolysis of chloride solution and for conversion of the electrolytic chlorine into pure ammonium chloride. *A*, glass stirring rod; *B*, platinum cathode; *C*, thermometer; *D*, Pyrex glass cell; *E*, stopcock to obtain samples of NaCl solution for titration with standard $AgNO_3$; *F*, platinum anode; *G*, stopcock; *H*, liquid nitrogen trap; *I*, manometer; *J*, activated charcoal trap for hydrogen purification; *K*, stopcock; *L*, chlorine jet; *M*, hydrogen inlet; *N*, explosion release; *O*, chlorine combustion chamber; *P*, ammonia inlet; *Q*, hydrogen chloride jet; *R*, two-liter reaction flask; *S*, outlet for excess hydrogen and ammonia; *T*, condensing surface for NH_4Cl sublimate; *U*, *V*, water outlet and inlet.

[1] H. L. Johnston and Clyde A. Hutchison, J. Chem. Phys. **8**, 869 (1940).

I. EXPERIMENTAL DESCRIPTION

A. Apparatus for the Electrolysis and for Recovery of the Cl_2

Figure 1 is a diagram of the apparatus used in the electrolysis and in the recovery of the electrolytic chlorine. An aqueous solution of pure NaCl was electrolyzed between platinum electrodes in a U-shaped Pyrex cell whose temperature was regulated by an external bath. A thermometer dipped directly into the electrolyte. The temperature was controlled to within ±2°C.

The Cl_2 liberated at the anode was solidified in a liquid nitrogen cooled trap from which it was distilled, to remove water vapor, and finally burned at a jet in an atmosphere of hydrogen. The HCl produced, together with an excess of H_2, passed through a second jet *Q* into a two-liter reaction chamber, where it combined with an excess of dry NH_3. The NH_4Cl thus produced was absorbed in triple-distilled water at the bottom of the reaction chamber. The gaseous residue, which consisted of a mixture of the excess H_2 and excess NH_3, escaped through the outlet *S*. The reaction chamber *R* was designed so

that no significant portion of the NH_4Cl escaped with the H_2 and NH_3 gases.

When the electrolysis was completed, the reaction chamber *R* was disconnected from the rest of the system, by opening the ground glass joints at the HCl and NH_3 inlets, and the aqueous NH_4Cl evaporated to dryness. The dry NH_4Cl was then sublimed *in situ*, under vacuum, onto the water cooled condensing surface *T*. The flask was cleaned; the sublimate was scraped off of *T* and the vacuum sublimation repeated.

The purified NH_4Cl was next dissolved in triple-distilled water. To this solution pure Na_2CO_3 was added in such quantity that its equivalent concentration remained slightly below that of the NH_4Cl. The resulting solution was evaporated to dryness and the dry salt fused in a platinum crucible, to drive off $(NH_4)_2CO_3$ together with the slight excess of NH_4Cl. The resulting pure NaCl was used to prepare crystals for the densimetric analysis (cf. *seq.*).

The amount of chloride ion converted to chlorine in the electrolysis was determined by titration of the residual electrolyte with a standard $AgNO_3$ solution, after the electrolysis.

B. Preparation of Reagents

NaCl used for the electrolysis, and in the preparation of standard crystals of normal isotopic composition for use as comparison crystals in the densimetric analyses, was prepared from Baker and Adamson's Reagent Quality NaCl by a method of purification similar to that employed by Richards and Wells[2] in their determination of the atomic weights of sodium and chlorine. Details of our procedure and evidence of its efficacy, are being published elsewhere.[3]

Hydrogen, used in the combustion of the electrolytic Cl_2, was commercial electrolytic hydrogen which was purified by passing it through charcoal at liquid nitrogen temperatures (Fig. 1, *J*). The charcoal had previously been degassed in vacuum at 400°C.

Ammonia gas, to combine with the HCl, was taken from a 100-lb. cylinder of du Pont liquid ammonia.

Na_2CO_3, used to decompose the NH_4Cl, was prepared from J. T. Baker's C.P. Na_2CO_3 by six recrystallizations from triple-distilled water.

Pure ethylene dibromide, used as flotation liquid for the densimetric analyses (cf. *seq.*), was prepared from Merck's Reagent Quality $C_2H_4Br_2$ (boiling point range 129°–132°C), previously dried over C.P. $CaCl_2$, by distillation in vacuum. The middle third of the distillate was retained. The isothermal density of the purified liquid remained constant to within experimental error limits ($\pm 4\times10^{-6}$ g/ml) during the several days that measurements were in progress.

C. The Isotopic Analyses

The isotopic analyses were made in the manner previously outlined[1] for LiF, and in the same apparatus. Details of manipulation will not be repeated here. Pure ethylene dibromide was found satisfactory for the flotation liquid, and crystals were grown in the manner described previously.[1] It was found necessary to anneal the crystals for 4 hours at a temperature 50° below their melting point and to store them over P_2O_5 under vacuum.[4] With these precautions, densities of individual crystals were reproducible to within about ±0.002°C (equivalent to $\pm 3.6\times10^{-6}$ g/ml in density).

The density of ethylene dibromide, as a function of the temperature, was determined for the approximate range 24.5 to 29.5°C. The determinations were made by careful hydrostatic weighings of an approximate 9-ml Pyrex glass bob in air, in pure distilled water, and in the ethylene dibromide.[5] Our experimental data are given elsewhere.[3] They are satisfactorily reproduced by the equation:

$$d\ (\text{g/ml}) = 2.16909 - 0.001995(t-24°)^2. \quad (1)$$

For the temperature interval with which we are concerned in the flotation of crystals for isotopic analyses the density—temperature coefficient of the ethylene dibromide is somewhat above the average for the 5° interval, and can be taken as a constant, with reasonable accuracy,

[2] T. W. Richards and R. C. Wells, "A revision of the atomic weights of sodium and chlorine," Carnegie Institution of Washington, Publication No. 28 (1905).

[3] H. L. Johnston and D. A. Hutchison, "Density of sodium chloride," Phys. Rev. **62** (July 1 and 15, 1942).

[4] Cf. Section II of reference 3 for details.

[5] To avoid possible small errors due to surface tension effects on the fine Pt wire suspension, we employed a small auxiliary bob attached to the suspension, after the manner of Osborne, McKelvey, and Bearce, Bull. Nat. Bur. Stand. Reprint No. 197 (1912).

TABLE I. Isotopic separation of Cl isotopes in the electrolysis of aqueous NaCl.

Run number	1	2	3	4	5	6	7	8	9
Average temperature, °C	40	40	40	40	25	13	40	40	40
Average current (amperes)	5	3	1	5	5	5	5	5	5
Moles of NaCl in starting material	0.83366	0.82851	0.76965	0.83298	0.75890	0.76519	3.36560	0.42020	4.31469
Equivalents of Cl liberated	0.15606	0.14117	0.10603	0.15145	0.17401	0.18219	0.64296	0.07826	1.00165
Mole fraction of NaCl decomposed	0.18720	0.17039	0.13777	0.18183	0.22929	0.23810	0.19104	0.18624	0.23215
Current efficiency[a]	0.67	0.65	0.71	0.69	0.75	0.84	0.67	0.63	0.78
Flotation temperatures of different crystal fragments relative to standard crystals taken as zero	0.041 0.039 0.039 0.038	0.039 0.038 0.037 0.037	0.039 0.038 0.038 0.035	0.040 0.038 0.038 0.037	0.042 0.041 0.041 0.036	0.041 0.041 0.040 0.039	0.045 0.043 0.041 0.041	0.078 0.077 0.077 0.077	0.034 0.035 0.033 0.034
Average flotation ΔT, °C	0.0393	0.0377	0.0375	0.0383	0.0400	0.0402	0.0425	0.0773	0.0340
Change in the atomic weight of Cl	−0.00196	−0.00188	−0.00187	−0.00191	−0.00199	−0.00200	−0.00212	−0.00386	−0.00170
α	1.0061	1.0057	1.0056	1.0059	1.0064	1.0064	1.0066	1.0060	1.0054

[a] Cf. p. 874 of reference 1.

with the value $-2.11\pm0.01\times10^{-3}$ g/ml/degree. With account taken of the thermal coefficient of expansion for NaCl,[6] namely, $\alpha_l=40.5\times10^{-6}$, one degree in the ΔT of flotation corresponds to 1.85×10^{-3} g/ml in the isothermal density of NaCl. This corresponds to 0.0499 unit in the atomic weight of chlorine and to 2.51 percent in the percentage distribution of chlorine isotopes. Determination of the flotation temperatures of pure NaCl crystals to within ±0.002°C, which is about the limit of our reproducibility, thus corresponds to 5×10^{-3} percent in the isotopic composition of chlorine.

II. THE DATA

In all, nine runs were made to evaluate the isotopic separation factor α and to determine the possible effects of certain experimental conditions on its value.[7] In the first series of three independent runs at 40°C the current across the cell was varied. In the fourth, fifth, and sixth runs, which were likewise independent, the current was kept constant at 5 amperes while the temperature was varied. The seventh and ninth runs were carried out under the same experimental conditions as runs 1 and 4. The eighth run was a re-electrolysis of the light fraction from the seventh run, in order to increase the isotopic separation and thereby increase the accuracy of the determination of α. Its α (cumulative[8]) is in exact agreement with the average for the four runs (1, 4, 7, and 9) made with the same experimental conditions of temperature and of current density, and likewise with the average of all eight single step runs. The records of these several runs are given in Table I.

With each run four crystal fragments, prepared from the NaCl made from the electrolytic chlorine, were annealed and floated. The table records the ΔT's from *every* crystal. Since there were no large or systematic differences among crystals from any one run, linear averages were taken for the computations of α.

α's for the several runs were computed from the equation.

$$\alpha=\frac{\log\left[1-F\left(1+\frac{1.86\times10^{-3}M_{\mathrm{NaCl}}}{d_{\mathrm{NaCl}}(A_{37}-A_{\mathrm{Cl}})}\Delta T\right)\right]}{\log\left[1-F\left(1-\frac{1.86\times10^{-3}M_{\mathrm{NaCl}}}{d_{\mathrm{NaCl}}(A_{\mathrm{Cl}}-A_{35})}\Delta T\right)\right]}; \quad (3)$$

in which F is the mole fraction of NaCl electrolyzed in a given run; M_{NaCl} is the molecular weight of *normal* NaCl; A_{Cl} the atomic weight of *normal* Cl; A_{35} and A_{37} the mass numbers of Cl_{35} and Cl_{37}, respectively; d_{NaCl} the density of normal NaCl at the flotation temperature for standard normal crystals of NaCl; and ΔT the

[6] Straumanis, Ievins, and Karlsons, Zeits. f. anorg. allgem. Chemie **238**, 175 (1938). Cf. also Eucken and Dannohl, Zeits. f. Elektrochemie **40**, 814 (1934).

[7] α is defined by the relationship

$$d\log \mathrm{Cl}^{35}=\alpha d\log \mathrm{Cl}^{37}. \quad (2)$$

[8] The cumulative α is the value (taken as constant through both steps of electrolysis) needed to yield the experimental ΔT of 0.0773 observed at the end of the second step.

flotation temperature of crystals prepared from the electrolytic chlorine minus the flotation temperature of standard normal crystals. This equation is an exact solution of Eq. (2)[7] in terms of the experimentally measured quantities F and ΔT. We used for the constants in the equation: $A_{35}=34.980$[9]; $A_{37}=36.978$[9]; $A_{Cl}=35.457$[10]; $M_{NaCl}=58.454$[10]; and d_{NaCl} (at 27.63°) = 2.16165 g/ml.[3]

The light fraction from run 9 was given two additional steps of electrolysis (making 3 steps in all) to increase further the isotope separation. The observed ΔT of 0.120° (equivalent to −0.0060 unit) in the third step is in line with the ΔT's of first- and second-step electrolyses and confirms the interpretation of the data but was less reliable than the earlier runs, in a quantitative sense, for the calculation of α because of the difficulty in preparing pure single crystals from the small amount of Cl_2 (600 cc) that was evolved in the third step.[11] Through an error in the analysis no ΔT was obtained for the second step of this series, which would have given an accurate α.

III. DISCUSSION OF RESULTS

The average α of the several single step runs at 40° and 5-amperes current is 1.0060, in exact agreement with the cumulative α recorded under run 8. The α's at 25° and at 13° are somewhat higher than for the runs at 40°, as might be expected, but the difference is only a little greater than would correspond to a ±0.002 experimental uncertainty in the flotation ΔT's (±0.0003 unit in α) and are matched by equal variations in runs 7 and 9, which were both run at 40°. Likewise, no significance can be attached to the slightly lower α's obtained with reduced current densities. We believe that

$$\alpha = 1.0060 \pm 0.0005$$

includes a liberal estimate of the error limits for electrolysis on a bright platinum anode over the temperature interval 25° to 40°C.

It is interesting to compare this with the value of α that can be computed from the data obtained by Yacouban,[12] who reduced an aqueous mixture of HCl and NaCl containing 36 kilograms of chloride ion to a residual solution containing 24 grams of Cl^-, by electrolysis with electrodes of Acheson graphite. The temperature was maintained between 8 and 12°C. Correcting for a 25-percent loss of material in the second stage of electrolysis, this corresponds to a reduction factor of 552 in the amount of Cl. Analysis of the residual 24 grams of Cl^- by titration with a standard $AgNO_3$ solution indicated an atomic weight increase of 0.016 unit which was regarded as about 5 times the experimental error of the analysis. Employing these data to solve the equation

$$(\alpha-1)\log\frac{Cl_i}{Cl_f}=\log\left(\frac{Cl_{35}}{Cl_{37}}\right)_i-\log\left(\frac{Cl_{35}}{Cl_{37}}\right)_f \quad (4)[13]$$

we obtain $\alpha = 1.0068 \pm 0.0014$, in good agreement with our own more precise values.

Isotopic separation factors have now been determined for the electrolysis of aqueous solutions of hydrogen,[14] lithium,[1,14] oxygen,[13,15] and chlorine. There is a marked drop, in the order named, from H to O but no significant drop, within expressed error limits, from O to Cl. However, the latter results and the comparison of both with lithium may not be strictly comparable since electrode metals were different in all three cases. It is not known, as yet, whether or not the separation factors for elements other than hydrogen are susceptible to the character of the electrode material. Any proper interpretation of these results should await somewhat further extension of experimental material.

---

[9] F. W. Aston, Proc. Roy. Soc. **A163**, 391 (1937).

[10] Tenth annual report of the committee on atomic weights of the International Union of Chemistry, J. Am. Chem. Soc. **62**, 669 (1940).

[11] The cumulative α for this three-step electrolysis was computed from the observed ΔT of 0.120° and the experimental F's and came out 1.0067.

[12] K. V. Yacouban, Helv. Chim. Acta. **22**, 808 (1939).

[13] H. L. Johnston, J. Am. Chem. Soc. **57**, 484 (1935).

[14] Cf. citations in reference 1.

[15] Klar and Kraus, Naturwiss. **22**, 119 (1934); Selwood, Taylor, Hipple, and Bleakney, J. Am. Chem. Soc. **57**, 642 (1935).

The Second Virial Coefficient for Gas Mixtures*

JAMES A. BEATTIE AND WALTER H. STOCKMAYER
Research Laboratory of Physical Chemistry, Massachusetts Institute of Technology, Cambridge, Massachusetts

(Received April 14, 1942)

The second virial coefficients B for methane, normal butane, and three mixtures of these gases were evaluated from the experimental data, and the interaction term B_{12} computed for methane-*n*-butane from 150° to 300°C. The results were used to study the methods of combination of constants in an equation of state. Computation of B_{12} from a Lennard-Jones expression similar to that used for a pure gas with σ and θ evaluated as $\sigma_{12}=\frac{1}{2}(\sigma_{11}+\sigma_{22})$ and $\theta_{12}=\sqrt{\theta_{11}\theta_{22}}$ where the subscripts 1 and 2 refer to the pure components gave exceptionally good results. This suggested a new method of combination of constants in the equation of state which led to the best results of any method so far used.

THE compressibilities[1] of methane, normal butane, and three mixtures of these gases have been used to study various methods of combination of constants in an equation of state. In the present paper the data on these five systems are applied to a study of the second virial coefficient.

Compressibility measurements on gases and on gas mixtures of constant composition may be correlated by an equation of the form:

$$pV=RT(1+B/V+C/V^2+\cdots), \qquad (1)$$

where the second virial coefficient B is a function of T for a pure gas, and of T and x_1, x_2, $\cdots$ (the mole fractions) for a gas mixture.

EXPERIMENTAL RESULTS

Now

$$B=\lim_{1/V\to 0} V\left(\frac{pV}{RT}-1\right). \quad (T, x=\text{constant}) \qquad (2)$$

Hence from a plot of $V[pV/RT)-1]$, computed from isothermal compressibility measurements on a pure gas or on a mixture of constant composition, against $1/V$ we can determine B as the intercept of the curve on the $1/V$ axis. In Table I the experimental values of B obtained in this manner for the five systems mentioned above are given.

TABLE I. Second virial coefficients for the system methane—normal-butane determined from the experimental data.

Mole fraction CH_4 / Temp. °C (Int.)	0	0.25066	0.50436	0.74895	1*
			B in liter/mole		
300	−0.1574	−0.0984	−0.0476	−0.0202	+0.0068
275	− .1760	− .1108	− .0564	− .0256	+ .0045
250	− .1981	− .1262	− .0651	− .0314	+ .0019
225	− .2245	− .1445	− .0761	− .0380	− .0009
200	− .2542	− .1645	− .0888	− .0451	− .0040
175	− .2873	− .1870	− .1034	− .0523	− .0075
150	− .3287	− .2147	− .1207	− .0613	− .0114

* Values for CH_4 computed from the Beattie-Bridgeman equation of state.

For a binary mixture the second virial coefficient B_m is related to those, B_{11} and B_{22}, of the pure components and the mole fractions x_1, x_2 of the components by the relation

$$B_m=x_1^2B_{11}+2x_1x_2B_{12}+x_2^2B_{22}, \qquad (3)$$

where B_{12} is the interaction constant, a function of temperature but not of composition. In Table II average experimental values of B_{12} for methane-*n*-butane are given from 150° to 300°. These were computed at a given temperature by first finding

$$2B_{12}-B_{11}-B_{22}=(B_m-x_1B_{11}-x_2B_{22})/x_1x_2 \qquad (4)$$

for each mixture at the temperature in question, averaging the three values of $(2B_{12}-B_{11}-B_{22})$, and then computing B_{12} from this average. Since

TABLE II. Values of B_{12} for methane-normal-butane. $B_{12}(\text{calcd.})=0.1102-78/T-54\times 10^4/T^3$

Temp. °C (Int.)	B_{12} (obs.)	B_{12} (calc.)	B_{12} (obs. −calc.)
		liter/mole	
300	−0.0292	−0.0288	−0.0004
275	− .0352	− .0354	+ .0002
250	− .0420	− .0427	+ .0007
225	− .0512	− .0508	− .0004
200	− .0604	− .0598	− .0006
175	− .0694	− .0699	+ .0005
150	− .0816	− .0813	− .0003

* Contribution from the Research Laboratory of Physical Chemistry, Massachusetts Institute of Technology No. 491.

[1] J. A. Beattie, W. H. Stockmayer, and H. G. Ingersoll, J. Chem. Phys. 9, 871–874 (1941).

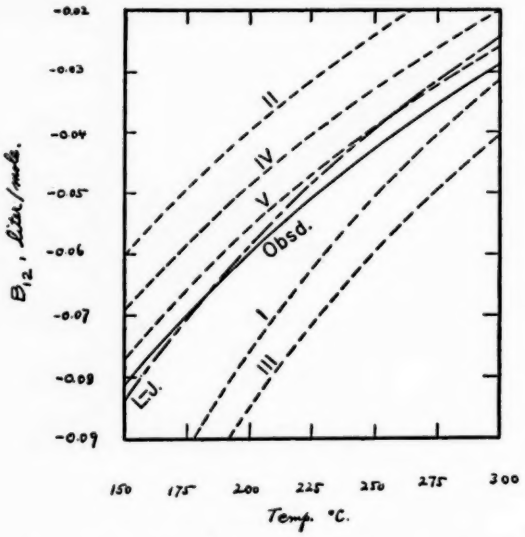

FIG. 1. Plot of B_{12} for methane-*n*-butane against temperature. The solid line represents the smoothed observed values; the dotted lines, the values from five methods of combination of constants in an equation of state; and the dot-and-dash line, the values from the Lennard-Jones potential.

differences of quantities of about the same size are involved the accuracy of the determination of B_{12} is not high.

According to the Beattie-Bridgeman equation of state

$$B_{12}=B_{012}-A_{012}/RT-c_{12}/T^3, \qquad (5)$$

where B_{012}, A_{012}, and c_{12} are interaction constants of the equation of state of mixtures. In order to smooth the experimental value of B_{12} we fitted them with an equation of this type, the constants being determined *empirically* from the experimental values of Table I. The result is

$$B_{12}\ (\text{liter/mole})=0.1102-78/T-54\times10^4/T^3; \qquad (6)$$

and values computed from this relation are given in Table II, and plotted in Fig. 1. It is evident that Eq. (6) reproduces the observed values of B_{12} well within the accuracy of their determination.

COMPUTATION OF B_{12} FROM AN EQUATION OF STATE FOR GAS MIXTURES

The equation of state constants for *n*-butane determined from all of the data up to the critical density do not reproduce the experimental B values well since, as has been pointed out before, the c constant is actually a function of density. Hence we redetermined the constants for *n*-butane from the second virial coefficients given in Table I. These values and the constants for methane (unchanged) are given in Table III.

In the earlier paper A_{012} was computed from the constants A_{011} and A_{022} of the pure gases by the usual relation:

$$A_{012}=A_{011}^{1/2}A_{022}^{1/2}; \quad \text{(square-root combination)} \qquad (7)$$

B_{012} by the two methods:

$$B_{012}=\tfrac{1}{2}(B_{011}+B_{022}), \quad \text{(linear combination} \qquad (8)$$

$$B_{012}=\tfrac{1}{8}(B_{011}^{1/3}+B_{022}^{1/3})^3; \quad \text{(Lorentz combination)} \qquad (8A)$$

and c_{12} by the two methods:

$$c_{12}=\tfrac{1}{2}(c_{11}+c_{22}), \quad \text{(linear combination)} \qquad (9)$$

$$c_{12}=c_{11}^{1/2}c_{22}^{1/2}. \quad \text{(square-root combination)} \qquad (9A)$$

There are thus four methods of computing the interaction constants of Eq. (5) from those of the pure gases:

Method I:
square root A_{012}, linear B_{012}, linear c_{12}.
Method II:
square root A_{012}, linear B_{012}, square root c_{12}.
Method III:
square root A_{012}, Lorentz B_{012}, linear c_{12}.
Method IV:
square root A_{012}, Lorentz B_{012}, square root c_{12}.

The values of B_{12} computed by Eq. (5) with each of these four methods of combination of constants and the values of constants given in Table III are plotted in Fig. 1. As was found before[1] Method IV gives the best over-all representation.

TABLE III. Values of the principal constants of the Beattie-Bridgeman equation of state for methane and low pressure normal butane.

Gas	R	A_0	B_0	c
	Units: liter/mole, normal atmos. °K			
CH_4	0.08206	2.2769	0.05587	12.83×10^4
n-C_4H_{10}	.08206	12.4805	.16020	975×10^4

COMPUTATION OF B_{12} FROM STATISTICAL MECHANICS

Equation (1) can be derived for a pure gas from classical statistical mechanics.[2] For molecules of spherical symmetry[3] the second virial coefficient B is given by

$$B=2\pi N\int_0^\infty (1-\exp(-W(r)/kT))r^2dr, \quad (10)$$

where N is Avogadro's number, $W(r)$ the mutual potential energy of a pair of molecules of separation r, and k is Boltzmann's constant. Although n-butane can hardly be considered to satisfy the condition of spherical symmetry, yet for practical purposes the assumption may not be too drastic.

TABLE IV. Values of the parameters in the Lennard-Jones potential.

$W(r)=\lambda r^{-12}-\mu r^{-6}$
$=4\epsilon[(\sigma/r)^{12}-(\sigma/r)^6]$,
$\epsilon=\mu^2/4\lambda$; $\sigma^6=\lambda/\mu$; $\theta=\epsilon/k$

Parameter	CH_4	$n-C_4H_{10}$	$CH_4-n-C_4H_{10}$
$2\pi N\sigma^3/3$ (cm³/mole)	70.3*	299.4*	158.3
θ°K	148*	268*	199*
$\epsilon\times10^{16}$ (erg)	204	370	275
σ(A)	3.820	6.191	5.006*
$\mu\times10^{10}$ (erg A⁶)	2.54	83.37	17.29
$\lambda\times10^{5}$ (erg A¹²)	0.0788	46.96	2.72
$\theta/T_{\text{critical}}$	0.78	0.63	

* All values in column computed from starred quantities.

Substitution of a Lennard-Jones[4] potential

$$W(r)=\lambda r^{-12}-\mu r^{-6},$$
$$=4\epsilon[(\sigma/r)^{12}-(\sigma/r)^6], \quad (11)$$
$$\epsilon=\mu^2/4\lambda; \quad \sigma^6=\lambda/\mu$$

into Eq. (10) gives:

$$B=\frac{2\pi N\sigma^3}{3}\sqrt{2}\left(\frac{\theta}{T}\right)^{\frac{1}{4}}\left[\Gamma\left(\frac{3}{4}\right)-\sum_1^\infty{}_n\, c_n\left(\frac{\theta}{T}\right)^{n/2}\right], \quad (12)$$

$$c_n=\frac{2^{n-2}}{n!}\Gamma\left(\frac{2n-1}{4}\right); \quad \theta=\epsilon/k.$$

The values of σ and θ were determined for methane and n-butane from the data of Table I by a method to be given in a later paper. The results are given in Table IV. Lennard-Jones and Devonshire[5] predicted on theoretical grounds that the ratio of θ to the critical temperature on the Kelvin scale is about 0.75 for gases obeying the (6, 12) potential and found that this is quite closely obeyed for several gases. For methane ($T_c=190.7$) this ratio is 0.78; for n-butane ($T_c=425.2$) it is 0.63. Either n-butane is not well approximated by the assumption of spherical symmetry or else on a corresponding states basis the temperature range of the data is too short to give the Lennard-Jones potential accurately.

For a binary mixture classical theory[6] leads to Eq. (1) where B_m is given by Eq. (3), and B_{12} by Eq. (10) with the use of the mutual potential energy $W_{12}(r)$ of molecule 1 and molecule 2. The calculation of W_{12} from W_{11} and W_{22} from theoretical considerations alone has not been carried out but the indications are that a good approximation can be made.

From experimental data on mixtures Lennard-Jones and Cook[6] found that

$$\sigma_{12}=\tfrac{1}{2}(\sigma_{11}+\sigma_{22}), \quad (13)$$

which corresponds to averaging collision radii when the relative kinetic energy is zero (Lorentz combination), is a good approximation; and Hirschfelder and Roseveare[7] used this equation and the relation

$$\mu_{12}=\mu_{11}^{1/2}\,\mu_{22}^{1/2} \quad (14)$$

for the treatment of mixtures.

We computed B_{12} for methane-n-butane from Eq. (12) and the relations:

$$\sigma_{12}=\tfrac{1}{2}(\sigma_{11}+\sigma_{22}),$$
$$\theta_{12}=\theta_{11}^{1/2}\,\theta_{22}^{1/2}. \quad (15)$$

The numerical values of σ_{12} and θ_{12} so computed are given in Table IV and the curve for B_{12} is

[2] W. H. Keesom, Comm. Phys. Lab., Leiden, Suppl. **24B**, 41 pp. (1912); H. D. Ursell, Proc. Camb. Phil. Soc. **23**, 685–697 (1925–27).

[3] For a treatment of polar molecules see W. H. Stockmayer, J. Chem. Phys. **9**, 398–402 (1941).

[4] J. E. Lennard-Jones, Proc. Roy. Soc. **106A**, 463–477 (1924); Physica **4**, 941–956 (1937); see also R. H. Fowler, *Statistical Mechanics* (The Macmillan Company, New York, 1936), pp. 292–312.

[5] J. E. Lennard-Jones and A. F. Devonshire, Proc. Roy. Soc. London, **163A**, 53–70 (1937).

[6] J. E. Lennard-Jones and W. R. Cook, Proc. Roy. Soc. **115A**, 334–348 (1927); see also Fowler, reference 4, and R. H. Fowler and E. A. Guggenheim, *Statistical Thermodynamics* (The Macmillan Company, New York, 1939), pp. 255–138.

[7] J. O. Hirschfelder and W. E. Roseveare, J. Phys. Chem. **43**, 15–35 (1939).

labelled L.-J. in Fig. 1. Equation (15) is equivalent to taking $\epsilon_{12}=\epsilon_{11}^{1/2}\epsilon_{22}^{1/2}$.

The success of this result suggests by analogy the Lorentz combination for B_{012} and square-root combination for A_{012}/B_{012} and c_{12}/B_{012} of Eq. (5), since B_0 is analogous to $2\pi N\sigma^3/3$ and A_0/RB_0 to θ. Thus:

$$B_{12}=B_{012}\left[1-\frac{A_{012}}{B_{012}RT}-\frac{c_{12}}{B_{012}T^3}\right], \quad (16)$$

where Eq. (8A) is used for the B_{012} outside the parenthesis, and equations similar to Eq. (7) for (A_{012}/B_{012}) and (c_{12}/B_{012}). Using in Eq. (16) the values of the equation of state constants given in Table III we find

$$B_{12}\ (\text{liter/mole})=0.09906-68.02/T-117\times10^4/T^3. \quad (17)$$

Values from this equation give the curve labelled V shown in Fig. 1. It is the best of the combination rules for computing B_{12} from the equation of state.

JULY, 1942 JOURNAL OF CHEMICAL PHYSICS VOLUME 10

Determination of the Lennard-Jones Parameters from Second Virial Coefficients

Tabulation of the Second Virial Coefficient*

WALTER H. STOCKMAYER AND JAMES A. BEATTIE
Research Laboratory of Physical Chemistry, Massachusetts Institute of Technology, Cambridge, Massachusetts

(Received April 14, 1942)

Values of $B/(2\pi N\sigma^3/3)$ to four decimal places as a function of θ/T are computed from $\theta/T=0.20$ to 1.00 for a Lennard-Jones (6, 12) potential. The equation $B/(2\pi N\sigma^3/3)=(\theta/T)^{\frac{1}{4}}[1.064-3.602(\theta/T)]$ computes the tabulated values fairly well. Thus σ and θ can be determined from experimental B values by plotting $BT^{\frac{1}{4}}$ against $1/T$ and finding the slope and intercept of the best straight line through the points. For methane and n-butane this method gave parameters that computed B values agreeing with observed values within the experimental uncertainty.

IN the preceding paper[1] second virial coefficients derived from a Lennard-Jones (6, 12) potential were applied to the compressibility data on methane, n-butane, and mixtures of these two gases. Let:

$$W(r)=\lambda r^{-12}-\mu r^{-6}=4\epsilon[(\sigma/r)^{12}-(\sigma/r)^6],$$

where

$$\epsilon=\mu^2/4\lambda,\qquad \sigma^6=\lambda/\mu.$$

The second virial coefficient B (cc/mole) becomes:

$$\frac{B}{\beta}=\sqrt{2}\left(\frac{\theta}{T}\right)^{\frac{1}{4}}\left[\Gamma\left(\frac{3}{4}\right)-\sum_1^\infty{}_n\frac{2^{n-2}}{n!}\Gamma\left(\frac{2n-1}{4}\right)\left(\frac{\theta}{T}\right)^{n/2}\right], \quad (1)$$

where

$$\theta=\epsilon/k,\qquad \beta=2\pi N\sigma^3/3;$$

and N is the Avogadro number, σ is in cm, ϵ in ergs, and k the Boltzman constant in ergs/°K, so that θ is in °K. Any other consistent set of units may, of course, be used.

To compute the values of B/β given in Table I as a function of θ/T we set $y=2(\theta/T)^{\frac{1}{4}}$ and computed the function for values of y increasing by

---

* Contribution from the Research Laboratory of Physical Chemistry, Massachusetts Institute of Technology, No. 492.

[1] J. A. Beattie and W. H. Stockmayer, J. Chem. Phys. **10**, 473 (1942).

TABLE I. Lennard-Jones second virial coefficients.

$$W(r)=4\epsilon[(\sigma/r)^{12}-(\sigma/r)^{6}]$$

$$B/\beta=\sqrt{2}\left(\frac{\theta}{T}\right)^{\frac{1}{4}}\left[\Gamma\left(\tfrac{3}{4}\right)-\sum_{1}^{\infty}{}_{n}\frac{1}{4n!}\Gamma\left(\frac{2n-1}{4}\right)2^{n}\left(\frac{\theta}{T}\right)^{n/2}\right];\quad \theta=\epsilon/k,\quad \beta=2\pi N\sigma^{3}/3$$

θ/T	0.00	0.01	0.02	0.03	0.04	0.05	0.06	0.07	0.08	0.09
					B/β					
0.20	+0.2434	+0.2185	+0.1933	+0.1677	+0.1417	+0.1154	+0.0887	+0.0617	+0.0345	+0.0070
0.30	− .0207	− .0487	− .0770	− .1056	− .1344	− .1635	− .1929	− .2225	− .2523	− .2823
0.40	− .3126	− .3431	− .3738	− .4047	− .4359	− .4673	− .4989	− .5307	− .5628	− .5951
0.50	− .6276	− .6604	− .6933	− .7264	− .7597	− .7932	− .8270	− .8610	− .8952	− .9296
0.60	− .9643	− .9992	−1.0343	−1.0696	−1.1051	−1.1408	−1.1767	−1.2129	−1.2493	−1.2859
0.70	−1.3228	−1.3599	−1.3972	−1.4347	−1.4724	−1.5103	−1.5485	−1.5870	−1.6257	−1.6646
0.80	−1.7037	−1.7431	−1.7828	−1.8227	−1.8628	−1.9032	−1.9438	−1.9846	−2.0256	−2.0669
0.90	−2.1084	−2.1502	−2.1923	−2.2346	−2.2772	−2.3201	−2.3632	−2.4065	−2.4501	−2.4939
1.00	−2.5380									

TABLE II. Deviations of B/β computed by Eqs. (2) and (3) from the values listed in Table I.

θ/T	0.2	0.3	0.4	0.5	0.6	0.7	0.8	0.9	1.0
				$\Delta(B/\beta)$					
Table I—Eq. (2)	−0.0041	+0.0010	+0.0007	−0.0002	−0.0004	±0.0000	+0.0004	−0.0006	−0.0041
Table I—Eq. (3)	+ .0136	− .0084	− .0129	− .0079	+ .0014	+ .0103	+ .0153	+ .0128	± .0000

increments of 0.05 from 0.8 to 2.2, that is for θ/T from 0.16 to 1.21. In order to construct a table for even values of θ/T in the range $(\theta/T)=0.20$ to 1.00 the approximate equation

$$\frac{B}{\beta}=0.71875-2.131899\frac{\theta}{T}-1.120795\left(\frac{\theta}{T}\right)^{2} \quad (2)$$

was used together with a deviation plot. Deviations of the values computed by Eq. (2) from those of Table I are given in Table II.

Table I covers the region from the critical to the Boyle temperature for all gases, and thus covers the experimentally accessible range for all except the permanent gases.

Another approximate equation, while not as accurate as Eq. (2), is particularly suited for a rapid estimate of θ and β and hence of λ and μ. It was found that the equation

$$\frac{B}{\beta}=\left(\frac{\theta}{T}\right)^{\frac{1}{4}}\left[1.064-3.602\frac{\theta}{T}\right] \quad (3)$$

reproduces the values in Table I as closely as B is known for many gases. (See Table II for the deviations.) Consequently from a plot of the experimental values of $BT^{\frac{1}{4}}$ against $1/T$ we can determine β and θ very quickly since $-3.602\beta\theta^{5/4}$ is the slope and $1.064\beta\theta^{\frac{1}{4}}$ the intercept on the $BT^{\frac{1}{4}}$ axis at $1/T=0$ of the best straight line through the experimental points. This procedure was followed in obtaining θ and β for methane and n-butane. Second virial coefficients determined from these values of θ and β agreed with the observed values within the experimental uncertainty.

The Electrostatic Influence of Substituents on Reaction Rates

III. Solvent Effect

F. H. WESTHEIMER, W. A. JONES,[1] AND ROBERT A. LAD[1]
Department of Chemistry, University of Chicago, Chicago, Illinois

(Received April 23, 1942)

The magnitude of the electrostatic effect of substituents on reaction velocity depends on the solvent in which the reaction is carried out. In order to investigate the influence of solvent, the first and second saponification constants of diethyl malonate and diethyl adipate have been measured, both in water and in 80-percent alcohol, in solutions of varying ionic strength. The saponification constants have been extrapolated to infinite dilution. The ratio of the first to the second velocity constant at infinite dilution in any one solvent is a measure of the effect of a charged substituent on the rate of saponification. The results obtained in water are compared with those for 80-percent alcohol, and it has been shown that they are in good qualitative agreement and in fair quantitative agreement with the predictions of the Kirkwood-Westheimer theory.

AN electrostatic theory of the effect of substituents on reaction rates requires that the substituent effect increases as the dielectric constant of the solvent is lowered. In particular, the theory advanced by Kirkwood and Westheimer[2,3] (which takes explicit account of the electrostatic forces which are transmitted through the solvent as well as those which are transmitted through the molecule itself) makes quantitative predictions concerning the relationship between molecular shape and dielectric constant, on one hand, and substituent effect, on the other.

It is a matter of some interest that Ritchie,[4] investigating the saponification of the esters of diacids, found in several instances that the ratio of the first to the second saponification constant is actually smaller in alcohol-water mixtures than in water itself. That is to say, Ritchie's results indicate that the negative charge of the ion of a half ester repels an hydroxide ion to a greater extent in water than in a solvent of much lower dielectric constant.

A reinvestigation of the matter has shown that Ritchie's experimental data are probably correct. However, in his work he neglected salt effects,[5] and these salt effects are of considerable magnitude, especially in the solvent of low dielectric constant. The quantitative predictions of electrostatic theory apply, of course, only to solutions so dilute that no such complications can arise.

In the present work, the first and second saponification constants of the diethyl esters of malonic and adipic acids were determined at several values of the ionic strength in both water and in 80-percent alcohol. When the rate constants were carefully extrapolated to infinite dilution, it was seen that, in conformity with theory, the electrostatic effect is greater in the solvent of lower dielectric constant.

The experimental work was carried out with malonates and adipates because the Kirkwood-Westheimer theory predicts strikingly different results for these two cases. The electrostatic effect of a charged substituent is computed by applying classical electrostatics to a model which consists of an inner region of low dielectric constant representing the activated complex, surrounded by an homogeneous solvent. This model, while most certainly an approximation, probably corresponds more closely with reality than does any other which has been advanced.[6] Furthermore, it provides a means of correlating the electrostatic effect with the shape of the molecules which enter into reaction. It is clear, on the basis of the model, that, for elongated particles like the activated complex which arises in the

[1] Samuel S. Fels Fellow in 1941.
[2] J. G. Kirkwood and F. H. Westheimer, J. Chem. Phys. **6**, 506 (1938); **7**, 437 (1939); F. H. Westheimer and J. G. Kirkwood, *ibid.*, **6**, 513 (1938).
[3] F. H. Westheimer and M. Shookhoff, J. Am. Chem. Soc. **62**, 269 (1940).
[4] M. Ritchie, J. Chem. Soc. 3112 (1931).
[5] J. N. Brønsted, Chem. Rev. **5**, 231 (1928).
[6] A brief discussion of other models is included in reference 2.

saponification of sodium ethyl adipate, most of the lines of force between the negative charges of the carboxylate ion and the hydroxide ion will travel through the solvent. The electrostatic effect of the substituent will be inversely proportional to the dielectric constant of the solvent. On the other hand, for shorter and, comparatively, broader molecules such as the malonates, most of the lines of force will flow through the molecule itself and relatively few through the external solvent. The effect of the solvent will, therefore, be minimized. These qualitative predictions have been borne out by the present study.

As yet, no explanation can be advanced for Ritchie's[4] striking results with the esters of dimethyl and diethylmalonic acid.

Previous experimental work which can be compared with the predictions of the present theory has, in general, been concerned with the ionization constants of substituted acids. The work of Schwartzenbach,[7] on the ionization constants of the dibasic acids in water and alcohol seems to be in general agreement with the work presented here; the experimental method, however, involving mixed solvent junctions, is not unassailable. The work of Kilpatrick and Mears[8] on the ionziation of substituted benzoic acids in methanol has been compared with the predictions of the present theory. Here the results are only in qualitative agreement with the theory.

EXPERIMENTAL

Method

The rates of saponification of the esters were determined by titrating, from time to time, the alkali present in the reaction mixture. The solutions containing the ester and alkali were forced into a 10-cc calibrated pipet, and the pipet emptied into standard acid. The excess acid was back-titrated with 0.01 *N* base. The only real modification of the procedure previously used[9] was the addition of glass jackets for the delivery pipets. Water from the thermostat was pumped through the jacket while samples were withdrawn.

The saponification of the adipates was carried out in a thermostat maintained at 20.0°±0.01°, while the measurements for the malonates were carried out in an insulated and stirred ice bath at 0.0±0.03°.

Materials

After vacuum fractionation, the diethyl adipate melted at −21°.[10] The diethyl malonate was carefully fractionated through a Podbielniak column, and boiled at 82.5–83° at 11-mm pressure. Sodium ethyl malonate was prepared following Walker's[11] general method. It was quite hygroscopic, but saponification showed that it was better than 99 percent pure. The potassium salt[11,12] was much easier to handle than the sodium salt, and its saponification value was 100.6 percent of the theoretical. Sodium and potassium ethyl adipates were made by Walker's method, and were 99.5 percent pure. Hydrogen ethyl adipate, prepared in a manner analogous to the preparation of hydrogen ethyl sebacate,[13] boiled at 140°/3 mm, and had a neutral equivalent of 100.1 percent of the theoretical.

Absolute alcohol was made by the barium oxide method and had a density of 0.78498 at 26.5°. It was diluted with conductivity water so that the resulting solution would be 80 percent alcohol by weight. The solutions of ester and of alkali were made up in water or 80-percent alcohol prior to use, and brought to temperature in the thermostat. A saponification experiment was initiated by mixing the solutions.

RESULTS

The saponification of the diethyl esters is complicated by the simultaneous saponification of the salt of the monoester formed during the reaction. The problem involved has been understood for some time, and both Ritchie[4] and Ingold[14] suggested methods of computing the first saponification constant; neither of these methods, however, appears convenient. An approximate method which permits rapid computation of the first saponification constant has been developed, and the derivation of the neces-

[7] G. Schwartzenbach, Helv. Chim. Acta **16**, 522, 529 (1933).
[8] Kilpatrick and Mears, J. Am. Chem. Soc. **62**, 3047 (1940).
[9] F. H. Westheimer and R. P. Metcalf, J. Am. Chem. Soc. **63**, 1339 (1941).
[10] J. Timmermans, Bull. Soc. Chim. Belg. **36**, 502 (1927).
[11] J. Walker, J. Chem. Soc. **61**, 696 (1892).
[12] M. Freund, Ber. **17**, 780 (1884).
[13] Organic Syntheses **19**, 45 (1939).
[14] C. K. Ingold, J. Chem. Soc. p. 2170 (1931).

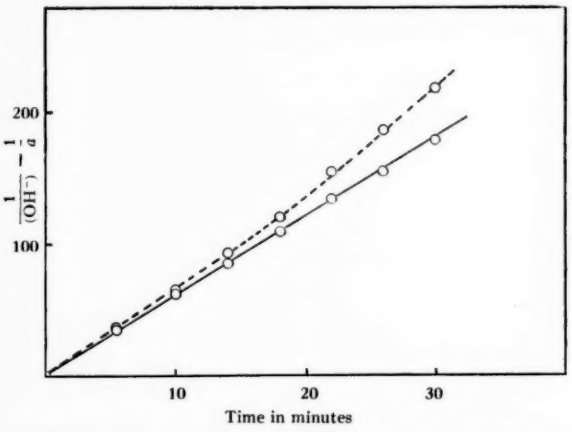

FIG. 1. The saponification of diethyl adipate in water at 20°. The dotted line shows the ordinary second-order equation (a is the initial concentration of hydroxide ion). The data corrected according to Eq. (11) are shown in the solid line.

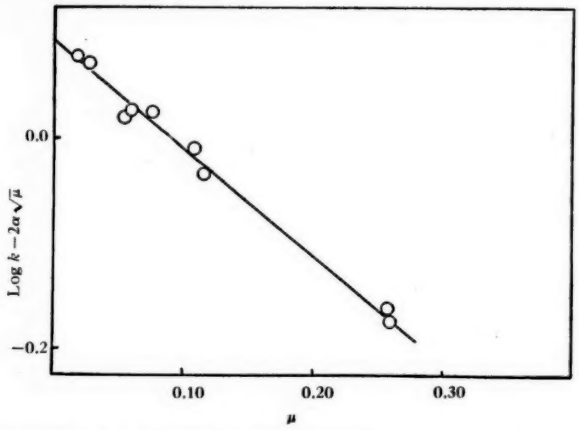

FIG. 2. The extrapolation to infinite dilution of the saponification constants for the monoethyladipate ion in water.

sary equations presented in Appendix A. The maximum error introduced by this computation is an over-correction of about 4 percent, and occurs when the constant is obtained from the amount of alkali consumed at about 40-percent reaction for the adipates at high ionic strength. The error usually introduced in the average rate constants is negligible. Application of Eq. (11) to the published data of Ingold[14] gave a constant identical with the one he had obtained.

Equation (11) involves c, the ratio of k_2 to k_1, where k_1 is the first and k_2 is the second saponification constant of the diester. Clearly, c is computed using the value of k_2 appropriate to the ionic strength at which the measurement of the first saponification constant is made. In practice, the values of k_2, the saponification constants of the ester salts were first obtained at several salt concentrations. Then the value of k_1 could be estimated from the alkali consumed at the beginning of the saponification of a diester. From k_2 and an approximate value of k_1, an approximate value of c could be obtained, and was introduced into the integrand of Eq. (11). A corrected value of k_1 was thus obtained. In some cases, it was necessary to repeat this process of approximation. To simplify the mathematics, the initial concentrations of alkali and ester were always made equal in the saponification of the diesters; this condition was of course unnecessary in the case of the monoester salts. (See Fig. 1.)

It was easily shown that the rate of water hydrolysis of the diesters and the monoester salts was negligible when compared to the measured rates of alkaline hydrolysis. Further, it could be shown that the monoester salt did not disproportionate to any large extent during the course of the reaction. Experiments demonstrating this were based on the extremely low solubility of the disalts (disodium adipate and disodium malonate) in alcohol.

The final values of the first saponification constants were plotted against μ, the ionic strength. In no case was the variation of the constant with salt concentration large, and the value at infinite dilution could easily be estimated. While the values of the first saponification constants of the diesters proved almost independent of the salt concentration, this was decidedly not true for the second saponification constants. Here the rate of reaction between the negative hydroxide ion and the negative ester-ion is greatly increased by the presence of salt, especially in the alcoholic solutions. The experimental value of k_2, the second saponification constant for ethyl adipate, varies more than threefold when μ, the ionic strength, is increased from 0.0065 to 0.096, and the value at an ionic strength of 0.0065 is almost double the extrapolated value for infinite dilution in 80-percent alcohol.

The extrapolation of the values of k_2 to infinite dilution could not be accomplished successfully by plotting k_2 against $\sqrt{\mu}$. A more refined method

TABLE I. The rates of saponification of adipates and malonates.

Conc. ester M/l	Conc. NaOH M/l	Conc. NaCl M/l	μ (corr)	k_1 in min.$^{-1}$ $(M/l)^{-1}$
		Diethyl adipate Water 20°		
0.005061	0.005020	——	0.0050	5.81
.005230	.005020	——	.0050	6.08
.005062	.005062	——	.0051	5.94
.005062	.005065	——	.0051	5.94
.005105	.004989	0.00664	.0116	6.40
.005105	.005068	.02001	.0231	6.20
.005153	.005015	.02667	.0317	6.14
.005078	.004990	.0330	.0383	5.80
.005103	.005030	.04674	.0518	5.88
.005153	.005045	.06668	.0718	5.78
.01108	.01108	——	.01108	5.70
		Diethyl adipate 80% alcohol 20°		
0.02000	0.02000	——	0.0200	0.348
.02000	.02021	——	.0202	.326
.02000	.02021	——	.0202	.320
.02000	.02042	0.03021	.0506	.330
.02000	.02048	.03410	.0546	.358
.05990	.05940	——	.0594	.336
.05990	.05940	——	.0594	.329
.02000	.02050	.04985	.0704	.330
.02000	.02060	.06820	.0888	.334
.02000	.02040	.07022	.0905	.334
.02000	.02000	.1000	.1200	.403
.02000	.02056	.1000	.1206	.332
		Sodium ethyl adipate Water 20°		
0.01109	0.01109	——	0.0180	(1.63[a])
.01001	.00999	——	.0260	1.712
.02068	.02068	——	.0534	1.745
.02280	.02248	——	.0592	1.860
.03189	.00981	0.0598	.108	2.085
.02000	.02000	.0626	.115	2.020
.01030	.01030	.232	.257	2.140
.01000	.01000	.232	.258	2.182
.01001	.00999	.0499	.273	1.981[b]
		Sodium ethyl adipate 80% alcohol 20°		
0.00302	0.00302	——	0.0065	0.0383
.00500	.00500	——	.0110	.0413
.01002	.01002	——	.0250	.0735
.00965	.0290	——	.0437	.0880
.0204	.0612	——	.0916	.116
.01090	.01090	0.0684	.0956	.120
		Diethyl malonate Water 0°		
0.004982	0.004966	——	0.00497	25.7
.004972	.005040	——	.00504	23.4
.005017	.005042	——	.00504	24.4
.004982	.005000	0.1000	.105	25.5
.004972	.005080	.1000	.105	22.2
.01109	.01109	——	.0111	21.1
		Diethyl malonate 80% alcohol 0°		
0.02000	0.01996	——	0.0200	1.184
.02000	.01996	——	.0200	1.212
.02035	.02035	——	.0204	1.200
.02000	.02032	0.02506	.0454	1.254
.02000	.02032	.02506	.0454	1.230
.05987	.05870	——	.0587	1.150
.05987	.05870	——	.0587	1.221
.02000	.02005	.05000	.0701	1.358
.02000	.02005	.05000	.0701	1.424
		Potassium ethyl malonate Water 0°		
0.01059	0.01988	——	0.330	0.181
.01051	.02975	——	.0434	.189
.01041	.03906	——	.0536	.191
.01042	.04011	0.02006	.0743	.199
.01004	.03891	.03000	.0829	.196
.01067	.03906	.05015	.1042	.204
.01072	.03893	.06005	.1140	.206
.01046	.03882	.07015	.1236	.205
.01062	.03868	.08130	.1349	.206
.01047	.03992	.1004	.1550	.210
		Sodium ethyl malonate 80% alcohol 0°		
0.02040	0.02040	——	0.0440	0.0167
.01052	.03066	——	.0442	.0185
.02040	.02040	0.0404	.0872	.0289
.03062	.06108	——	.1007	.0276
.01011	.03011	.0989	.1442	.0470

[a] Preliminary experiment with potassium ethyl adipate.
[b] Hydrogen ethyl adipate used.

Table II. Saponification constants for adipates and malonates, extrapolated to infinite dilution.

Compound	Solvent	Temperature	k^0 in min.$^{-1}$ $(M/l)^{-1}$
Diethyl adipate	Water	20°	5.97
	80% alcohol	20°	0.339
Ethyl adipate ion	Water	20°	1.23
	80% alcohol	20°	0.0217
Diethyl malonate	Water	0°	23.7
	80% alcohol	0°	1.11
Ethyl malonate ion	Water	0°	0.134
	80% alcohol	0°	.00401

of extrapolation[15] was, therefore, adopted. It was assumed that the activity coefficient, γ, of an ion is given by the following equation:

$$\log \gamma = -\alpha Z^2 \sqrt{\mu} + \beta\mu,$$

where α is the Debye-Hückel constant, Z the ionic charge, and β is a constant. Applying the Brønsted theory[5] of the critical complex, it

[15] This method has been applied to ionic equilibria. See H. S. Harned and B. B. Owen, J. Am. Chem. Soc. **52**, 5079 (1930).

TABLE III. Values of $\Delta \log k$ for infinite dilution.

Compounds	Solvent	Temperature	$k_1^0/2k_2^0$	$\Delta \log k$
Adipates	Water	20°	2.39	0.38
	80% alcohol	20°	7.80	0.89
Malonates	Water	0°	89.	1.94
	80% alcohol	0°	139.	2.14

becomes apparent that a plot of $(\log k_2 - 2\alpha\sqrt{\mu})$ against μ should be a straight line, and that the value of the expression in parentheses for $\mu=0$ is just $\log k_2^0$ where k_2^0 is the value of k_2 at infinite dilution. This method proved highly satisfactory, and an accurate extrapolation could be made. While this method assumes that the Debye-Hückel limiting law holds for 80-percent alcohol as well as for water, the values of k_2^0 obtained are probably independent of this assumption. Only the limiting value of k_2 is desired, and the experimental fact that the plots are linear suggests that the extrapolation involves no great error. The straight lines were actually obtained by the method of least squares. The error in the extrapolation is no greater than the error in the measurements themselves, and probably does not exceed 0.02 log unit. (See Fig. 2.)

The observed and extrapolated velocity constants are tabulated in Tables I and II. The ionic strength changes somewhat during the saponifications; the value of μ recorded is the average value for the particular experiment. However, μ is given in moles per liter, instead of the customary units of moles per 1000 grams. The former unit is the one for which the Debye-Hückel equation was derived.

The saponification constants for the malonates in water are in rough agreement with the values obtained by Ritchie.[4] The saponification of malonic ester,[16] in contrast to the saponification of acetoacetic ester,[17] is a normal second-order reaction. Apparently the ionization of diethylmalonate in very dilute alkali is too slight to interfere with the kinetics of the reaction. The ratio of k_1^0/k_2^0 for the adipates in water is quite close to the ratio found by Ingold,[12] but the individual constants differ from his by a factor of almost 2. No explanation of this difference is available, but the values of the constants here reported have been checked, not only by the authors, but also by Dr. Donna Price.

The effect of the negative charge of the ester-ion on the rate of saponification can be judged from the value of the ratio $k_1^0/2k_2^0$. (The statistical factor of 2 has been introduced because there are two ester groups in the diester which can be attacked.) In Table III the values of $k_1^0/2k_2^0$, and the values of $\log (k_1^0/2k_2^0)$ or $\Delta \log k$ are presented.

DISCUSSION OF RESULTS

It has been pointed out before that k_1 is almost independent of ionic strength, while k_2 increases with increasing salt concentration; this increase is very much greater in aqueous alcohol than in water. The ratio $k_1/2k_2$ is, therefore, quite strongly dependent on the ionic strength. Even in the lowest salt concentration at which the present work was carried out, the value of the ratio is almost the same in water as in 80-percent alcohol. But the value of $k_1^0/2k_2^0$ for the adipates is much greater in 80-percent alcohol than in water. And only at infinite dilution has the ratio of the velocity constants theoretical significance.

Furthermore, it is qualitatively clear that the predictions concerning the influence of shape on solvent effect have proved correct. The electrostatic equation which relates the first to the second saponification constant of the ester of a dibasic acid is as follows:

$$\Delta \log k = e^2/2.303 D_E R \mathbf{k} T,$$

where e is the electronic charge, $\mathbf{k}$ is Boltzmann's constant, R is the distance between the negative charges in the activated complex derived from the ester-ion. D_E, the effective dielectric constant, is a function of the sizes and shapes of the molecules involved and of the external dielectric constant. For elongated molecules such as the adipates where the external dielectric constant is quite important, D_E should approximate the

TABLE IV.

Compound	Solvent	Temperature	Δpk (or ΔpK)	R
Diethyl adipate	Water	20°	0.38	8.20
Diethyl adipate	80% alcohol	20°	0.89	8.25
Adipic acid	Water	25°	0.38	7.75
Diethyl malonate	Water	0°	1.94	4.90
Diethyl malonate	80% alcohol	0°	2.14	5.15
Malonic acid	Water	25°	2.26	4.10

[16] H. Goldschmidt and V. Scholz, Ber. **36**, 1333 (1903).
[17] H. Goldschmidt and L. Oslan, Ber. **33**, 1140 (1900).

dielectric constant of the solvent. In actual fact, the values of $\Delta \log k$ for the adipates are inversely proportional to the dielectric constant of the solvent, increasing from 0.38 to 0.89 as the dielectric constant falls from 79 to 34.

On the other hand, the effect of changing solvent is expected to be, and actually is, much smaller for the malonates. In this case changing the solvent from water to 80-percent alcohol caused an increase in $\Delta \log k$ from 1.94 to 2.14.

It can be concluded, therefore, that at least qualitatively, the Kirkwood-Westheimer theory accounts for the change in velocity constant with change in solvent. The agreement is noteworthy because it explains the great difference in behavior which obtains with molecules of different shapes.

The quantitative application of the theory is, however, accompanied by certain difficulties. The first and perhaps the most important of these lies in the fact that it is necessary to treat 80-percent alcohol as an homogeneous solvent. There will, nevertheless, be a certain tendency for water, rather than alcohol, to cluster around the ions.[18] A further difficulty arises because of the shapes of the molecules involved, which do not correspond to the shapes (a sphere, a prolate ellipsoid with the charges at the foci) for which a mathematical solution of the electrostatic problem is convenient. While the adipates may, perhaps, reasonably be represented by a prolate ellipsoid, the approximation in the case of the malonates is necessarily poor. Here an average size must be taken for diethyl malonate, the monoethylmalonate ion and the activated complexes arising from these ions plus hydroxide ion. These ions are very different in size and in shape, none of them corresponds very well with a sphere (or ellipsoid), and the location of the charges with respect to the center of any sphere which might be chosen is very different for the monoester and the diester.

Further, while the approximate length R for the malonates and the adipates can be estimated, no accurate measure of this quantity is available. Nevertheless, the values of R were in each case computed in the same manner as in previous papers,[19] and the values listed in Table IV. In addition to the values of R obtained from the saponification data, Table IV contains the values of R obtained by carrying out similar computations for the first and second ionization constants of malonic and adipic acids in water. In these computations, the spherical model was used for the malonates; the results are not appreciably different using the ellipsoid instead. Despite the difference in molecular volume between the esters and the acids, the values of Δpk (as Ingold[14] has noted) are about the same for the two cases.

In order to carry out the computations presented in Table IV, it was necessary to have tables of D_E, similar to those previously published,[2] but which would apply to lower values of the dielectric constant of the solvent. These tables have been prepared, and are given in Appendix B.

The lengths R are all of the right order of magnitude. In the case of the adipates, the three values of R agree within 0.5A, and this result is as satisfactory as could be desired. However, in the case of the malonates, the agreement is poorer. While the values of R are individually reasonable, they differ among themselves by more than an Angstrom unit. Furthermore, in this case, this difference in length corresponds to a marked divergence of $\Delta \log k$. However, in view of the difficulties already noted which must arise in quantitative application of the theory to the malonates, the agreement is perhaps not unsatisfactory.

ACKNOWLEDGMENT

The authors are indebted to the Samuel S. Fels Fund for the financial support of this research.

APPENDIX A

Derivation of the equation for the computation of the first saponification constant of diesters.

Let a be the initial concentration of NaOH and of diester, x, y, and h the instantaneous concentrations of diester, monoester, and hydroxide ion at time t.

Then

$$-dh/dt = k_1hx + k_2hy \qquad (1)$$

where k_1 and k_2 are the first and second saponification

[18] See, for example, G. Scatchard, J. Chem. Phys. **9**, 34 (1941).

[19] F. H. Westheimer and M. Shookhoff, J. Am. Chem. Soc. **61**, 555 (1939).

TABLE V. Values of $D_E\sqrt{x}$.

$\sqrt{x}$ \ D	10	20	30	40	60
			$\cos\vartheta=-1$		
0.1	0.24	0.24	0.24	0.25	0.25
0.2	.58	.62	.62	.64	.64
0.3	1.1	1.2	1.2	1.3	1.3
0.4	1.8	2.1	2.3	2.3	2.4
0.5	3.0	3.7	4.1	4.3	4.5
0.6	4.5	6.2	7.2	7.7	8.4
0.7	6.8	11.	13.	14.	17.
0.8	10.	17.	22.	27.	29.
0.9	13.	25.	36.	46.	64.
1.0	16.	33.	49.	65.	98.
			$\cos\vartheta=-\frac{1}{2}$		
0.1	0.23	0.24	0.24	0.24	0.24
0.2	.56	.58	.58	.60	.60
0.3	.99	1.1	1.1	1.1	1.1
0.4	1.7	1.9	2.0	2.0	2.1
0.5	2.7	3.2	3.5	3.6	3.8
0.6	4.1	5.3	6.0	6.4	6.9
0.7	6.0	8.9	11.	12.	13.
0.8	8.6	15.	19.	23.	28.
0.9	12.	22.	32.	41.	56.
1.0	15.	30.	45.	60.	90.
			$\cos\vartheta=0$		
0.1	0.23	0.23	0.23	0.23	0.23
0.2	.52	.54	.54	.54	.54
0.3	.90	.96	.99	.99	1.0
0.4	1.4	1.6	1.7	1.7	1.7
0.5	2.3	2.6	2.8	2.9	3.0
0.6	3.4	4.3	4.7	5.0	5.4
0.7	5.0	7.2	8.4	9.2	10.
0.8	7.4	12.	16.	18.	21.
0.9	10.	19.	27.	34.	46.
1.0	13.	27.	40.	53.	80.

TABLE VI. Values of xD_E.

$\sqrt{x}$ \ D	10	20	30	40	60	78
0.1	0.02	0.02	0.02	0.02	0.02	0.02
.2	.08	.08	.08	.08	.08	.08
.3	.19	.20	.20	.20	.20	.20
.4	.37	.38	.38	.38	.38	.39
.5	.65	.70	.70	.70	.72	.72
.6	1.1	1.2	1.3	1.3	1.3	1.3
.7	1.8	2.1	2.3	2.3	2.4	2.4
.8	2.9	3.8	4.2	4.5	4.7	4.9
.9	4.8	7.3	8.7	9.7	11.	12.
.95	6.2	11.	14.	16.	20.	22.
1.0	8.1	16.	24.	33.	49.	64.

constants of the diester.

$$-dx/dt=k_1hx, \tag{2}$$

$$dy/dt=k_1hx-k_2hy. \tag{3}$$

So

$$-dy/dx=1-cy/x, \tag{4}$$

where $c=k_2/k_1$. On integration,

$$y=a^{1-c}x^c/(1-c)-x/(1-c), \tag{5}$$

and

$$x=h+[a+cx/(1-c)-a^{1-c}x^c/(1-c)]. \tag{6}$$

Equation (6) is completely equivalent to Ritchie's[4] Eq. (7). Now, as a first approximation, the diester and hydroxide concentration are always equal, since $k_1>k_2$. The term in brackets in Eq. (6) is, therefore, small, and replacing x by h here will cause an error of the second order. Therefore, as a good approximation,

$$x=h+a+ch/(1-c)-a^{1-c}h^c/(1\quad c). \tag{7}$$

Likewise, to a good approximation,

$$y=h^c/(1-c)[a^{1-c}-h^{1-c}]. \tag{8}$$

Substituting the approximate Eqs. (7) and (8) into Eq. (1)

$$-dh/dt=k_1h^2+k_1h^2\{a/h+c/(1-c)-(a/h)^{1-c}/(1-c) +c/(1-c)[(a/h)^{1-c}-1]\}. \tag{9}$$

Since the term in braces is small compared with unity, Eq. (10) is a good approximation to Eq. (9),

$$-dh/h^2\{1-c/(1-c)+(a/h)^{1-c}/(1-c) -a/h-c/(1-c)[(a/h)^{1-c}-1]\}=k_1dt. \tag{10}$$

And on integration,

$$1/h-1/a+\int_a^h\{c/(1-c)-(a/h)^{1-c}/(1-c)+a/h +c/(1-c)[(a/h)^{1-c}-1]\}\frac{dh}{h^2}=k_1t. \tag{11}$$

TABLE VII. Values of $D_E(\text{Charge})/(\lambda^3-\lambda)^{\frac{1}{2}}$.

λ \ D	10	20	30	40	60
2.3	2.5	3.0	3.3	3.4	3.6
2.0	3.5	4.7	5.2	5.7	5.9
1.8	4.7	6.7	7.8	8.5	9.3
1.6	6.6	11.	14.	15.	17.
1.4	9.9	18.	25.	31.	40.
1.3	12.	24.	35.	45.	63.
1.2	15.	30.	46.	61.	90.
1.1	19.	39.	58.	78.	117.
1.0	∞	∞	∞	∞	∞
			Values of $D_E(\text{Dipole})/(\lambda^3-\lambda)^{\frac{1}{2}}$		
2.3	0.54	0.57	0.59	0.59	0.59
2.0	.88	.94	.97	.97	1.0
1.8	1.3	1.4	1.5	1.5	1.6
1.6	2.2	2.7	2.8	2.9	3.0
1.4	4.8	6.7	7.6	8.1	8.9
1.3	8.2	13.	16.	18.	21.
1.2	16.	29.	39.	49.	62.
1.1	31.	62.	92.	125.	188.
1.0	∞	∞	∞	∞	∞

The indicated integration is performed graphically. The equation is a good approximation when h is at least half of a, and c is small.

APPENDIX B

Tables V, VI and VII supplement Table II in the first and Table II in the second papers of this series.[2] Specifically, Table V gives the values of $\sqrt{x}D_E$ for the case (analagous to the ionization of dibasic acids) in which two equal charges are placed at a distance r from the center of a sphere of radius b and $\sqrt{x}=r/b$. The angle made by the

lines joining these charges with the center of the sphere is called ϑ. Table VI gives the values of xD_E for the case (analagous to the ionization of a dipole substituted acid) in which a charge and a dipole are on a diameter at a distance r from the center of a sphere, and $\sqrt{x}=r/b$. Table VII gives the values of D_E (charge)$/(\lambda^3-\lambda)^{\frac{1}{2}}$ and of D_E(dipole)$/(\lambda^3-\lambda)^{\frac{3}{2}}$ for the cases in which two charges, or one charge and a dipole, are placed at the foci of a prolate ellipsoid of revolution. These tables again can be applied to cases analogous to the ionization of dibasic acids, or of dipole substituted acids. The ratio of the major axis of the ellipsoid to the distance between the foci is designated as λ.

JULY, 1942 JOURNAL OF CHEMICAL PHYSICS VOLUME 10

Statistical Thermodynamics of Rubber. II[1]

FREDERICK T. WALL
Noyes Chemical Laboratory, University of Illinois, Urbana, Illinois

(Received March 27, 1942)

The statistical theory of rubber elasticity is extended by postulating that the total volume of a piece of rubber remains constant during a stretching process. The modified theory is found to be in better agreement with observation than any previous molecular theory. In addition, it is shown theoretically that rubber should obey Hooke's law with respect to shear.

INTRODUCTION

DURING recent years, considerable progress has been made in connection with theories of rubber elasticity. Two general types of theories have been advanced, one from a macroscopic point of view and the other from a molecular point of view. As an example of the former, there is the theory of M. Mooney,[2] who arrived at an equation which agrees well with observation. For molecular theories, there is the work of Guth and Mark,[3a] Kuhn,[3b] and Pelzer[3c] who carried through calculations of a statistical nature.

More recently, the author[1] extended the statistical theory along lines which avoided some of the earlier difficulties. In the present paper, the calculations will be carried still further and the molecular theory will be related to the macroscopic theory of Mooney. It will also be shown theoretically that although rubber does not obey Hooke's law for ordinary elongation, it should obey Hooke's law for shear.

It will be supposed that the individual rubber molecules are long chain hydrocarbons capable of assuming various lengths and shapes as a result of free rotation about carbon-to-carbon valence bonds. When a piece of rubber is under no stress, the rubber molecules will have a certain distribution of shapes. When the rubber is subjected to a stress, however, the molecules will assume another distribution of lower probability. The theory here advanced will relate this probability to the entropy of strain, thus providing a means of arriving at the mechanical properties of rubber.

Two postulates will now be made. I. When a macroscopic piece of rubber is strained, the components of the lengths of the individual molecules (along some set of axes) will change in the same ratio as does the corresponding dimension of the piece of rubber. II. When a piece of

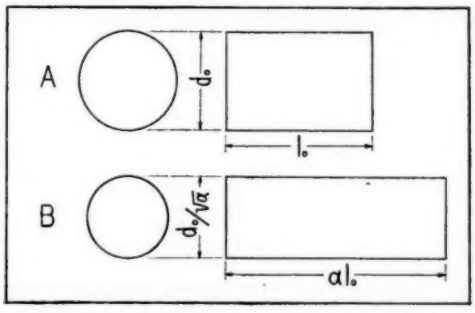

FIG. 1. A. Cylindrical piece of rubber in unstretched condition. B. Same piece of rubber after stretching.

[1] For the first paper of this series, see F. T. Wall, J. Chem. Phys. **10**, 132 (1942).
[2] M. Mooney, J. App. Phys. **11**, 582 (1940).
[3] (a) E. Guth and H. Mark, Monats. F. Chem. **65**, 93 (1934); Naturwiss. **25**, 353 (1937). (b) W. Kuhn, Kolloid Zeits. **68**, 2 (1934); **76**, 258 (1936); **87**, 3 (1939). (c) H. Pelzer, Monats. F. Chem. **71**, 444 (1938). See also H. Mark, *High Polymers* (Interscience Publishers, New York, 1940), pp. 69–78 for a general discussion of the subject.

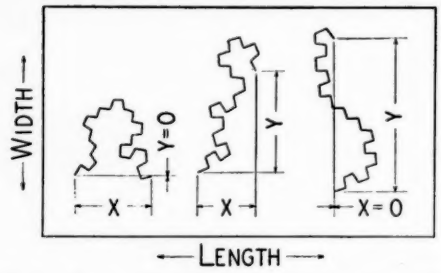

FIG. 2. Plane projections for rubber-like molecules.

rubber is elongated, no change in total volume takes place. The first assumption was made in the earlier paper of this series[1] whereas the second was not. Experimental support for the second postulate has been given by Holt and McPherson.[4] Our first problem is to investigate the effect of this second assumption on the equation of state for rubber.

STATISTICAL CALCULATIONS

Consider a cylindrical piece of rubber of length l_0 and diameter d_0 in its unstretched condition (Fig. 1). If this piece of rubber is stretched so that its length is increased by a factor α, then the diameter must change by a factor $1/\sqrt{\alpha}$ in view of postulate II. Within the piece of unstretched rubber, the molecules might appear as illustrated in Fig. 2. Let x, y, and z equal the components of the distance between the ends of a molecule along the directions indicated (z values being measured perpendicular to the plane of the paper). Then according to postulate I, when the rubber is stretched along its length by a factor α, all of the x values will increase by that factor and the y and z values will change by the factor $1/\sqrt{\alpha}$.

If the rubber molecules are uniformly long, the probability of finding a molecule with x, y, and z values in the range x to $x+dx$, y to $y+dy$, and z to $z+dz$ will be given by

$$p(x, y, z)dxdydz=\frac{\beta^3}{\pi^{\frac{3}{2}}}\times\exp\left[-\beta^2(x^2+y^2+z^2)\right]dxdydz \quad (1)$$

for the unstretched configuration. In expression (1), β is a constant depending upon the number of atoms in the molecular chain and the distance between adjacent atoms. For convenience, let us change expression (1) to cylindrical coordinates (x, r, ϕ) where $r^2=y^2+z^2$ and $\tan\phi=z/y$. Then (1) becomes

$$rp(x, r, \phi)dxdrd\phi=\frac{r\beta^3}{\pi^{\frac{3}{2}}}\times\exp\left[-\beta^2(x^2+r^2)\right]dxdrd\phi. \quad (2)$$

Integrating over the angular coordinate, we obtain

$$2\pi rp(x, r)dxdr=\frac{2\beta^3 r}{\sqrt{\pi}}\exp\left[-\beta^2(x^2+r^2)\right]dxdr \quad (3)$$

for the probability of finding molecules with x and r values in the ranges x to $x+dx$ and r to $r+dr$.

When the rubber is stretched, distribution (3) will be changed to

$$2\pi rp'(x, r)dxdr=\frac{2\beta^3 r}{\sqrt{\pi}}\times\exp\left[-\beta^2(x^2/\alpha^2+\alpha r^2)\right]dxdr, \quad (4)$$

where $\alpha=l/l_0$. The problem now is to determine the probability of finding the system with the distribution (4) when its most probable distribution is given by (3).

To accomplish this, let us first divide the configuration space into elements of size $2\pi r_i\Delta r_i\Delta x_i$, each element being located in the neighborhood of r_i and x_i. Let s_i equal the number of molecules in the ith cell and p_i equal the probability of finding a molecule in that cell. Also let $n_i=Np_i$ be the most probable number of molecules to be found in the ith cell, N being the total number of molecules. If P_0 is the probability of finding the system with its most probable distribution and if P is the probability of finding it with some other distribution characterized by s_1, s_2, s_3, etc., then

$$\ln(P/P_0)=\sum_i s_i\ln(n_i/s_i). \quad (5)$$

Equation (5) was derived in the first paper of this series[1] and will now be used directly. In the present instance, the quotient n_i/s_i will be given by dividing expression (3) by (4):

$$\frac{n_i}{s_i}=\frac{p(x_i, r_i)}{p'(x_i, r_i)}=\exp\left[-\beta^2x_i^2(1-1/\alpha^2)-\beta^2r_i^2(1-\alpha)\right]. \quad (6)$$

[4] W. L. Holt and H. T. McPherson, J. Research Nat. Bur. Stand. **17**, 657 (1936).

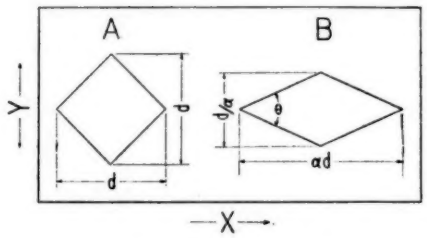

FIG. 3. A. Square cross section of rubber before shear. B. Cross section of same piece of rubber after pure shear of amount $\gamma=\alpha-1/\alpha=[2(\csc\theta-1)]^{\frac{1}{2}}$.

Hence

$$\ln\frac{P}{P_0}=-\beta^2(1-1/\alpha^2)\times\sum_i s_i x_i^2-\beta^2(1-\alpha)\sum_i s_i r_i^2. \quad (7)$$

But $\sum_i s_i x_i^2=N\langle x^2\rangle_{Av}$, where $\langle x^2\rangle_{Av}$ is the average value of x^2 for the distribution (4). Likewise $\sum_i s_i r_i^2=N\langle r^2\rangle_{Av}$, where $\langle r^2\rangle_{Av}$ is also calculated by use of (4). Upon integration it is found that $\langle x^2\rangle_{Av}=\alpha^2/(2\beta^2)$ and $\langle r^2\rangle_{Av}=1/(\alpha\beta^2)$. Therefore

$$\ln(P/P_0)=-N(\alpha^2-1)/2-N(1-\alpha)/\alpha,$$
$$=-N(\alpha^2+2/\alpha-3)/2. \quad (8)$$

It can be established readily that P has its maximum value (equal to P_0) when $\alpha=1$.

The entropy change accompanying the stretch can now be written. Evidently

$$S=k\ln(P/P_0)=-Nk(\alpha^2+2/\alpha-3)/2. \quad (9)$$

If the stretch is carried out isothermally, then the total energy of the rubber is unchanged providing only free rotation effects are utilized in rearranging the molecules. Hence the work done *on* the rubber must equal $-T\Delta S$ or

$$W=(NkT/2)(\alpha^2+2/\alpha-3). \quad (10)$$

The restoring force will be given by $(\partial W/\partial l)_T$ which is

$$f=(NkT/l_0)[(l/l_0)-(l_0/l)^2]. \quad (11)$$

Equation (11)* differs from the corresponding equation derived without postulate II[1] only in that the term $(l_0/l)^2$ has replaced a term (l_0/l). At first glance, this may not appear to be a significant improvement, but there is reason to believe that (11) is superior to the earlier form.

To show this, let us first rewrite Eq. (10):

$$W=(G/4)E(\alpha)+(G/4)F(\alpha), \quad (12)$$

where

$$G=NkT,$$
$$E(\alpha)=\alpha^2+1/\alpha^2+2/\alpha+2\alpha-6, \quad (13)$$

and

$$F(\alpha)=\alpha^2-1/\alpha^2+2/\alpha-2\alpha.$$

Equation (12) is identical with Mooney's equation[2] except that Mooney had a different coefficient for $F(\alpha)$ as follows:

$$W=(G/4)E(\alpha)+(H/4)F(\alpha). \quad (14)$$

Since Eq. (12) is closer to (14) than any other equation derived by statistical means, and since (14) gives excellent agreement with observation,[2] we see that the present theory is almost complete. Moreover, we have shown that the molecular and macroscopic theories are compatible. It will be recognized that $E(\alpha)$ and $F(\alpha)$ are, respectively, *symmetric* and *antisymmetric* with regard to replacing α by its reciprocal. If $H=G$ (as the present molecular theory predicts) then there will be no symmetry between extension and compression processes. On the other hand, if $H\neq G$, then compression will have some resemblance to extension as far as the work required is concerned. Accordingly, H/G is a measure of the asymmetry of compression and extension, as pointed out by Mooney. To get Eq. (14) from the statistical theory, it would be necessary to introduce a perturbation which would add terms resembling an energy of compression to the energy of extension.

RUBBER SUBJECTED TO SHEAR

The statistical theory will now be extended to a treatment of pure shear. Consider a bar of rubber of square cross section arranged so that the diagonals of the square lie on a pair of cartesian axes (Fig. 3). Now let the rubber be sheared so that its cross section becomes a rhombus of area equal to that of the original square. For such a process, no effect will be noticed in the z direction, so that direction will be disregarded.

The original distribution of molecules with

* An equation similar to (11) was derived by E. Guth and H. M. Jones by a different method. Ind. and Eng. Chem. **33**, 624 (1941).

respect to x and y values will be

$$p(x, y)dxdy = (\beta^2/\pi) \times \exp[-\beta^2(x^2+y^2)]dxdy. \quad (15)$$

After the shear, the distribution becomes

$$p'(x, y)dxdy = (\beta^2/\pi) \times \exp[-\beta^2(x^2/\alpha^2+\alpha^2y^2)]dxdy, \quad (16)$$

assuming an extension in the x direction by a factor α. Substituting into Eq. (5), there is obtained

$$\ln \frac{P}{P_0} = \sum_i s_i[-\beta^2 x_i^2(1-1/\alpha^2) - \beta^2 y_i^2(1-\alpha^2)]. \quad (17)$$

Performing the indicated summation gives

$$\ln \frac{P}{P_0} = -N(\alpha^2-1)/2 - N(1-\alpha^2)/(2\alpha^2),$$
$$= -N(\alpha^2+1/\alpha^2-2)/2. \quad (18)$$

Hence

$$W = NkT(\alpha^2+1/\alpha^2-2)/2. \quad (19)$$

But the amount of shear (γ) is measured by[5]

$$\gamma = \alpha - 1/\alpha. \quad (20)$$

Therefore

$$W = NkT\gamma^2/2 = G\gamma^2/2. \quad (21)$$

Equation (21) shows that rubber should obey Hooke's law with respect to shear even though it does not obey Hooke's law for extension. The quantity G is called the modulus of rigidity.

DISCUSSION

One of the first points to be clarified is the significance of N, the total number of molecules. Assuming the validity of Eqs. (10) and (21) we must recognize that the apparent number of molecules depends upon the state of vulcanization, because increased vulcanization increases G, the modulus of rigidity. Since vulcanization involves linking molecules together at various points, it is clear that N must be taken as the total number of molecular segments between linkage points, such points being regarded as the ends of the "molecules." The chain segments between such vulcanization bridges arrange themselves more or less at random, subject only to the condition that their ends are in fixed positions. The vulcanization bridges (or ends of "molecules") are assumed to respond to external constraints in accordance with postulate I.

From the foregoing discussion, it is seen that increased vulcanization increases the apparent number of molecules and hence the modulus of rigidity. If an experimental value for the rigidity is used to calculate a molecular weight by use of Eqs. (10) or (21), then the calculated molecular weight will be the average weight of the chain segments between points of vulcanization. Increased vulcanization decreases the "molecular weight" insofar as the concept of molecular weight is used in this theory.

The range of validity of the equations derived in this theory depends upon the degree of vulcanization. A slightly vulcanized sample of rubber will have long enough chain segments so that the probability distributions which were used will be valid up to several hundred percent elongation. On the other hand, a highly vulcanized sample will have such short chain segments that the statistical arguments will fail after a small amount of elongation. This follows because a short molecule is more likely to be found near its maximum length than is a long molecule. When an appreciable number of molecules approach their maximum lengths, then the external stretching force must become much greater than that predicted by Eq. (11). This is in agreement with the findings of R. H. Gerke.[6]

The prediction that rubber should obey Hooke's law for shear is particularly interesting. Mooney[2] quotes some unpublished results which directly confirm this point. On the basis of those experiments, Mooney assumed Hooke's law applying to shear as one of the postulates for his macroscopic theory.

[5] A. E. H. Love, *Mathematical Theory of Elasticity* (Cambridge University Press), second edition, p. 34.

[6] R. H. Gerke, Ind. Eng. Chem. **22**, 73 (1930); Rub. Chem. Tech. **3**, 304 (1930); also see reference 2 for a convenient summary and for graphs of data.

Letters to the Editor

THIS section will accept reports of new work, provided these are terse and contain few figures, and especially few halftone cuts. The Editorial Board will not hold itself responsible for opinions expressed by the correspondents. Contributions to this section should not exceed 600 words in length and must reach the office of the Managing Editor not later than the 15th of the month preceding that of the issue in which the letter is to appear. No proof will be sent to the authors. The usual publication charge ($3.00 per page) will not be made and no reprints will be furnished free.

Atomic Weight Comparisons from Density and X-Ray Data: Fluorine, Calcium, and Carbon

CLYDE A. HUTCHISON
Department of Chemistry, University of Buffalo, Buffalo, New York
June 15, 1942

WHEN values of the densities and of the x-ray grating spaces of two crystalline substances are known, their molecular weights may be compared by means of the relationship,

$$M_1 = M_2\left\{\frac{\rho_1}{\rho_2}FR_g^3\right\}, \qquad (1)$$

where the numerical subscripts refer to the two crystalline substances; M is a molecular or atomic weight; ρ is a density; F is a factor depending on the crystal geometries and arrangements and number of molecules in the unit cells; and R_g is the ratio of the true x-ray grating spaces of the crystals. Since the R_g's may be determined with high precision by well-known methods and are independent of the absolute values of x-ray wave-lengths or Avogadro's number, the development of a "temperature of flotation" technique[1] for precise determination of crystal densities makes available a general physical method of high precision for atomic weight comparisons.

Hutchison and Johnston[2] have used Eq. (1) in the comparison of the atomic weights of fluorine and calcium. We wish to call attention to the density and x-ray data of Bearden[3] and of Tu[4] on diamond which make possible a comparison of the atomic weights of calcium and carbon and hence of carbon and fluorine. In Table I is listed a set of values which has been employed in Eq. (1), which becomes in this case,

$$M_{Ca} = M_C\left[\left\{\frac{\rho_{\text{calcite}}}{\rho_{\text{diamond}}}FR_g^3\right\}-1\right]-48.$$

This set of values yields 40.0842 ± 0.0049 for the atomic weight of calcium. The uncertainty in the comparison may be stated as an uncertainty of ±0.0049 in the atomic weight of calcium obtained in Eq. (1) when a given value of the atomic weight of carbon is used on the right-hand side of this equation.

TABLE I.

$\rho^{20°C}$calcite	Bearden[a]	2.71030 ±0.00003 g cm^{-3}
$\rho^{20°C}$diamond	Bearden (reference 3)	3.51540 ±0.00004 g cm^{-3}
F		$\varphi^{20°C}$calcite/4
$\varphi^{20°C}$calcite	Bearden[a]	1.09594 ±0.00001
$R_g^{20°C}$	Tu (reference 4)	3.40430 ±0.00002
	Bearden[a] (reference 3)	
M_C	Baxter and Hale[b]	12.0104
	Scott and Hurley[c]	

[a] J. A. Bearden, Phys. Rev. **38**, 2089 (1931). The value used is that given by Bearden as a best mean of his results and those of Defoe and A. H. Compton, Phys. Rev. **25**, 618 (1925).
[b] Baxter and Hale, J. Am. Chem. Soc. **59**, 506 (1937).
[c] Scott and Hurley, J. Am. Chem. Soc. **59**, 1905 (1937).

The density of diamond at 20°C was computed from Bearden's data using 0.354×10^{-5} deg.$^{-1}$ as the cubic coefficient of thermal expansion. This is three times the value[5] of the linear coefficient. Tu's density data appear unreliable due to some error as has been mentioned by Bearden.[3]

The R_g was calculated directly from the angle measurements using the expression,

$$R_g = \frac{\sin\theta_2(1-\delta_2/\sin^2\theta_2)}{\sin\theta_1(1-\delta_1/\sin^2\theta_1)}, \qquad (2)$$

where 2 refers to diamond and 1 to calcite. R_g was calculated from the first-order angles of Tu for both calcite and diamond and also from the first-order angle of Tu for diamond and the fourth-order angle of Bearden[6] for calcite.

TABLE II.

Carbon		Calcium	Fluorine
Best chemical value[a] (reference 2)	12.0104	40.0842 ±0.0049	18.9961 ±0.0015
Gas density values[b,c]* based on CO and CO_2	12.010 to 12.011	40.0812 ±0.0049 to 40.0886 ±0.0049	18.9952 ±0.0015 to 18.9974 ±0.0015
Mass spectrographic[d] value	12.0114	40.0915 ±0.0049	18.9983 ±0.0015

[a] See reference *c*, Table I.
[b] Cawood and Patterson, Trans. Roy. Soc. **A236**, 77 (1936).
[c] Woodhead and Whytlaw-Gray, J. Chem. Soc., p. 846 (1933).
[d] R. T. Birge, Rev. Mod. Phys. **13**, 233–239 (1941).
* The gas density data of Moles (Moles and co-workers, series of papers in Annales. Soc. Españ. Fís. Quín. References in annual reports of Int. Comm. on atomic weights) give extremely low values and are not included here.

The two results agree within the experimental uncertainty and the mean was used. The δ's were calculated from Bearden's[3, 6] values of the indices of refraction. The data were obtained at 18°C and R_g at 20°C was computed using the data from the *International Critical Tables*[5] and of Cooksey and Cooksey[7] on the linear coefficients of thermal expansion of diamond and calcite, respectively. In all cases the Mo $K_{\alpha1}$ line was used.

From the value of the atomic weight of calcium obtained in this manner the atomic weight of fluorine may be calculated from the data of Hutchison and Johnston.[2] The value of the atomic weight of carbon given in Table I is the best chemical value. In Table II is given a set of values of the atomic weight of carbon and the resulting values of the atomic weights of calcium and fluorine computed from density and x-ray data.

It will be seen that if the chemical value of the atomic weight of carbon is used, the resulting atomic weight of

calcium is in agreement with the value, 40.085, obtained by Hönigschmid and Kempter,[8] and somewhat higher than the recent value given by Birge.[9] It is in disagreement with the older value of Richards and Hönigschmid[10] or the more recent value of Kendall, Smith, and Tait.[11] The value obtained for the atomic weight of fluorine is in agreement with the gas density data[2] but in disagreement with the mass spectrographic value of 18.999.[2]

If the mass spectrographic value of the atomic weight of carbon is used, the value obtained for calcium is improbably high but the value obtained for fluorine is much nearer the mass spectrographic value and in agreement with only the highest of the gas density values.[2]

[1] C. A. Hutchison and Johnston, J. Am. Chem. Soc. **62**, 3165 (1940).
[2] C. A. Hutchison and Johnston, J. Am. Chem. Soc. **63**, 1580 (1941).
[3] J. A. Bearden, Phys. Rev. **54**, 698 (1938).
[4] Y. Tu, Phys. Rev. **40**, 662 (1932).
[5] *International Critical Tables*, Vol. 3, p. 21.
[6] See reference a, Table I.
[7] C. D. Cooksey and D. Cooksey, Phys. Rev. **36**, 85 (1930).
[8] Hönigschmid and Kempter, Zeits. f. anorg. allgem. Chemie **163**, 315 (1927); **195**, 1 (1931).
[9] See reference d, Table II.
[10] Richards and Hönigschmid, J. Am. Chem. Soc. **32**, 1577 (1910).
[11] Kendall, Smith, and Tait, Nature **131**, 688 (1933).

Heat of Dissociation of Cyanogen

N. C. Robertson and R. N. Pease
Department of Chemistry, Princeton University, Princeton, New Jersey
May 28, 1942

In a recent communication Herzberg[1] has criticized the value given by White[2] for the heat of dissociation of cyanogen into two cyanide radicals. White found a probable value of 146(±4) kcal./mole and assigned a minimum value of 138(±1.5) kcal./mole for this quantity.

We have recently investigated the kinetics of the thermal reaction of hydrogen with cyanogen over the temperature range 575–675°, and the conclusions with regard to the nature of this process may throw some light on this question. The results of our study, the details of which are soon to be published, are consistent only with a chain mechanism. This appears to involve the initial dissociation of cyanogen into free cyanide radicals with chain ending by the recombination of these radicals. The most plausible series of reactions is:

1. $(CN)_2 \rightarrow 2\ CN.$
2. $CN + H_2 \rightarrow HCN + H.$
3. $H + (CN)_2 \rightarrow HCN + CN.$
4. $H + HCN \rightarrow H_2 + CN.$
5. $CN + CN \rightarrow (CN)_2.$

If this mechanism is accepted, the absolute rate of formation of hydrogen cyanide, neglecting the inhibiting reaction 4, may be calculated as twice the rate of reaction of an equilibrium concentration of cyanide radicals with hydrogen. Hartel and Polanyi[3] obtained the reasonable value of 7 kcal. for the activation energy of step 2. It develops that if the equilibrium concentration of cyanide radicals is calculated using the *minimum* value assigned by White for $D(C_2N_2)$, the calculated rate is too low by at least a power of ten. If the value of 77 kcal./mole found by Kistiakowsky and Gershinowitz[4] is taken, the calculated rate is too high by about 10^5. A value between these extremes in the range 120–130 kcal./mole seems to be indicated.

The over-all activation energy for the reaction with hydrogen is approximately 72 kcal., which is entirely consistent with the observed absolute rate and with the proposed mechanism. Combining this value with the activation energy for step 2, one obtains 125–130 kcal./mole for the heat of dissociation of cyanogen. It might be mentioned that Hogness and T'sai[5] found that 2240A, corresponding to 127 kcal./mole, is the maximum wave-length effective for the photo-polymerization of cyanogen; and this reaction from all evidence also involves the initial dissociation of cyanogen into radicals.

Herzberg's comment regarding the relative values of $D(C_2N_2)$ and $D(CN)$ seems well taken from the chemical standpoint since the $C \equiv N$ bond is stable at very high temperatures.

[1] G. Herzberg, J. Chem. Phys. **10**, 306 (1942).
[2] J. U. White, J. Chem. Phys. **8**, 459 (1940).
[3] H. v. Hartel and M. Polanyi, Zeits. f. physik. Chemie **B11**, 97 (1930).
[4] G. B. Kistiakowsky and H. Gershinowitz, J. Chem. Phys. **1**, 432 (1933).
[5] T. R. Hogness and Liu-Sheng T'sai, J. Am. Chem. Soc. **54**, 123 (1932).